This is to certify that the
thesis entitled
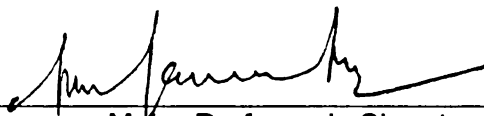
ENERGY BASED EQUIVALENT APPROACH FOR EVALUATING FIRE RESISTANCE OF REINFORCED CONCRETE BEAMS

presented by

PURUSHOTHAM PAKALA

has been accepted towards fulfillment
of the requirements for the

_____M.S._____   degree in   _____CIVIL ENGINEERING_____

_____
Major Professor's Signature

_____9th December 2009_____

Date

PLACE IN RETURN BOX to remove this checkout from your record.
TO AVOID FINES return on or before date due.
MAY BE RECALLED with earlier due date if requested.

DATE DUE	DATE DUE	DATE DUE

ENERGY BASED EQUIVALENT APPROACH FOR EVALUATING FIRE RESISTANCE OF REINFORCED CONCRETE BEAMS

By

Purushotham Pakala

A THESIS

Submitted to
Michigan State University
in partial fulfillment of the requirements
for the degree of

MASTER OF SCIENCE

Civil Engineering

2009

ABSTRACT

ENERGY BASED EQUIVALENT APPROACH FOR EVALUATING FIRE RESISTANCE OF REINFORCED CONCRETE BEAMS

By

Purushotham Pakala

Provisions of fire resistance is one of the key considerations in building design since fire represents most severe hazard experienced by built infrastructure during their life time. Current fire resistance provisions do not account for critical factors in evaluating fire resistance of reinforced concrete (RC) members and hence are not applicable for realistic fire performance assessment of RC members. Rational design approaches for evaluating realistic fire resistance of RC members can be achieved through the use of time equivalency. Existing time equivalency methods have a number of limitations and are derived for protected steel members and may not be applicable for RC members.

This thesis presents the development of an energy based approach for evaluating time equivalent of RC members under realistic fire scenarios. To generate large amount of data required for development of energy based method, a macroscopic finite element model has been extended to cover beams with T and I cross-sections. The validated numerical model is used to undertake a set of parametric studies on RC beams. Data from the parametric studies is used for validating the proposed energy based approach. Regression analysis has been applied to the data set and a correlation between the ratio of time equivalent predicted by the finite element model and equal energy method has been established. Based on the results, it is shown that the proposed energy based approach provides a better estimate of time equivalent for RC beams than current approaches.

Dedicated to

my family and friends

who have always been with me

during various phases of my life.

ACKNOWLEDGEMENTS

Finally I would like to thank my family members for my academic success. Without their moral support and sacrifices, it would not have been possible for me to pursue this graduate degree.

TABLE OF CONTENTS

LIST OF TABLES

LIST OF FIGURES

xiii

CHAPTER 1

1. INTRODUCTION

1.1 General

Reinforced Concrete (RC) structural systems are frequently used in high rise buildings due to several advantages they provide over other construction materials. Provision of appropriate fire safety measures is one of the key considerations in buildings since fire represents one of the severe hazards to which buildings may be subjected to in their design life time. One of the main advantages of RC construction is its high fire resistance properties. This leads to achieving required fire resistance ratings without the use of any external fire protection measures.

The main objective of fire safety provisions is to limit the probability of death, injury, and property loss, during a fire [Buchanan, 2002]. These fire safety objectives are achieved by providing active and passive fire protection systems. Active fire protection systems, such as sprinklers, are those which become functional in the event of fire and control the fire through an external device. Passive fire protection systems, such as fire

resistance, are inherent within the structural system and do not require any device to get activated. Thus, active and passive fire protective systems can be used independently or jointly to achieve fire safety objectives in buildings. The most important component of passive fire protection is fire resistance which is defined as the duration during which a structural element exhibits resistance with respect to structural integrity, stability, and temperature transmission, when exposed to fire. Fire resistance depends on type of fire exposure, structural member type, applied load and characteristics of the constituent materials of the structural member.

1.2 Fire resistance of structural members

Fire resistance provisions for RC members in codes and standards are prescriptive in nature and are derived based on results from standard fire resistance tests or through empirical calculation methods. Standard fire resistance tests are conducted on structural components such as beams, walls, floors or columns according to national standards [ASTM E119a or ISO 834]. The standards require the test specimens be constructed in a similar manner as in real building. Some standards such as ASTM E119 specify the dimensions of the specimen to be tested along with the size of the furnace being used for the standard fire test. The test specimens are often loaded with service loads (generally 50% of the room temperature capacity) and are subjected to standard fire exposure which follows a predefined time-temperature relationship as shown in Figure 1.1. The test is continued until a prescribed failure criterion is met. The time to reach failure point is termed as the fire resistance of the member. This time is rounded off to nearest half hour

2

(30 or 90 minutes) or hour (1, 2, 3 or 4) and this value represents the fire resistance rating.

The fire resistance of structural component depends on a number of factors including type of fire scenario, applied load, material properties and structural configuration (restraint). Figure 1.1 also shows time-temperature curves of two representative design fires. Design fire (Fire 1) is short hot fire whereas the other design fire (Fire 2) is moderate fire. It can be seen from Figure 1.1 that the temperature in standard fire increases continuously without a decay (cooling) phase, whereas in design fires there is a well defined decay phase. The presence of decay phase in design fires significantly influences the fire response of structural members. Though standard fire resistance tests are very helpful in assessing the comparative performance of structural members, they do not account for important factors such as realistic fire scenario, loading and failure criterion. Also, the standard fire resistance tests are often carried out on individual elements without any consideration to structural interactions and restraint conditions at supports. These interactions provide considerable amount of redistribution of moments that will have significant influence on the fire resistance of RC members as shown in a number of studies [Dwaikat 2009]. Figure 1.2 illustrates the loading and support conditions encountered by structural members during standard fire resistance test and in a real building. The presence of end restrains, member continuity, and structural members' interaction at joints in a building will modify the fire response of RC members compared to that under a standard fire resistance test.

Fire response of RC members is highly influenced by the material properties of constituent materials, namely concrete and reinforcing steel. The high temperature

3

material properties that are important are thermal, mechanical and deformation properties. Thermal properties influence the amount of heat transferred to a structural member whereas mechanical properties determine the extent of loss in strength and stiffness of the member. Deformation properties influence the extent of deformations in the structural components. All these properties change with increasing temperature and also depend on the characteristics of concrete and steel.

Structural configuration refers to geometric and support conditions of the structural member. The support conditions define the level of restraint at the ends which in turn influences the fire resistance of RC beams. Recent studies showed that axial restraint can improve the fire resistance of RC beam by arch action. However, the axial restraint under large deflections in the span may lead to buckling and premature failure of the beam [Dwaikat 2009].

Designing a structural component through prescriptive based methods involves adherence to predetermined requirements specified in codes and does not give the designer the freedom to implement innovative and cost-effective engineering approaches to fire safety. Also prescriptive based approaches provide same level of fire safety to RC members irrespective of the fire severity, magnitude of loading, compartment characteristics and member dimensions. In addition, these ratings are derived based on standard fire exposure without due consideration to important factors such as fire exposure, load level and support conditions. Thus the current provisions in codes and standards may not provide a realistic assessment of the fire performance of RC beams.

In contrast to prescriptive based codes, performance based fire design comprises of evaluating performance of structural elements under realistic fire, loading and restraint

scenarios. In a performance based evaluation, the structural components are designed taking into account realistic fire exposure, support conditions, loading and failure criterion. Performance based approach gives the designers the opportunity to use innovative strategies for design of structural components, provided that equivalent fire safety can be demonstrated. Generally performance based design requires detailed calculations and numerical simulations.

Of the various factors, fire scenario has the greatest influence on fire resistance and is not properly accounted for in prescriptive based approaches. In order to evaluate or design a structural component for fire resistance, the worst case fire scenario that the structural component might be subjected to during its design life time should be known. In other words, the designer should be aware of the destructive potential of a fire to which the structure might be subjected to. The destructive potential of fire is defined as the fire severity and it depends on a number of factors such as the fuel load (occupancy type), compartment size and location of openings, type of lining materials and area of compartment. Knowing the fire severity, a designer could design the structure by making sure that the structural fire resistance is greater than the severity of fire. In order to ensure that the above criteria are met for performance based design, severity of realistic fire exposure should be related to that of standard fire exposure. This correspondence is often established by a simplified approach termed as equivalent fire severity.

1.3 Fire performance of RC beams under design fires

As illustrated above, fire severity is one of the main factors that influence the performance of a beam under fire. If the fire severity under design fire is linked to the

performance of an RC beam under a standard fire scenario then an equivalency can be established. Therefore, a designer can evaluate the performance of RC beam exposed to a design fire using the currently available data from standard fire tests, without the need of conducting fire tests or detailed finite element analysis on the beams under design fire exposure. The equivalency for beam response under design and standard fire exposures is generally expressed using the term "time equivalent", which can be defined as the time of exposure to standard fire that would result in the same fire severity as that under design fire exposure. A review of the literature shows that there are very few methods and empirical formulae for evaluating time equivalent of RC members [CIB, Eurocode, Ingberg, Law, Pettersson]. Further, there are a number of drawbacks in these methods and empirical formulae since they do not account for all the critical factors governing fire response. Also, these methods are mainly derived for protected steel members and are not validated over the full range of fire scenarios for RC members. Furthermore, there is significant variation among various time equivalent approaches. Hence, there is a need for an appropriate time equivalent method for establishing equivalency between standard and design fire exposure.

1.4 Objectives

Currently, fire resistance of RC beams is established based on standard fire tests which have numerous drawbacks. To overcome these limitations, the current study is focused on developing a simplified engineering approach for evaluating fire resistance of RC beams under realistic fire, loading and restraint conditions. Establishing such simplified

approaches require large set of data which can be generated through numerical studies utilizing finite element based computer models.

Recently Dwaikat and Kodur [2008] have developed a macroscopic finite element based numerical model for fire resistance analysis of RC beams. However this model is for RC beams with rectangular sections only, but in real life situations RC beams with T and I cross-sections are often used. Hence the current study aims at extending the macroscopic finite element model to evaluate the fire performance of RC beams with rectangular, T and I cross-section. Using the updated numerical model, parametric studies will be conducted to quantify the influence of various parameters on the fire response of RC beams. Data generated from parametric studies will be used to develop a time equivalent approach for evaluating equivalent fire resistance of RC beams under design fire exposure.

1.5 Outline of thesis

This thesis is divided into six chapters and four appendices. Chapter 2 provides a review of literature relevant to the behavior of RC beams under fire conditionsPrevious experimental and analytical studies on fire response of RC beams are reviewed and currently available time equivalent methods for RC beams are discussed.

Chapter 3 presents the extension of macroscopic FE model for tracing the fire response of RC beams with T and I cross sections. Predictions from the model are compared with those obtained from test data and other numerical models to demonstrate the validity of the model.

Results from a set of parametric studies on the fire response of RC beams are presented in Chapter 4. Factors influencing the fire resistance of RC beams are discussed.

Chapter 5 presents the development of semi-empirical energy based approach for evaluating the time equivalent of RC beams under realistic fire, loading and support conditions. Chapter 6 presents the key conclusions derived from the research and main recommendations for further research.

Figures
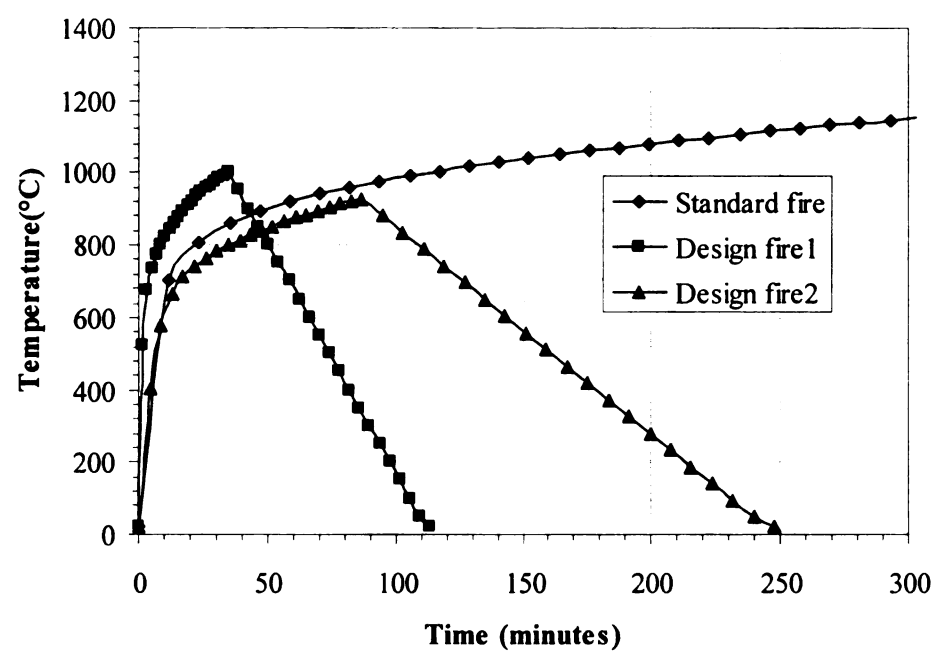
Figure 1.1 - Time-temperature curves of standard and representative design fires

9
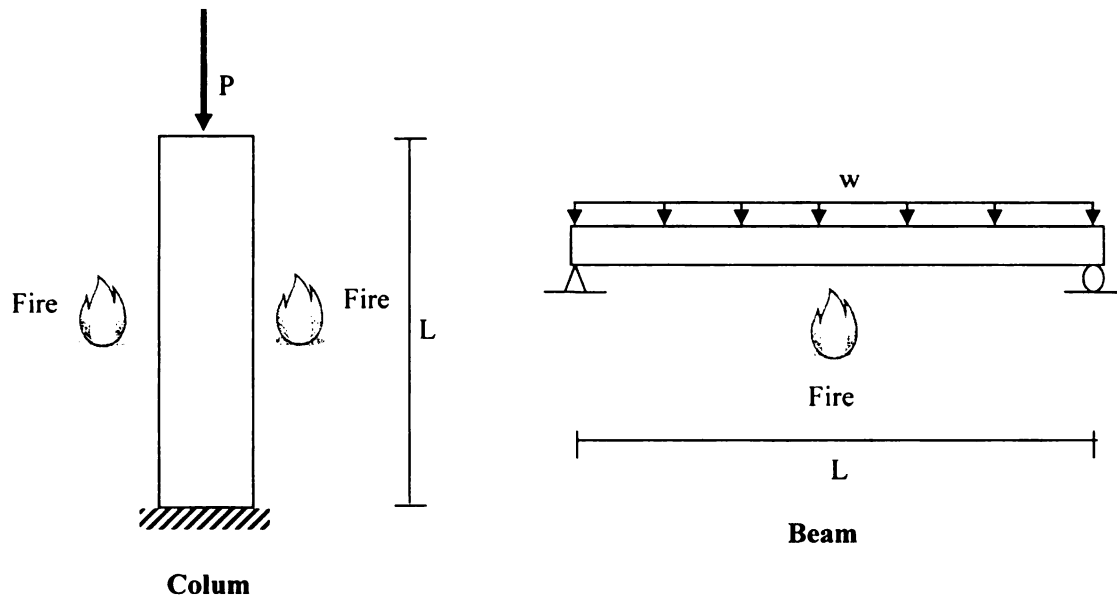
(a) Fire resistance evaluation through standard fire test
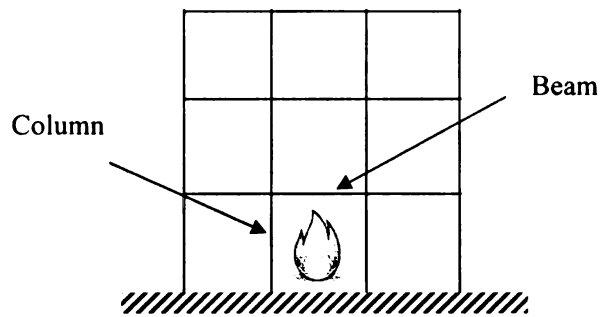
(b) Actual conditions in a building

Figure 1.2 - Comparison of loading and boundary conditions of structural members encountered in standard fire testing and an actual building

CHAPTER 2

2. LITERATURE REVIEW

2.1 General

Current methods of evaluating fire resistance of RC beams utilize prescriptive based approaches which are developed using data from standard fire resistance tests. The standard fire resistance tests are conducted under a standard fire exposure and do not take into consideration realistic fire scenarios that depend on compartment characteristics such as fuel load and ventilation properties. Thus the prescriptive based methods for evaluating fire resistance of RC beams may not be applicable for evaluating fire resistance under performance based codes wherein the fire resistance of the member is to be evaluated under realistic conditions. Evaluation of fire resistance under realistic conditions requires detailed finite element analysis. However, currently there are only very limited finite element based computer models for modeling the fire response of RC members.

This chapter presents a brief overview of the behavior of RC beams under fire conditions. Both experimental and numerical studies that are reported in the literature to characterize the fire behavior of RC beams are reviewed. In addition, different time equivalent methodologies for evaluating the equivalent fire resistance of structural members are reviewed.

2.2 Response of RC beams under fire

The response of RC beams under fire conditions is different from that of room temperature. This is due to the fact that under fire conditions the loads on the beam remain the same or may even reduce (due to evacuation of people), but the strength and stiffness of the beam deteriorates with fire exposure time. The temperatures in the beam increase with time due to heat transfer from the fire through the exposed surface of the beam. The increasing temperatures results in loss of strength and stiffness of the constituent materials (namely concrete and steel) which leads to reduction in the moment (capacity) as well as increase in the deflection of the beam. This process will continue until the capacity of the beam deteriorates to the level of applied moment (load), at which point the beam is considered to have failed. The duration at which the capacity of beam equals the applied load is termed as the fire resistance of the beam.

Behavior of an RC beam subject to a standard fire exposure is illustrated in Figure 2.1. It can be seen from the figure the capacity of the beam decreases with time under increasing fire temperatures. The decrease in the capacity of the beam is not significant in the initial stages of fire exposure but as the time progresses the capacity of the beam decreases gradually due to increase in fire temperature. The degradation in the capacity of the beam

continues until it reaches a value where it can no longer sustain the applied moment (load) resulting in failure of the beam. The fire exposure time at which the failure of the beam occurs is defined as the fire resistance of the beam.

The fire resistance of RC beams is mostly evaluated through full-scale fire-resistance tests or prescriptive based methodologies. In the fire test, the building element is subjected to a standard fire exposure specified in ASTM E119a [2008] or ISO834 [1975] and the fire exposure is continued until failure of the element or required fire resistance rating is attained. The failure of a structural element in standard fire resistance test is based on stability, integrity and insulation failure criterion. To meet the stability failure criterion, the structural element should be able to perform its load-bearing capacity for the duration of the test without collapse. Integrity failure criterion requires that the structural element does not develop any cracks/openings that allow the fire/smoke to pass through it. The insulation failure criterion is said to be met when the average increase in unexposed side temperature of the assembly is below 140°C and a maximum temperature increase does not exceed 180°C at a single point.

In lieu of standard fire tests or complex set of calculations, codes and standard provisions often relate fire resistance of RC members to minimum cross-section dimensions and the concrete cover to the reinforcement. These prescriptive based approaches, derived based on standard fire resistance tests have numerous drawbacks and do not lead to realistic assessment of fire resistance.

2.3 State-of-the-art review – Fire resistance of RC beams

A review of literature shows that there has been limited number of experimental and numerical studies on the behavior of RC flexural members (beams) exposed to fire. An overview of previous experimental and numerical (analytical) fire resistance studies on RC beams is presented here.

2.3.1 Experimental studies

Experimental studies aimed at characterizing the behavior of RC beams under fire have been undertaken by Dotreppe and Franssen [1985], Lin et al. [1981], Lin and Ellingwood [1987], Shi et al. [2004] and Dwaikat [2009]. Dotreppe and Franssen [1985] tested an RC beam of rectangular cross-section under ISO834 standard fire exposure to evaluate its fire resistance rating. The beam had a span length of 6.5 m with 200 mm x 600 mm cross-sectional dimensions. The beam was reinforced with 2Ø12 mm bars as compression reinforcement and 3Ø22 mm bars as tension reinforcement. The beam was made up of siliceous aggregate concrete having a compressive strength of 15 MPa. Two concentrated loads were applied on the beam, each at a distance of 1.625 m from the support. The study concluded that the presence of steep fire induced thermal gradients in the cross-section produces large deflections in the beam even in early stages of fire exposure.

Lin et al. [1981] tested eleven rectangular RC beams subjected to ASTM E119 standard fire exposure. All the test specimens had a cross-sectional dimension of 305 mm x 355 mm with a total length of 9.76 m. The beams were reinforced with #6 (Ø19 mm) and #8 (Ø25 mm) bars of ASTM A615 designation. The measured average yield strength of #6 bars was 435.8 MPa while that of #8 bars was 434.4 MPa. Normal weight concrete was

14

used for fabrication of ten beams while sanded lightweight concrete was used to fabricate single beam. The compressive strength of concrete at 28 days ranged between 27-33 MPa. The study investigated the effect of aggregate type, beam continuity and moment redistribution on the fire behavior of RC beams. Lin et al. [1981] observed that the loads required on overhang of the beam to accomplish the continuity effect in beams increased during the first 15 minutes of fire test, reached maximum value after 30 to 45 minutes into the test and then remained constant for the remaining duration. Also mid-span deflection of specimens tested as continuous beams increased at a constant rate for the first two-third duration of fire test and then increased sharply for the remaining duration. The study concluded that continuous beams as compared to simply supported beams undergo significant redistribution of moments during fire exposure and this helps in enhancing their fire resistance.

Lin and Ellingwood [1987] tested six full-scale concrete beams to study the behavior of RC beams exposed to fire. Five of the six test specimens had a cross-sectional dimension of 533 mm x 229 mm, while the sixth one was 610 mm deep and 254 mm wide. All the six beams were 8.2 m in total span with a fire exposed span of 6.1 m and an unexposed cantilever loaded in order to provide continuity over one support. Cross-sectional details as well as the elevation of typical beams are shown in Figure 2.2. All the six beams were fabricated with normal-weight concrete having a compressive strength of 2.76 MPa. Four beams were exposed to ASTM E119 standard fire, while the other two beams were subjected to short duration high-intensity (SDHI) design fire. During the test furnace atmosphere, concrete and steel temperatures, deformations in beam such as deflection, expansion were measured for each beam. Though shear cracks developed during the early

15

stages of fire tests, all the beams failed by flexure rather than by shear. The fire resistance of the beams(failure times) ranged from 3 hr 26 min to 4 hr 8 min. Major conclusion of this study is that the shear failure in RC beams is unlikely under fire exposure conditions. Other notable conclusion was that the temperature history in the reinforcement is the most important factor that affects fire response of RC beams.

Shi et al. [2004] tested six RC rectangular beams with varying concrete cover thickness by exposing them to time-temperature curve in a specially designed electric furnace. All the six beams were of 1.3 m long with a cross-section width of 100 mm. The section depth of the cross-section varied between 180 mm to 200 mm. The beams were reinforced with 2Ø10 mm bars in compression and 2Ø10 mm bars in tension. The test specimens were made with crushed limestone aggregate concrete having 28 day cube strength of 39 MPa and rebars having yield strength of 270 MPa. The main objective of the study was to study the effect of bottom and lateral concrete cover thickness on the fire response of RC beams. All beams were simply supported at both ends. One of the beams was tested in order to obtain the ultimate moment capacity at room temperature while another beam was heated without any applied load. Remaining four beams were subjected to load level of about 50% of ultimate capacity at room temperature in the form of two concentrated loads.

Shi et al. [2004] observed that the temperature distribution across the section depth is nonuniform and the gradients change continuously with an increase in the furnace temperature. The authors also observed that the temperature distribution in the top zone is similar for all test specimens irrespective of the amount of bottom concrete cover thickness and whether the specimen is loaded first before subjecting to heating. They

16

concluded that an increase in bottom concrete cover thickness up to a certain threshold increases the fire resistance of RC beams. Further increase in bottom concrete cover thickness, beyond the threshold value, does not improve the behavior (fire resistance) due to the widening of concrete cracks in the tension zone of concrete. The study also found that any increase in lateral concrete cover thickness beyond that of bottom concrete cover thickness, has negligible effect on the fire resistance of RC beams.

Dwaikat [2009] tested six RC beams to study the influence of critical factors such as concrete strength, load level, fire scenario, fire induced spalling, and axial restraint on the fire resistance of RC beams. Two of the beams were tested under ASTM E119 standard fire exposure [ASTM E119a 2008] while the remaining four beams were tested under typical design fire scenarios. Typical layout of tested beams is illustrated in Figure 2.3 along with the cross-sectional dimensions and material properties. Two of the six beams were fabricated with normal strength concrete (NSC), while the other four beams were fabricated with high strength concrete (HSC). Coarse aggregate used in both type of concretes were of carbonate aggregate. The average compressive cylinder strength at 28 days for NSC and HSC beams was 52.2 MPa and 93.3 MPa respectively. These tests were carried out to investigate the effect of variables such as concrete strength, axial restraint, type of fire exposure and load level on the fire behavior of RC beams. Dwaikat[2009] observed that the measured temperatures in HSC and NSC beams were close to each other. Measured mid-span deflection and spalling of HSC beam was higher than that of NSC beams. In addition, the axial restraint force in axially restrained beams increased with fire exposure time. Major conclusions from the study include that the fire resistance of HSC beams is lower than that of NSC beams due to faster degradation of

concrete strength and fire induced spalling in HSC. Fire resistance of RC beams exposed to design fire was higher as compared to standard fire exposure, due to the presence of the decay phase which leads to recovery of strength and stiffness.

The above discussed experimental studies were aimed at characterizing the behavior of RC beams under fire conditions. Effect of various parameters such as continuity, moment redistribution, concrete cover, concrete strength, load ration, fire scenario, fire induced spalling and axial restraint force on behavior of RC beams was studied. In most cases standard fire exposure was used and the results obtained from such tests might not represent actual performance under realistic fire conditions. Further, most of the fire resistance experiments were conducted on beams with rectangular cross section, but T and I cross sections were not considered.

2.3.2 Analytical studies

A review of literature indicates that a number of numerical studies were carried out by researchers (Dotreppe and Franssen [1985], Ellingwood and Lin [1991], Poh et al. [1995], Kang and Hong [2004], and Kodur and Dwaikat [2008, 2008b]) on the fire behavior of RC beams. Dotreppe and Franssen [1985] applied a finite element approach for the fire resistance analysis of RC beams. In this approach, the structure is divided into beam elements and sectional approach is used to evaluate strength at various time steps. As the study of mechanical behavior of concrete at high temperatures is complicated, the model employed a step-by-step analysis taking into account material and geometrical non-linearities. The model used Newton-Raphson procedure to perform iterative nonlinear structural analysis.

Ellingwood and Lin [1991] developed mathematical models for predicting thermal and structural response of RC beams subjected to standard and design fire exposures. The model utilizes sectional analysis approach for evaluating fire resistance of RC beams and accounts for change in thermal and mechanical properties of constituent materials, high temperature creep and shrinkage. Based on the results, the authors concluded that the most important factor that affects the behavior of RC beams is the temperature history in the reinforcement. Also the authors indicated that compressive strength and stiffness of concrete have less influence on fire resistance of RC beam.

Poh et al. [1995] developed a general numerical model to calculate the nonlinear behavior of load-bearing members (beams and columns) exposed to fire. According to this model, the structural member is discretized into a series of segments of appropriate lengths. Each segment is assumed to be represented by a cross section at its mid-length. The cross section is further divided into a number of small elements (subareas). The method uses a three tiered approach involving the elemental analysis, cross-section analysis and the overall global analysis of the structure. The structural behavior of each tier is characterized by appropriate action (internal or external) and deformations (including strains and curvatures) associated with the element. The governing equations are expressed in a succinct matrix format in terms of action-deformation relationships. These governing equations are solved by an iterative technique using two separate iterative loops namely, first loop which determines the behavior of the cross section and the other determines the behavior of the member. The first loop takes into account material nonlinearity while the second loop iterates on geometric nonlinearity. The material nonlinearity in the first loop is treated as a combination of linear component and

a correction component that accounts for material nonlinearity. Thus, the behavior of cross section is determined by a linear equation, and it is progressively corrected for material nonlinearity effects to be used in subsequent iterations. The method takes into account various factors such as axial forces, biaxial bending, restraints, material and geometric nonlinearity, unloading and reloading, residual or initial stresses, and initial out-of-straightness of the member. The numerical model is validated by comparing the results obtained from the model with those obtained from a series of restrained and unrestrained columns tested in laboratory by Poh and Bennetts [1995].

Kang and Hong [2004] proposed an analytical method for the thermal behavior of RC beams under fire conditions. The analysis was performed in two different levels; cross-sectional analysis and member solution. Sectional analysis is performed by the use of segmentation scheme which divides the length of the beam into segments of appropriate length. Mechanical changes at segmented section such as strain changes due to increase in temperature are integrated into the member behavior in the member solution. The model is based on the analytical formulation suggested by Poh et al. [1995] which uses action-deformation relationships, and numerical method proposed by Lie et al. [1993]. The method accounts for material deterioration, material nonlinearity and nonlinear strain changes of concrete with increasing temperature.

Apart from the above mentioned numerical models, special purpose finite element based computer programs such as SAFIR, developed at University of Liège in Belgium [Franssen et al. 2004] , can be applied to evaluate the performance of RC beams subjected to fire. A separate or combined (coupled or uncoupled) thermal and structural analysis can be performed in SAFIR to model the behavior of RC beams exposed to fire.

Fire resistance analysis of structural members can also be done using various commercial microscopic finite element based packages such as ANSYS, ABAQUS. However the analysis involves significant amount of complexity and effort. Results obtained from such programs are difficult to interpret and such complex level of analysis might not be necessary for the analysis of conventional RC beams. These factors limit the use of such microscopic finite element based models in practical situations.

To overcome the complexities of microscopic finite element models, Kodur and Dwaikat [2008] developed a macroscopic finite element based numerical model for tracing the response of RC members (beams and columns) exposed to fire. The model uses moment-curvature relationships to predict the behavior of an RC beam in the entire range of loading up to collapse under fire. The beam is divided into number of longitudinal segments and the mid-section of each segment is assumed to represent the behavior of the whole segment. The fire resistance analysis is carried out at various time steps, till failure occurs in the beam. The model accounts for creep and transient strain components, high temperature material properties, geometric and material nonlinearity and material softening. Based on the detailed validation the authors concluded that the model is capable of undertaking fire resistance analysis of RC beams for any value of span length, aggregate type, fire scenario, loading and sectional dimensions.

Kodur and Dwaikat [2008b] applied above developed finite element model to study the effect of parameters such as fire scenario, load level, concrete cover thickness, failure criteria, aggregate type and span length on the flexural response of RC beams exposed to fire. Sectional dimensions and properties of beam are illustrated in Figure 2.4. Based on these parametric studies, Kodur and Dwaikat [2008b] concluded that the type of failure

criterion, load level, fire scenario, concrete cover thickness and aggregate type have significant influence on fire resistance of RC beams while the span length has a minor effect.

2.3.3 Code provisions

Provisions for evaluating fire resistance of RC beams are generally specified in building codes and standards. These provisions, derived based on results of standard fire resistance tests, are generally related to factors such as minimum member dimensions and concrete cover thickness.

ACI 216.1 standard [2007] gives specifications for fire design of concrete and masonry structures. The standard specifies minimum beam width and concrete cover thickness to achieve a required fire resistance rating in RC beam as presented in Table 2.1. These requirements differ for restrained and unrestrained support conditions, but the definition of support conditions is not clearly addressed in the code. Hence, it is unclear whether restrained case refers to rotational restraint, or axial restraint or both rotational and axial restraints. Canadian provisions for fire resistance design, which are available in NBCC [2005], are similar to that of ACI 216.1.

Eurocode 2 [2004] provides tabulated data for evaluating fire resistance of RC beams. The required fire resistance of RC beams is related to minimum width and nominal axis distance, which is defined as the distance measured from the center of main reinforcing bar to the fire exposed surface of the member. Table 2.2 shows the minimum dimensions and axis distances, as specified in Eurocode 2, required for achieving fire resistance

22

rating in simply supported beams. These tables also provide possible combinations of minimum width and axis distance for achieving a required fire resistance rating.

In addition, Eurocode 2 [2004] also provides simplified calculation method, advanced calculation methods and tabulated data for determining fire resistance of RC beams. Simplified calculation method is based on cross-section analysis. Advanced calculation methods provide a realistic fire resistance assessment of a structure. These methods generally involve a detailed thermal and structural analysis model and require the use of advanced computer packages.

The above review of fire resistance provisions for RC beams in standards and codes shows that the fire resistance of a RC beam is mostly related to the cross-section dimensions and the concrete cover thickness without consideration to important facts such as fire scenario, material strength, amount of ventilation, loading and failure criteria. Thus these prescriptive based approaches may not yield realistic performance of beam under practical design situations.

2.3.4 Summary

Most of the previous experimental and analytical studies on RC beams were conducted under standard fire exposure. These standard fire resistance tests though helpful in assessing comparative performance of structural members, they do not take into account important factors such as realistic fire scenario, loading, restraint and failure criteria, which influence the fire behavior of RC beams. Thus, current prescriptive based fire resistance approaches may not be applicable for evaluating fire resistance under recently introduced performance based codes.

2.4 Time equivalent methods

As illustrated in Section 2.3, the main drawback in current prescriptive based fire resistance approaches is that they are derived for standard fire exposure without any consideration to realistic fire scenario. The fire scenario experienced by a beam varies from one compartment to other and is a function of fuel load, ventilation and size of compartment. Also, the absence of decay phase in the standard fire tests is a serious misrepresentation of fire scenario and this can have significant influence on fire resistance of RC beams.

Recently, there is a move towards performance based fire safety design since this facilitates realistic and rational assessment of fire safety under actual conditions present in a building. Such performance based fire safety design can be carried out through the use of calculation methods. However, undertaking performance based approach can present design challenges since numerous fire scenarios have to be considered. Further, tests or detailed finite element analysis are quite expensive and it may not be possible to undertake fire resistance tests or simulations for all possible fire scenarios. One way of overcoming such problem is by establishing an equivalency between the severity of a design fire and a standard fire exposure. Such an approach will facilitate the establishment of fire resistance information under any possible design fire scenario, provided the fire resistance is known for a standard fire exposure. Therefore, existing data from standard fire resistance tests or detailed finite element analysis can be utilized for evaluating performance under design fire scenarios. In order to ensure that the above criteria are met for performance based design, the severity of design fires should be related to standard fire exposures and can be done using equivalent fire severity.

24

Equivalent fire severity, commonly referred to as time equivalent, can be used to gauge the fire resistance of a structural member by comparing the severity of a design fire to that of a standard fire exposure. A review of literature indicates that there are a number of methods and empirical formulae for evaluating the equivalent fire severity. These methods include equal area method, maximum temperature method, minimum load capacity method, maximum deflection method and other empirical formulae such as CIB, Law and Eurocode methods. More details on these methods are presented in the following sub sections.

2.4.1 Equal area method

The equal area method proposed by Ingberg [1928], is based on the concept that two fires have equal fire severity if the areas under each of the time-temperature curves are equal, beyond a certain reference temperature (about 20°C – room temperature). The concept of equal area method is illustrated in Figure 2.5 where the fire temperatures from standard and design fire exposures are plotted as a function of time. According to this method, the area under the design fire (time-temperature) curve is computed first (area B in Figure 2.5). Then the area bound under the standard fire (time-temperature) curve, which is a function of time, is calculated at various time steps (area A in Figure 2.5). The time equivalency (t_e) is defined as the time at which the area under the standard time temperature curve (area A in Figure 2.5) is equal to that of design fire curve (area B in Figure 2.5).

Though the equal area concept was one of the earlier advancements in the area of fire engineering, it has many technical insufficiencies. This method is purely empirical

because the units of areas under comparison are not meaningful [Buchanan 2002]. The equal area concept can give an incorrect fire resistance assessment in case of a design fire that has significant variations from standard time-temperature curve. This is because the heat transfer from a fire to the structural element is mainly by radiation which is not directly proportional to the temperature difference, but it is proportional to the fourth power of the temperature difference. This method of comparing standard fire and a realistic fire underestimates the heat transfer in a short hot fire and overestimate the heat transfer in long cold fire, though both of them have equal areas under time-temperature curves [Nyman 2002]. Despite these technical inadequacies, equal area concept can be used to correct the results from a standard fire-resistance test if the time-temperature curve measured in a furnace is not followed within the limits described in the standard [ASTM E119a 2008].

2.4.2 Maximum temperature method

To overcome some of the deficiencies in equal area concept, Law [1971], Pettersson et al. [1976] and others developed maximum temperature concept for predicting equivalency between standard and design fire exposure in protected steel members. According to this method, equivalent fire severity is the time of exposure to standard fire that would result in the same maximum temperature in a protected steel member as would occur in a complete burnout of the fire compartment [Buchanan 2002]. Maximum temperature concept is illustrated in Figure 2.6, which shows the time-temperature curves for a design fire and a standard fire and also the corresponding protected steel temperatures. To determine the time equivalency, first the peak protected steel temperature resulting from

the design fire exposure (temperature at point B in Figure 2.6) is computed. The second step is to evaluate the steel temperature resulting from the standard fire exposure at various time steps. Time equivalency is then defined as the time at which the protected steel temperature under standard fire exposure (temperature at point A in Figure 2.6) is equal to the maximum steel temperature computed for the design fire exposure (temperature at point B in Figure 2.6).

This method is mainly derived for protected steel structural members exposed to fire and may not be applicable for RC members. In addition, this method may not be accurate if the maximum temperatures, used for computing the time equivalent, are much greater or lower than those which would cause failure in a particular building [Buchanan 2002].

In this method, rebar temperatures (instead of protected steel temperatures) can be used to evaluate time equivalency in the case of RC beams. However, computing rebar temperatures requires thermal analysis of the beam and significant computational effort, which limits the usefulness of this method in practical applications. Further, the method is not validated for RC beams.

2.4.3 Minimum load capacity method

In lieu of equal area and maximum temperature methods, minimum load carrying capacity method can be employed to establish equivalency between standard fire and design fire exposure. The concept of minimum load capacity is illustrated in Figure 2.7 where the variation of load carrying capacity is plotted as a function of time for an RC beam under both standard and design fire exposures. It can be seen from the figure that the capacity of RC beam decreases with fire exposure time due to gradual increase in

cross sectional temperature. However, for an RC beam exposed to design (realistic) fire, the strength decreases initially during the growth phase of fire, followed by an increase as the temperatures decrease in the decay phase as shown in Figure 2.7.

To calculate time equivalency in this method, the first step is to compute the minimum load capacity of the RC beam under design fire (load capacity at point B in Figure 2.7). The second step is to compute the load capacity of the beam under standard fire exposure as a function of fire exposure time. Time equivalency is the time at which the load capacity at point A in Figure 2.7 is equal the load capacity at point B in Figure 2.7.

This method utilizes various governing factors, such as fire scenario, beam characteristics, high temperature material properties, load level and support conditions, to establish time equivalency. Thus, the method generally results in a better estimate of the time equivalency as compared to other methods. However this method bases the failure of an RC beam only on strength capacity and does not account for deflection limit state which may be the governing failure criterion under some scenarios. In addition, the method requires detailed finite element analysis which limits its use in practice.

2.4.4 Maximum deflection method

In addition to the above discussed methods, time equivalency can be computed using maximum deflection method. The concept of computing time equivalency using maximum deflection method is illustrated in Figure 2.8, where the variation of deflection is plotted as a function of time for an RC beam subjected to standard and design fire exposures. To compute the time equivalency, first the maximum deflection of the beam subjected to design fire exposure is calculated (deflection at point B in Figure 2.8). Next

28

the deflection of the beam under standard fire exposure is computed as a function of fire exposure time. Time equivalent is defined as the time point when deflection at point A is equal to that at point B (Figure 2.8).

The maximum deflection method takes into account the deflection failure criteria, which makes it more reliable for estimating time equivalency for RC beams. A deflection failure criterion is important because failure in an RC beam can occur if the integrity cannot be maintained under large deflections. Large deflections can lead to the development of wider cracks that leave the reinforcement directly exposed to fire and cause failure of the beam.

With the exception of the equal area method, all three methods namely maximum temperature method, minimum load capacity method and maximum deflection method require detailed finite element analysis and thus can not be easily applied in design situations.

2.4.5 Empirical formulae

In addition to above methods, several empirical time equivalent formulae have been developed for evaluating time equivalency between standard and design fire exposure. These formulae are mainly derived based on the maximum temperature of protected steel members exposed to design fires. Widely used time equivalent formulae include the CIB formula, Law formula and Eurocode formula.

2.4.5.1 CIB formula: CIB formula [CIB 1986], derived by Pettersson [1973] is one of the most widely used time equivalent formula for evaluating fire resistance and establishes equivalency based on the fuel load (amount of combustible materials present) and ventilation parameters of the compartment. According to this formula, the equivalent time of design fire exposure to a standard fire exposure as per ISO 834 [1974] test is expressed as:

$$t_e = k_c w e_f \qquad (2.1)$$

where

t_e = time equivalency in minutes,

e_f = fuel load (MJ/m^2 floor area),

k_c = parameter to account for different compartment linings,

w_f = ventilation factor (m$^{-0.25}$),

$$= \frac{A_f}{\sqrt{A_v A_t \sqrt{H_v}}} \qquad (2.2)$$

A_f = floor area of the compartment (m^2),

A_v = total area of the openings in the walls (m^2),

A_t = total area of the internal bounding surfaces of the compartment (m^2) and

H_v = height of the windows (m).

CIB formula is valid only for compartments with vertical openings in walls and is not valid for compartments having horizontal openings in the roof [Buchanan 2002].

2.4.5.2 Law formula: Another expression for calculating the time equivalency was developed by Law[1971] based on a series of tests conducted on small scale and larger-scale compartments. The time equivalent is given by:

$$t_e = \frac{A_f e_f}{\Delta H_c \sqrt{A_v(A_t - A_v)}}$$ (2.3)

where

t_e = time equivalency in minutes, and

ΔH_c = calorific value of the fuel (MJ /kg).

Similar to CIB formula, Law's formula is valid only for compartments with vertical openings in the walls and is not applicable for rooms with horizontal openings in the roof. In general, time equivalent predicted by Law formula is slightly higher than that time equivalent predicted by CIB formula [Buchanan 2002].

2.4.5.3 Eurocode formula: Eurocode [1994] provides an empirical formula for calculating the time equivalency and is given by:

$$t_e = k_b w e_f$$ (2.4)

where

t_e = time equivalency in minutes,

k_b = parameter to account for compartment linings,

w = ventilation factor,

$$= \left(\frac{6.0}{H_r}\right)^{0.3}\left[0.62 + \frac{90(0.4 - \alpha_v)^4}{1 + b_v \alpha_h}\right] > 0.5$$ (2.5)

31

$$\alpha_v = A_v/A_f, \qquad\qquad 0.025 \leq \alpha_v \leq 0.25 \qquad\qquad (2.6)$$

$$\alpha_h = A_h/A_f, \qquad\qquad \alpha_v \leq 0.2 \qquad\qquad (2.7)$$

$$b_v = 12.5(1 + 10\,\alpha_v - \alpha_v{}^2), \qquad\qquad (2.8)$$

H_r = ceiling height (m) and

A_h = area of horizontal openings in roof (m^2).

Eurocode formula is similar to CIB formula, however, the compartment lining parameter

(k_c) is replaced by k_b and the ventilation factor (w) is also altered to take into account the

effect of horizontal opening that might be present in the roof.

Values for the compartment lining factors k_c and k_b for thermal conductivity (k), specific

heat (c_p) and density (ρ) are shown in Table 2.3. The value of b is defined as follows

$$b = \sqrt{Thermal\ Inertia} = \sqrt{k\rho c_p} \qquad\qquad (2.9)$$

where

k = thermal conductivity,

ρ = density and

c_p = specific heat

Unlike CIB formula, time equivalency predicted by Eurocode formula is independent of

the height of opening, but depends on the height of compartment ceiling. Both CIB and

Eurocode formulae give identical results for small compartments with tall windows, but

the Eurocode formula gives lower fire severities for large compartments having tall

ceilings and low window heights [Buchanan 2002].

32

2.5 Comparison of various time equivalent methods

Though the above empirical formulae are useful in computing equivalency, the results from these formulae are not consistent and the time equivalent computed by these formulae shows a significant variation even for similar fire exposure. Further, these formulae are mainly derived for protected steel members and may not be fully applicable for RC members.

To illustrate the variation in time equivalency predicted by various methods and empirical formulae, the above formulae was applied for evaluating the equivalent fire resistance of an RC beam. The RC beam used in the case study is a simply supported beam of 6 m span length and is made of concrete with a compressive strength of 30 MPa and reinforced with steel rebars having yield strength of 400 MPa. This beam is subjected to a representative design fire shown in Figure 2.9 and the time equivalency is calculated based on equal area method and empirical formulae discussed above. CIB formula gives a time equivalent of 174 minutes whereas Law and Eurocode formulae predict a time equivalent to be 132 and 155 minutes respectively. Time equivalent predicted by equal area method is about 232 minutes. It can be clearly seen that there is a wide variation in time equivalent predicted by equal area method and empirical formulae. This can be attributed to the fact that the above empirical formulae have been derived based on the maximum temperature in protected steel members and may not be fully applicable to RC members. Detailed computation of time equivalency by equal area method and formulae is illustrated in Appendix A and the results are summarized in Table 2.4.

2.6 Summary

The response of RC beams under fire conditions is different from that of room temperature due to deterioration in strength and stiffness of the beam with temperatures. The fire response depends on various parameters such as fire scenario, loading condition and failure criterion. Most of the previous experimental and analytical studies on RC beams were conducted under standard fire exposure and the fire resistance analysis was carried out using sectional analysis procedure. The current provisions in codes and standards base the fire resistance on sectional dimensions and concrete cover thickness without any consideration to fire exposure, load and concrete strength.

The use of time equivalent approach provides an attractive proposition for evaluating equivalent fire resistance under design fire scenarios. However, most of the existing time equivalent methods are derived for protected steel members and may not be applicable for RC beams. Thus there is a clear need for a time equivalent approach for evaluating fire resistance of RC beam under design fire scenarios.

Tables

Table 2.1 - ACI minimum width and cover thickness requirements for achieving fire resistance in RC beams [ACI 216.1 2007]

Restraint condition	Beam width (mm)	Cover for corresponding fire-resistance rating, mm				
		1 hour	1-1/2 hour	2 hours	3 hours	4 hours
Restrained	125	20	20	20	25	30
	175	20	20	20	20	20
	≥ 250	20	20	20	20	20
Unrestrained	125	20	25	30	Not permitted	Not permitted
	175	20	20	20	45	75
	≥ 250	20	20	20	25	45

Table 2.2 - Eurocode 2 specifications for fire resistance rating of simply supported RC beams [Eurocode 2 2004]

Beam dimensions (mm)/ Fire resistance (min)		30	60	90	120	180	240
Possible combinations of beam width and axis distance (mm)	Beam width	80	120	150	200	240	280
	Axis distance	25	40	55	65	80	90
	Beam width	120	160	200	240	300	350
	Axis distance	20	35	45	60	70	80
	Beam width	160	200	300	300	400	500
	Axis distance	15	30	40	55	65	75
	Beam width	200	300	400	500	600	700
	Axis distance	15	25	35	50	60	70

Table 2.3 - Values of k_b and k_c for computing time equivalency using CIB and Eurocode empirical formulae

Formula	Compartment lining parameter	$b = \sqrt{k\rho c_p}$			General
		High (>2500)	Medium (720-2500)	Low (<720)	
CIB	k_c	0.05	0.07	0.09	0.10
Eurocode	k_b	0.04	0.055	0.07	0.07

35

Table 2.4 - Time equivalent (in minutes) of an RC beam as obtained from existing methods

CIB formula	Law formula	Eurocode formula	Equal area method
174	132	155	232

Figures
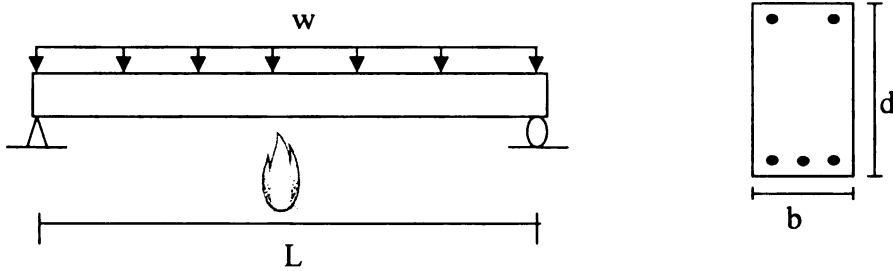
(a) Elevation and cross section of Simply Supported Beam
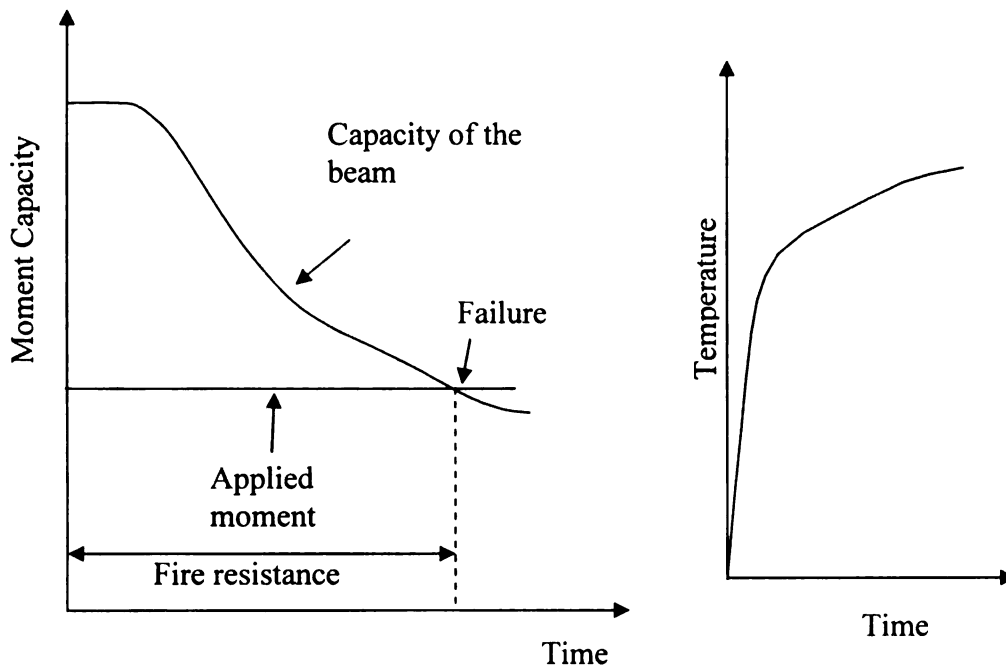
(b) Variation of capacity of beam with fire exposure time

(c) Time-temperature curve for a standard fire exposure

Figure 2.1 - Variation of strength capacity of a typical RC beam under fire conditions

37

Beams 1 to 5

Beam 6
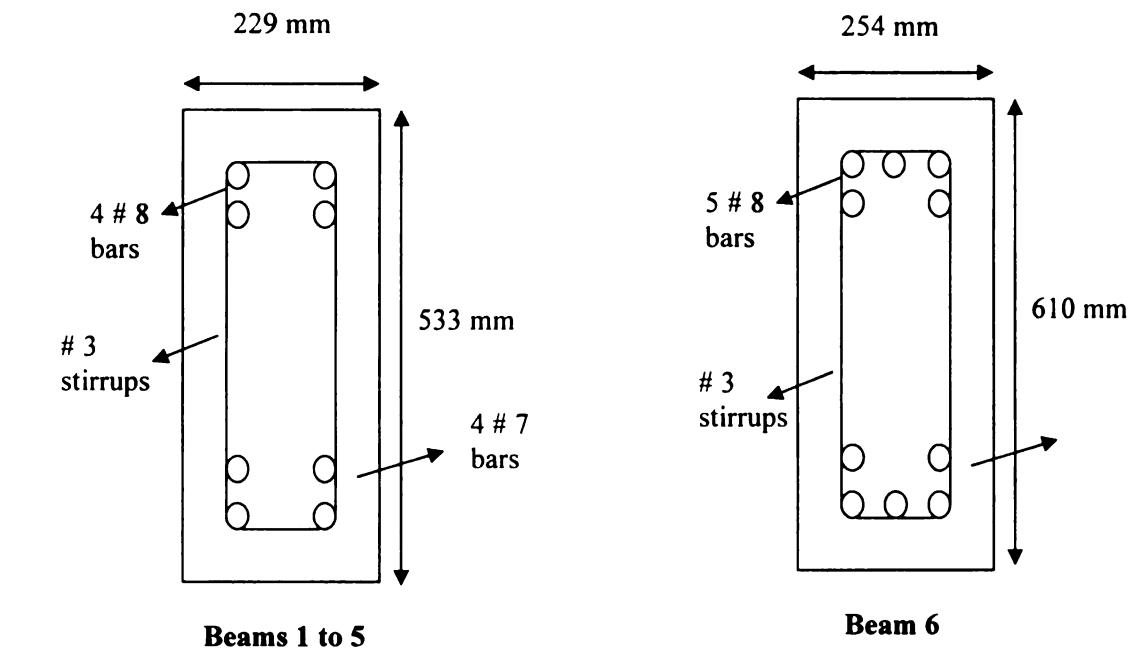
(a) Cross-sectional details
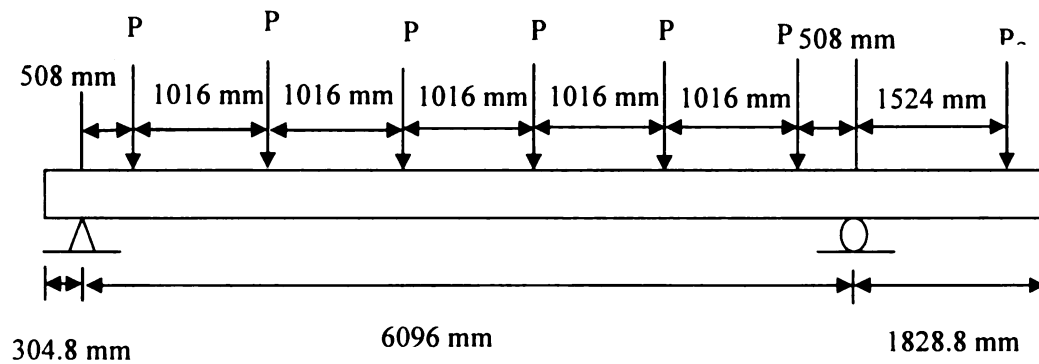
(b) Elevation

Figure 2.2 - Layout of beams tested by Lin and Ellingwood [1987]

38

38 mm

2 φ 13 mm

3 φ 19 mm

38 mm

254 mm

406 mm

f'_c = 58.2 MPa

f_y = 420 MPa

φ 6 mm
stirrups

(a) Cross Section

50 kN   50 kN

1.4 m   1.4 m

3.96 m

(b) Elevation
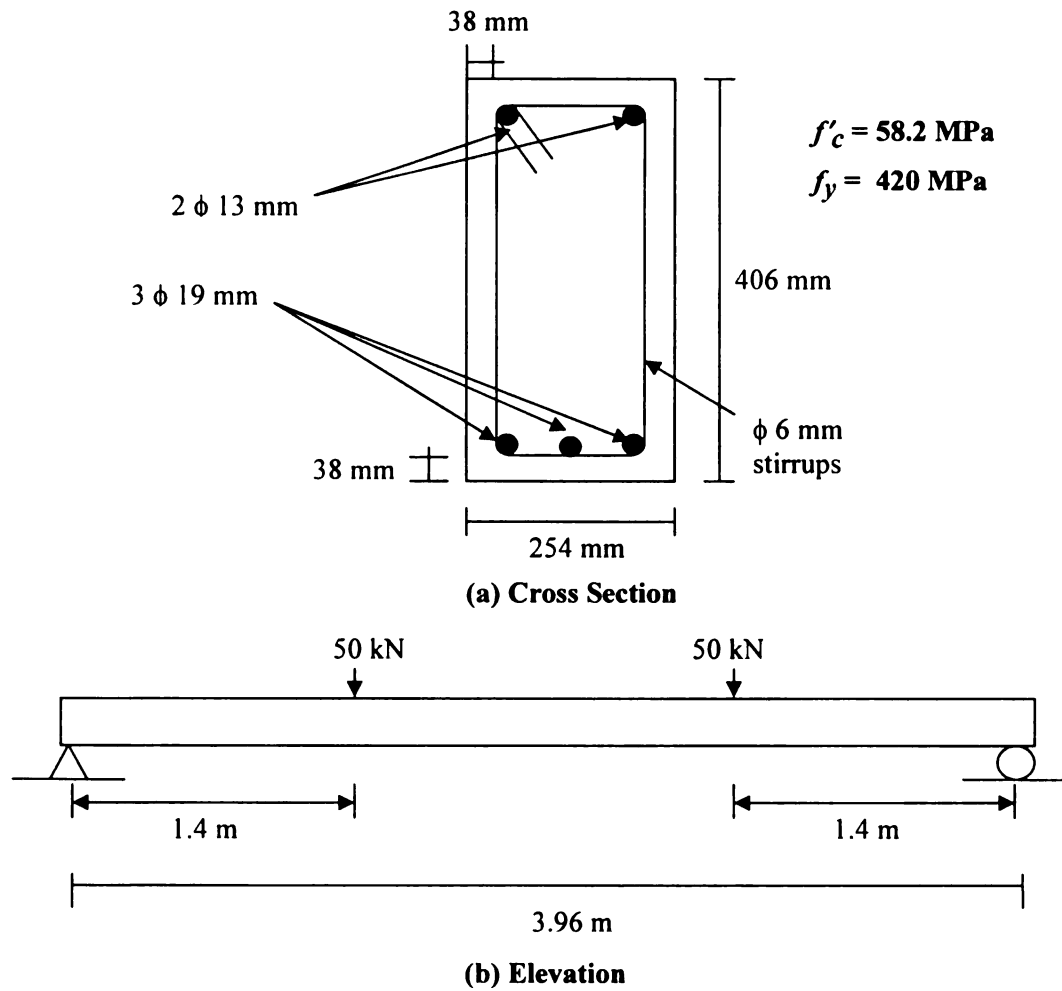
Figure 2.3 - Typical layout of beam tested by Dwaikat [2009]

40 mm

2 φ 14 mm

3 φ 20 mm

40 mm

500 mm

300 mm

$f'_c = 30$ MPa

$f_y = 400$ MPa

φ 10 mm stirrups

(a) Cross Section

20 kN/m

6 m

(b) Elevation
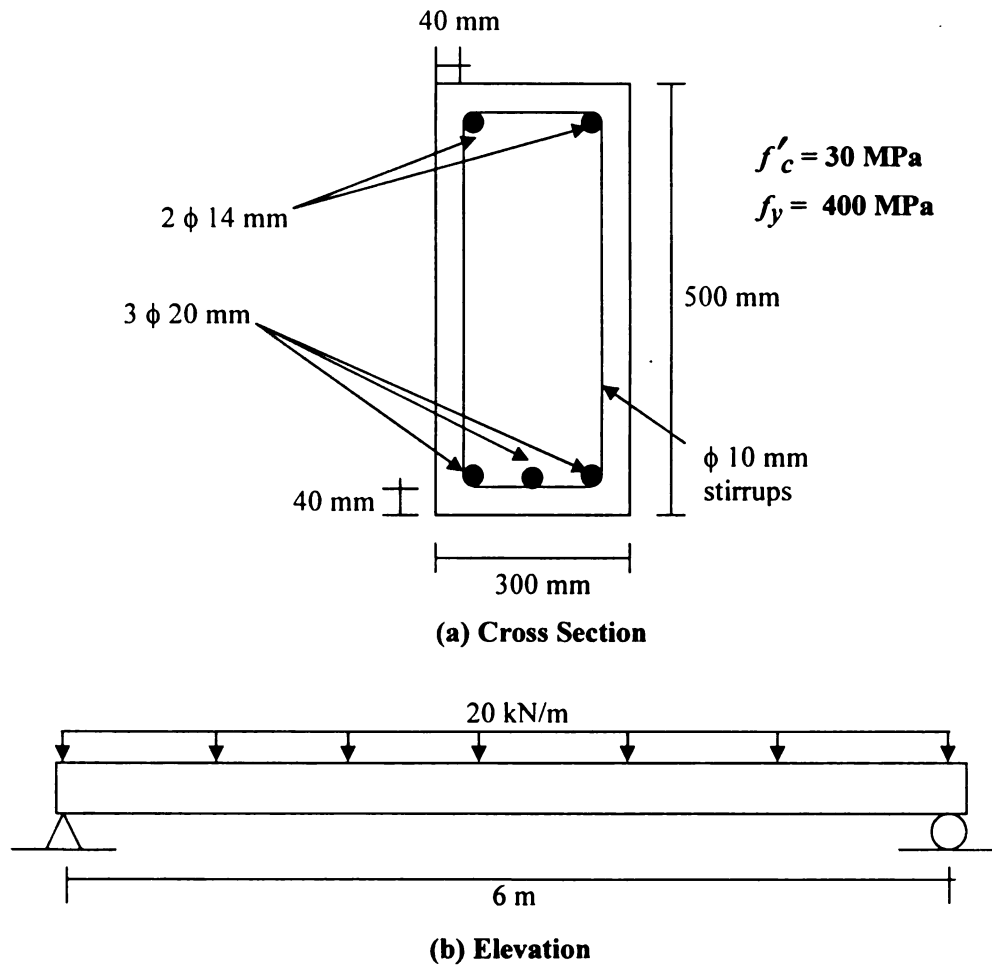
Figure 2.4 - Layout of RC beams used by Kodur and Dwaikat[2008b] in parametric studies
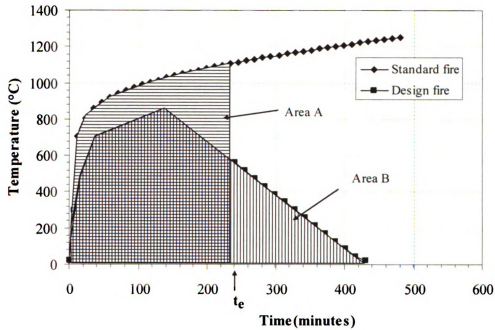
Figure 2.5 - Illustration of equivalent fire severity calculation using equal area method
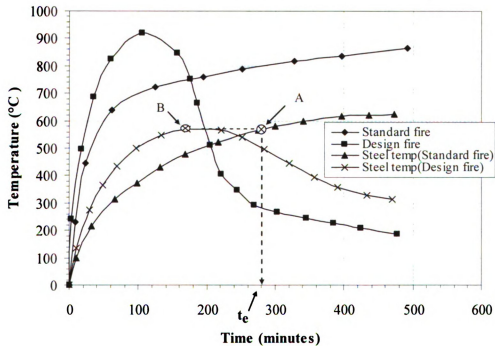
Figure 2.6 - Illustration of equivalent fire severity computation using maximum temperature method
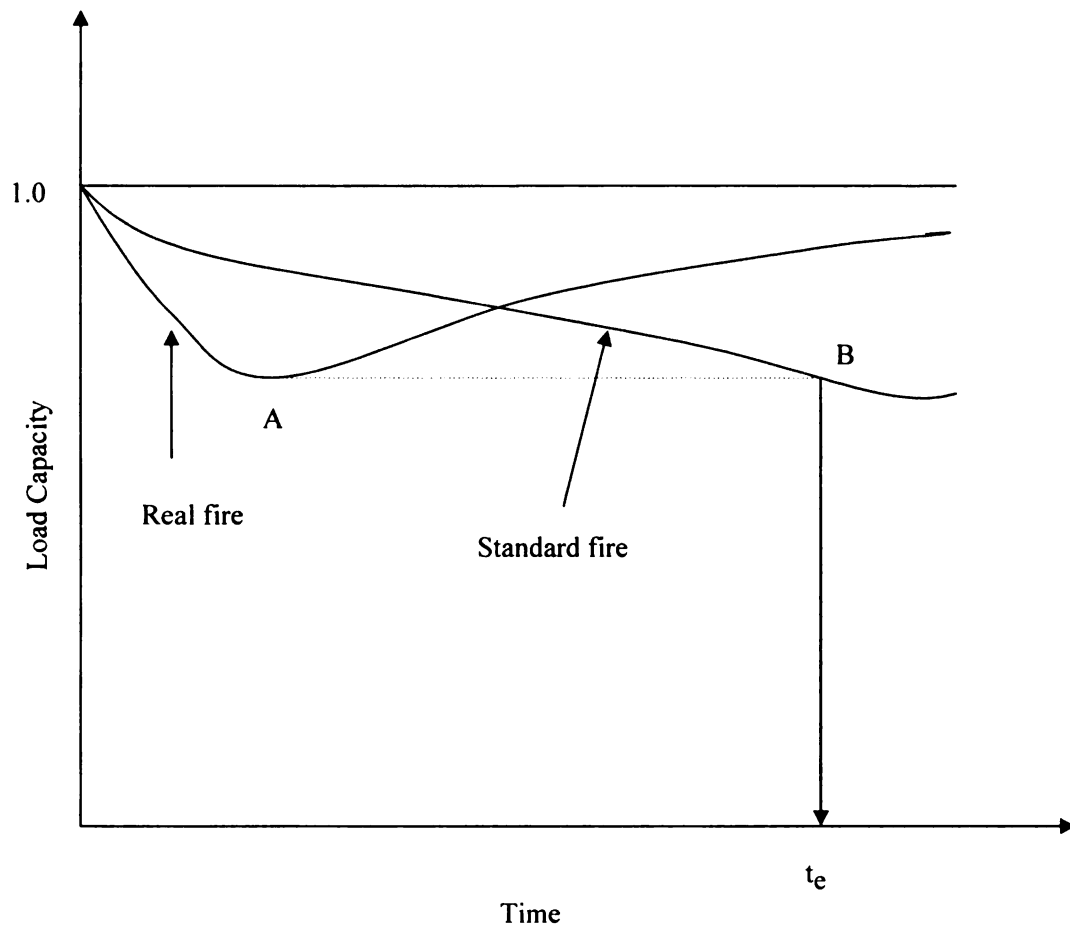
Figure 2.7 - Illustration of equivalent fire severity calculation using minimum load capacity method
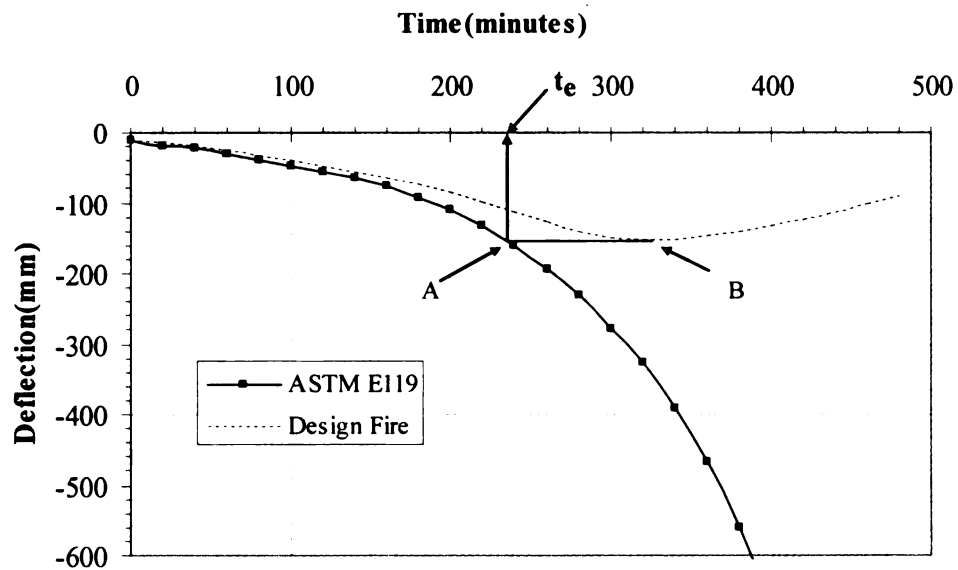
Figure 2.8 - Illustration of equivalent fire severity calculation using maximum deflection method
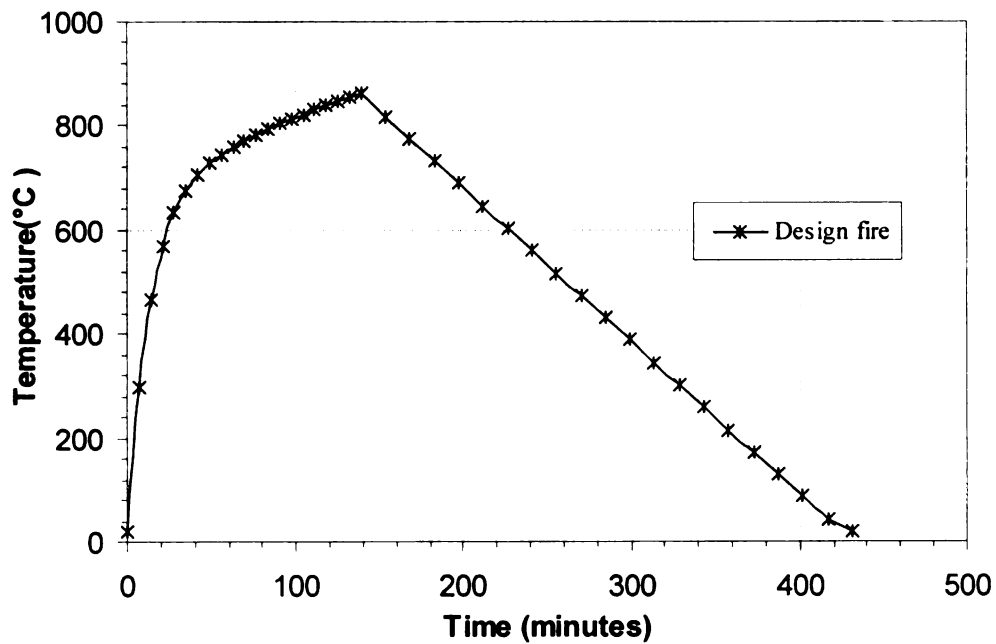
Figure 2.9 - Representative design fire scenario used in comparison of various time equivalent methods

CHAPTER 3

3. NUMERICAL MODEL

3.1 General

Fire resistance of RC beams can be evaluated by conducting detailed analysis using microscopic finite element models. In this approach an RC beam is discretized into a two or three dimensional mesh, and the fire performance is evaluated by undertaking coupled or uncoupled thermal and structural analysis at various time increments. This analysis is quiet complex and generally requires significant amount of computational time and effort.

In lieu of microscopic finite element models, a macroscopic finite element analysis can be applied to evaluate fire resistance, wherein a RC beam is divided into a number of segments along the span length. For each segment, moment-curvature (M- κ) relations are generated at various time steps. These M- κ relationships are utilized to trace the response of the beam at different time steps till failure occurs. Strain components such as creep and

transient strain, high temperature material properties, geometric, material nonlinearity and material softening can be accounted for in this analysis. The results obtained from such analysis (models) are easy to interpret and can be used in practical design situations. This type of macroscopic models has been developed for evaluating fire resistance of RC beams with rectangular cross section. In the current study the approach is extended for predicting fire response of RC beams with T, I and inverted T sections.

3.2 Macroscopic finite element model

In the macroscopic finite method, the structural member (beam or column) is divided into a number of segments along its length, and the mid-section of each segment is assumed to represent the behavior of the whole segment. The cross section of the segment is further divided into elements forming a two-dimensional mesh. The fire resistance analysis is carried out at various time steps, until failure occurs in a beam. At each time step, the analysis is carried out by

- Evaluating fire temperature resulting from fire exposure,

- Conducting heat transfer analysis in each segment to predict cross sectional temperature,

- Performing strength and deflection analysis by:

  o Generating moment-curvature (M-κ) relationships in various segments,

  o Conduct nonlinear structural analysis to compute strength and deflections.

The fire temperature is evaluated for a given fire scenario, i.e., standard or design, which is generally represented by temperature-time relations. Then, heat transfer analysis is performed by applying the finite element approach and temperature distribution across

45

the mid-section of each segment is developed. Figure 3.1 shows layout of a typical RC beam and it's idealization for analysis. The beam is idealized as a set of segments along its span (Figure 3.1(c)). The mid-section of each segment is further discretized into elements as shown in Figure 3.1(d).

The computed cross-sectional temperature distribution is utilized to undertake strength analysis of various segments of the beam. As part of this strength analysis moment-curvature relationships are generated for various segments. These relationships are generated as a function of time for each segment, based on the high temperature properties of constituent materials. Thus material nonlinearity is accounted for in the analysis. Strain components namely thermal, mechanical and creep strains are included in generation of M-κ relationships for both concrete and reinforcing steel. Additionally, transient strain for concrete is also accounted for in computing total strain. The model accounts for geometrical nonlinearity, material nonlinearity and material softening. The generated moment-curvature relationships are used to undertake a nonlinear structural analysis to predict the fire response of the RC beam. Typical moment-curvature relationships of an RC beam, generated by the model are shown in Figure 3.2. It can be seen from figure 3.2 that the moment capacity of the beam decreases with fire exposure time. This can be attributed to reduction in material strength and stiffness as a result of increased temperatures in concrete and steel. In addition, the ultimate curvature (curvature at collapse) increases with time of fire exposure. This is due to deterioration of stiffness as well as the increase in creep strain which becomes significant prior to failure. The model is capable of estimating fire resistance of beams exposed to any given fire time temperature curve. The computer model also generates temperatures, stresses,

strains, moments and deflections at each time step. These output parameters are used to check the failure of the beam. At every time step, each beam segment is checked against four pre-determined sets of failure criteria, which include prescriptive thermal criteria, and performance-based strength and deflection considerations. The analysis terminates when failure of the beam occurs under any specified limiting criteria. The four sets of failure criteria that can be applied to define failure of an RC beam are:

1) When the temperature in steel rebars (tension reinforcement) exceeds the critical temperature which is 593 °C for reinforcing steel.

2) When the beam is unable to resist the applied load.

3) When the maximum deflection in the beam exceeds $L/20$ at any fire exposure time, where L is span length.

4) When the rate of deflection exceeds the limit given by the following expression:

$$\frac{L^2}{9000d} \text{ (mm/min)}$$

where: L = span length of the beam (mm), and d = effective depth of the beam (mm).

The above discussed model is capable of predicting the fire performance of beam with rectangular cross section only. However, in practice T and I cross section beams are often used in buildings and bridge applications. To cater for wide range of design situations, the macroscopic finite element model has been extended to cover T, I and inverted T shaped cross-sections.

3.3 Extension of macroscopic finite element model for T/I beams

In the extended model, the analysis starts by dividing the beam into longitudinal segments and each segment cross-section is further discretized into a number of elements. Then sectional analysis is carried out at various cross sections along the length of the beam. The sectional response generated at different cross-sections is used to predict the fire response of RC member. A flow chart showing the numerical procedure for tracing the fire behavior of RC beams is shown in Figure 3.3 and the detailed description of the procedure associated with the analysis is presented in the following sections.

3.3.1 Fire temperatures

The fire temperatures are calculated from the specified time-temperature relationships for a given type of fire exposure i.e., standard or design. The time-temperature relationship for ASTM E119a [2008] standard fire exposure is approximated by the following equation:

$$T = 750(1 - \exp(-3.79553\sqrt{t_h})) + 170.41\sqrt{t_h} + T_o \qquad (3.1)$$

where

t_h = time (hours),

T_o = initial temperature (°C) and

T = fire temperature (°C)

The temperatures for design fire exposure are calculated based on parametric fire time-temperature equations given in Eurocode1 [1994] or SFPE [2004]. These equations can be used to predict the temperature of design fires for any combination of fuel load,

48

ventilation openings and lining materials. According to Eurocode1 specifications the approximate time-temperature relationship for the burning period of fire is given as:

$$T = 1325(1 - 0.324e^{-0.2t*} - 0.204e^{-1.7t*} - 0.472e^{-19t*}) + T_o \qquad (3.2)$$

where

T_o = initial temperature (°C),

T = fire temperature (°C), and

$t*$ = fictitious time (hours) = Γt

t = time (hours), and

$$\Gamma = \frac{\left(F_v/F_{ref}\right)^2}{\left(b/b_{ref}\right)^2}$$

F_v = ventilation factor (m$^{0.5}$) = $A_v\sqrt{H_v}/A_t$,

F_{ref} = 0.04,

A_v = area of window opening (m^2),

H_v = height of window opening (m),

A_t = total internal surface area of room (m^2),

$b = \sqrt{k\rho c_p}$ (Ws$^{0.5}$/m^{2}K),

$k\rho c_p$ = thermal inertia,

k = thermal conductivity (W/mK),

ρ = density (kg/m^3),

c_p = specific heat (J/kgK), and

b_{ref} = reference value of thermal inertia = 1900.

During the decay phase of design fire, the fire temperatures are computed using the modified decay rate specified by Feasey and Buchanan [2000] and is given as follows:

$$\frac{dT}{dt} = \left(\frac{dT}{dt}\right)_{ref} \frac{\sqrt{F_v/0.04}}{\sqrt{b/1900}}$$ (3.3)

Eurocode1 gives a reference decay rate $\left(\dfrac{dT}{dt}\right)_{ref}$ of 625°C per hour for fire with duration of burning less than half an hour and 250°C per hour for fires with over two hours of burning period.

3.3.2 Thermal analysis

For the thermal analysis, the beam is divided into a number of segments along its length and the mid-section of each segment is assumed to represent the behavior of the whole segment. The mid-section is further divided into elements forming a two-dimensional mesh. Temperature distribution in this mid-section is computed using finite element method based heat transfer analysis. Steel reinforcement is not specifically considered in the thermal analysis because it does not significantly influence the temperature distribution in the beam cross section [Lie and Irwin 1993]. The beam is assumed to be exposed to fire from three sides and maintained at ambient conditions on the fourth side as shown in Figure 3.4(d).

The governing heat transfer equation used for analysis of beam cross-section is given as:

$$k\nabla^2 T + Q = \rho c \frac{\partial T}{\partial t} \qquad (3.4)$$

where

k = *thermal conductivity,*

ρc = heat capacity,

T = temperature,

t = time, and

Q = heat source.

The mechanism for heat transfer on the boundary of RC beam is by convection and radiation. Therefore, the heat flow per unit area (heat flux) to RC beam can be written as:

$$q_{con} = h_{con}(T - T_f) \quad \text{and} \qquad (3.5)$$

$$q_{rad} = \sigma\varepsilon(T^4 - T_f^{\,4})$$

$$= \sigma\varepsilon(T^2 + T_f^{\,2})(T + T_f)(T - T_f) = h_{rad}(T - T_f)$$

(3.6)

where

q_{con} = convective heat flux(W/m^2),

q_{rad} = radiative heat flux(W/m^2),

h_{con} = convective heat transfer coefficient(W/m^2°K),

h_{rad} = radiative heat transfer coefficient(W/m^2°K),

σ = Stefan- Boltzmann constant = 5.67×10^{-8}(W/m^2°K^4),

ε = emissivity,

T = temperature on the boundary of RC beam, and

T_f = temperature of the fire.

The total heat flux transferred to the exposed surface of an RC beam through its boundaries is:

$$q = q_{con} + q_{rad} = (h_{con} + h_{rad})(T - T_f) \qquad (3.7)$$

Therefore, the governing heat transfer equation on the boundary of RC beam is obtained by balancing the energy transfer across the boundary and can be written as:

$$k\left(\frac{\partial T}{\partial y}n_y + \frac{\partial T}{\partial z}n_z\right) = -h(T - T_f) \qquad (3.8)$$

where

   n_y and n_z = components of the vector normal to the boundary in the plane of the

   cross section, and

   $h = h_{con} + h_{rad}.$

As the cross-section of the beam is exposed to fire from three sides and ambient conditions prevail on the fourth side, two types of boundary conditions exists, namely:

- Fire exposed boundaries where the heat flux is governed by the following equation:

$$k\left(\frac{\partial T}{\partial y}ny + \frac{\partial T}{\partial z}nz\right) = -hf(T - Tf) \qquad (3.9)$$

- Unexposed boundary where the heat flux equation is given by:

$$k\left(\frac{\partial T}{\partial y}ny + \frac{\partial T}{\partial z}nz\right) = -hc(T - To) \qquad (3.10)$$

where

h_f = heat transfer coefficient on the fire side,

h_c = heat transfer coefficient on the cold side,

T_f = fire side temperature, and

T_o = cold side temperature.

Eq. (3.4) is solved through Galerkin finite element formulation using four node quadrilateral elements (Q4). In this approach, element stiffness matrix (K_e), mass matrix (M_e), and nodal load vectors (F_e) are formulated as follows:

$$K_e = \int_A \left[k \frac{\partial N}{\partial x} \frac{\partial N^T}{\partial x} + k \frac{\partial N}{\partial y} \frac{\partial N^T}{\partial y} \right] dA + \int_\Gamma N\alpha N^T \, ds \qquad (3.11)$$

$$M_e = \int_A \rho c N N^T \, dA \qquad (3.12)$$

$$F_e = \int_A NQ \, dA + \int_\Gamma N\alpha T_\infty \, ds \qquad (3.13)$$

where

N = vector of shape function,

α = h_c or h_f depending on the boundary Γ,

T_∞ = fire or ambient temperature depending on the boundary Γ, and

s = distance along the boundary.

After computing the elemental matrices, they are assembled into global stiffness and mass matrices and formulated into a system of differential equations as follows:

$$M \dot{T} + KT = F(t) \qquad (3.14)$$

53

where

K = global stiffness matrix,

M = global mass matrix,

F = equivalent nodal heat flux, and

$\dot{T}$ = temperature derivative with respect to time.

Eq. (3.14) is solved using finite difference algorithm of trapezoidal family (θ algorithm) in the time domain. This algorithm computes the temperature distribution at any time step using the information available at previous time step, and can be written as [Williams 1990]:

$$T_{n+1} = T_n + h(\theta \dot{T}_{n+1} + (1-\theta)\dot{T}_n) \tag{3.15}$$

Multiplying both sides of Eq. (3.15) by M and using Eq. (3.14) at the beginning and the end of the time interval (t_n, t_{n+1}), the following equation can be obtained:

$$(M + h\theta K)T_{n+1} = (M - h(1-\theta)K)T_n + h(\theta F_{n+1} + (1-\theta)F_n) \tag{3.16}$$

where

h = time step,

T_n and T_{n+1} = temperature at the beginning and the end of time step,

F_n and F_{n+1} = equivalent nodal heat flux at the beginning and the end of time step, and

θ = a constant between 0 and 1.

Knowing the temperature at ambient conditions (zeroth time step), Eq. (3.16) begins marching in time to give temperatures at the following time step (first time step), and this procedure is repeated for subsequent time steps. At each time step, Eq. (3.16) should be

solved using an iterative process due to nonlinearity of both material properties and boundary conditions. Furthermore, for unconditional stability of the numerical calculations, the value of θ should be more than or equal to 0.5 [Williams 1990].

3.3.3 Strength analysis

3.3.3.1. General

The computation of temperature distribution is followed by strength analysis in which the moment-curvature relationships are generated for each segment represented by the mid-section. The basic assumptions made in the strength analysis are:

- Plane sections remains plane before and after bending.

- Tensile strength of concrete, at elevated temperatures, is taken into account in the model based on the reduction factors given in Eurocode 2 [2004].

- No bond-slip exists between concrete and steel reinforcement.

The strength analysis is carried out in two stages. First, the moment-curvature (M-κ) relationships for each segment are generated. Then the deflection of the beam is computed at each time step using the generated moment-curvature relationships.

Strength calculations are carried out using the same discretized cross-section as for thermal analysis as shown in Figure 3.4(c). It is assumed that temperatures, strains, stresses, deformations in each element are represented by those at the centre of the element. The temperature in each element is computing by taking an average of the temperatures at the nodes of that element. Similar assumption is used for steel reinforcement, where in the values of temperature, stress, strain in each bar is represented by those at the centre of the bar. Temperature at the center of steel reinforcement is

approximated by the temperature in the element at the location of the center of the rebar cross-section (in the concrete).

The total strain in concrete at any time step comprises of four components namely thermal, mechanical (or stress related strain), creep strain, and transient strain. Thus the total strain can be written as:

$$\varepsilon_t = \varepsilon_{th} + \varepsilon_{me} + \varepsilon_{cr} + \varepsilon_{tr} \qquad (3.18)$$

where

ε_t = total strain in concrete element,

ε_{th} = thermal strain in concrete element,

ε_{me} = mechanical strain (or stress related strain) in concrete element,

ε_{cr} = creep strain in concrete element, and

ε_{tr} = transient strain in concrete element.

The thermal strain (ε_{th}) is a function of temperature and can be obtained by knowing the temperature and thermal expansion of type of concrete. In general, the thermal strain can be written as follows:

$$\varepsilon_{th} = \alpha T_c \qquad (3.19)$$

where

α = coefficient of thermal expansion, and

T_c = concrete temperature.

56

The mechanical strain (or stress related strain) (ε_{me}) is a function of both the applied stress and the temperature. It includes the elastic and plastic components of strain resulting from applied stress.

The creep strain (ε_{cr}) is a function of time, temperature and the applied stress level. This creep strain can be computed based on Harmathy's [1993] approach, which can be written as:

$$\varepsilon_{cr} = \beta_1 \frac{\sigma}{f_{c,T}} \sqrt{t} \, e^{d(T-293)}$$

(3.20)

where

$$\beta_1 = 6.28 \times 10^{-6} \, \text{s}^{-0.5},$$

$$d = 2.658 \times 10^{-3} \, \text{K}^{-1},$$

T = concrete temperature (°K) at time t (sec),

$f_{c,T}$ = concrete strength at temperature T, and

σ = stress level in the concrete at the current temperature.

The transient strain (ε_{tr}) is a function of applied stress and the temperature [Anderberg and Thelandersson 1976]. This transient strain occurs only during the first time heating of concrete under load to approximately 600°C, and can be computed using the relationship proposed by Anderberg and Thelandersson [1976]. Accordingly, the transient strain can be written as follows:

$$\Delta\varepsilon_{tr} = k_2 \frac{\sigma}{f_{c,20}} \Delta\varepsilon_{th}$$

(3.21)

where

57

k_2 = a constant ranges between 1.8 and 2.35 (a value of 2 will be used in the

analysis),

$\Delta\varepsilon_{th}$ = change in thermal strain,

$\Delta\varepsilon_{tr}$ = change in transient strain, and

$f_{c,20}$ = strength of concrete at room temperature.

Similar to concrete, the total strain in steel reinforcement at any time step comprises of three components namely thermal, mechanical (or stress related strain) and creep strain. Thus the total strain in steel reinforcement can be written as follows:

$$\varepsilon_{ts} = \varepsilon_{ths} + \varepsilon_{mes} + \varepsilon_{crs} \tag{3.22}$$

where

ε_{ts} = total strain in steel reinforcement,

ε_{ths} = thermal strain in steel reinforcement,

ε_{mes} = mechanical strain in steel reinforcement, and

ε_{crs} = creep strain in steel reinforcement.

The thermal strain can be computed by knowing the values of coefficient of thermal expansion and temperature of the reinforcing steel. Eurocode 3 [1995] provides a linear coefficient of thermal expansion for use in the design equations. According to Eurocode 3, the thermal strain of steel can be approximated as follows:

$$\varepsilon_{ths} = 14 \times 10^{-6} (T - 20) \tag{3.23}$$

where

T = temperature in °C.

The creep strain in steel is computed based on Dorn's theory and the model proposed by Harmathy [1967] with some modifications to account for different values of yield strength of steel. Accordingly, the creep strain in steel can be written as:

$$\varepsilon_{crs} = (3Z\varepsilon_{t0}^2)^{1/3} \theta^{1/3} + Z\theta \qquad (3.24)$$

where

$$Z = \begin{cases} 6.755 \times 10^{19} \left(\dfrac{\sigma}{f_y}\right)^{4.7} & \dfrac{\sigma}{f_y} \leq \dfrac{5}{12} \\ 1.23 \times 10^{16} \left(e^{10.8(\sigma/f_y)}\right) & \dfrac{\sigma}{f_y} > \dfrac{5}{12} \end{cases},$$

$$\theta = \int e^{-\Delta H/RT} dt,$$

$$\frac{\Delta H}{R} = 38900°K,$$

t = time (hours),

$$\varepsilon_{t0} = 0.016 \left(\frac{\sigma}{f_y}\right)^{1.75},$$

σ = stress in the steel, and

f_y = yield strength of steel.

The distribution of strain, stress, and internal forces for the beam cross-section at any fire exposure time is shown in Figure 3.5. At each time step, for an assumed value of curvature of the beam, the total strain in any element of concrete or rebar can be written as:

$$\varepsilon_t = \varepsilon_o + \kappa y \qquad (3.25)$$

where

ε_o = total strain at the geometrical centroid of beam cross-section,

κ = curvature of the beam, and

y = the distance measured from geometrical centroid of beam cross-section.

Thus, the total strain can be computed for a segment at any given fire exposure time using Eqs. (3.18)-(3.25) . At each time step, a value of ε_0 and κ are assumed and the total strain is computed using Eq.(3.25) and an iterative process is applied till equilibrium and compatibility conditions are satisfied. The analysis at each time starts with the converged value of strain (ε_0) at previous time step. The individual strain components like thermal, transient, creep strain for concrete are evaluated using Eqs.(3.19)-(3.21). The thermal, creep strain for reinforcing steel are also evaluated using Eqs. (3.23)- (3.24). Using the value of total strain and individual strain components, the mechanical strain of each element can be computed by subtracting the various strain components from the total strain (using Eqs. (3.18) and (3.22)) as follows:

For concrete,

$$\varepsilon_{me} = \varepsilon_t - \varepsilon_{th} - \varepsilon_{cr} - \varepsilon_{tr} \tag{3.26}$$

For steel,

$$\varepsilon_{mes} = \varepsilon_{ts} - \varepsilon_{ths} - \varepsilon_{crs} \tag{3.27}$$

Having known the value of mechanical strain, the stress in the element can be computed using the material specific stress-strain relationships.

3.3.3.2 Generation of M-κ relationships

The M-κ relationships are generated using the same rectangular network of elements used for thermal analysis (Figure 3.4(c)). The M-κ relationships are established by iterating the central total strain (ε_O) and the curvature (κ). At the beginning of each time step, curvature and central total strain in concrete is assumed. Then, the total strain in concrete and rebar elements are computed from the assumed values of strain and curvature. These strain values are used to compute the stresses in rebars and concrete elements by using the constitutive laws of respective materials. Once the stresses are known, the forces are computed in the concrete elements and rebars as a product of stress and the area of element. The computed force in each element is subsequently used to verify the equilibrium condition (total compressive force to be equal to total tensile force) for the assumed value of curvature and strain. If the equilibrium is not satisfied the curvature is incremented and the iteration process is continued until the computed forces satisfy compatibility, equilibrium and convergence criteria. When these conditions are satisfied the corresponding moment and curvature are computed. Thus at the end of iterative procedure, a point on the moment-curvature curve is obtained.

The value of the central total strain is incremented to generate subsequent points on the moment curvature curve. This process is repeated again for each time step, to compute various points on the moment-curvature curve at that given time step. Thus, various points on the moment-curvature curve are generated at a given time step and also at various time steps.

3.3.3.3 Computation of deflection

The mid-span deflection of the beam at each time step is computed using the generated moment-curvature relationships. For any given time step, the curvatures along the member is integrated twice numerically to estimate the mid-span deflection of the beam using the following equation

$$\delta_{AB} = \int_A^B \theta_{AB}\, dx \qquad (3.28)$$

where, θ_{AB} is the rotation between any two points A and B of the member, which can be calculated as:

$$\theta_{AB} = \int_A^B \varphi_{AB}\, dx \qquad (3.29)$$

where, φ_{AB} is the curvature between any two points A and B of the member.

The step-by-step procedure involved in the numerical integration is illustrated in Figure 3.6. In this approach the beam is divided into segments and using the moment-curvature relationship for each segment, the curvature for the corresponding moment distribution at any location along the length of the beam is determined. The curvature is then integrated twice along the member using Eq.(3.28) and Eq.(3.29), to compute the mid-span deflection of the beam.

Therefore this model can be used to compute the temperatures, moment and curvature values, deflection of the beam for any specified duration of fire exposure. These output parameters namely temperature, strength (capacity) of the beam, deflection can be subsequently used to evaluate the failure of the beam using the failure conditions described earlier.

62

3.4 Computer program

3.4.1 General

The numerical procedure described in Section 3.2 through Section 3.3 requires significant computational effort at each time step as iterative process is needed to satisfy equilibrium, compatibility and convergence criterion. To facilitate the vast amount of calculations, the numerical procedure has been incorporated into a computer program written in FORTRAN language.

3.4.2 Beam discretization

The given RC beam is divided into several longitudinal segments and the central cross section at mid-length of the segment is assumed to represent the behavior of each segment. The cross section is further divided into elements. The number of longitudinal segments and the number of elements in the cross section along with the dimensions of the elements in each direction has to be specified in the input file. The program allows the user to specify uniform and non-uniform grid size in the cross sectional mesh generation.

3.4.3 Material properties

Two sets of material properties for both concrete and the reinforcing steel as specified in Eurocode 2 [2004] and ASCE Manual [Lie 1992], and reproduced in Appendix B, are incorporated into the computer program. Appropriate formulas for both thermal and mechanical properties of concrete and steel as a function of temperature are built into the program. The user has the option of selecting the desired material properties and should

specify the choice of relevant material model codes in the input file. Further, the user can select either siliceous aggregate concrete or carbonate aggregate concrete. The user has to specify the modulus of elasticity of steel and concrete, the 28-day compressive strength of concrete, yield strength of steel, initial moisture content of concrete, material model code and type of aggregate in the concrete as input in the input file.

3.4.4 Program input

The input for the program is divided into two categories namely input for thermal analysis and input for structural analysis. Input for the thermal analysis includes the number of horizontal and vertical division of the beam cross-section, grid size along vertical and horizontal directions, aggregate type, moisture content in concrete, number of reinforcing bars, location of center of rebars in the cross section, type of fire exposure, and duration of fire exposure time.

Input for structural analysis requires the user to specify the material properties (concrete and reinforcing steel), structural geometry, boundary conditions, loading conditions and the number of longitudinal segments required along the span of the beam.

3.4.5 Program output

Similar to the input for the model, the output from the model comprises of thermal output file and structural output file. At each time increment, the thermal analysis generates the temperature at each node. This temperature distribution serves as one of the input for structural analysis for generating moment curvature curves. Additionally, the deflection of the beam and rate of deflection of the beam is written in the output file at each time step.

3.5 Validation

In order to validate the numerical model, presented above, predictions from the model are compared with data generated from tests and finite element analysis for three RC beams namely B1, B2 and B3. Beam B1 is a RC beam with a rectangular cross-section tested by Dwaikat [2009], while beams B2 and B3 are typical RC beams with T, I cross-sections respectively. Since there is no test data available on the fire performance of RC beams with T and I cross-section, results obtained for beams B2 and B3 from the model are compared with the results obtained from SAFIR [Franssen et al. 2004].

3.5.1 Rectangular beam B1

Predictions from the computer program are compared with test data generated on a rectangular RC beam. Beam B1, shown in Figure 3.7, was tested by Dwaikat [2009] under standard fire conditions. The simply supported rectangular beam of 254 mm x 406 mm had a span length of 3960 mm. The beam was made of carbonate aggregate concrete with a 28 day compressive strength of 52.2 MPa. The beam was reinforced with 2Ø13 mm bars as compressive reinforcement and 3Ø19 mm bars as tension reinforcement. Shear reinforcement consisted of Ø6 mm stirrups spaces at 150 mm over the length of the beam and bent at 135° into the concrete core. The main reinforcing bars (tensile and compressive rebars) and shear reinforcement were having yield strength of 420 MPa and 280 MPa respectively. The beam had a clear concrete cover thickness of 38 mm to the surface of stirrups. The beam was tested after 16 months of casting. The measured compressive strength of concrete on the day of testing was 58.2 MPa. The beam was tested by applying two point loads of 50 kN/m at a distance of 1.4 m from the end

supports and this represented an equivalent load ratio of 54%. Load ratio is defined as the ratio of applied load to the capacity at room temperature. Details about the beam properties are presented in Table 3.1, and the sketch of the beam is shown in Figure 3.7. This beam was analyzed using the macroscopic finite element model by simulating ASTM E119 fire conditions. Figure 3.8 shows the comparison of measured and predicted temperatures for rebar and two concrete locations (at a depth of 200 mm and 300 mm from the surface of beam). It can be seen that there is a good agreement between the measured and predicted temperatures. Initially there is a temperature plateau at about 100°C for rebar and concrete temperatures and this can be attributed to the evaporation of water in concrete which consumes significant amount of energy [Dwaikat 2009]. The figure also shows that the measured temperatures in concrete decrease with increasing depth from the bottom surface. This is mainly due to low thermal conductivity and high thermal capacity of concrete which reduces heat penetration into the inner layers of concrete. The slight discrepancies in the measured and predicted temperatures can be attributed to variation in the high temperature material properties reported. The same discrepancies between the temperatures measured from the test and those predicted by the model were observed by Dwaikat[2009].

The measured and predicted mid-span deflection is presented in Figure 3.9. It can be seen from the figure that the mid-span deflection predicted by the current model vary significantly from those measured in the test. This difference can be attributed to variability in the high temperature properties of concrete and rebar specified in codes. High temperature material properties specified in codes are developed using data obtained from limited material property tests. However these material properties show

66

considerable variations due to differences in test methods, conditions and procedures used during test. Kodur et. al. [2008] reviewed high-temperature concrete constitutive relationships and illustrated the considerable variations in the high-temperature properties of concrete.

Based on the results obtained from the model, fire resistance of the beam is evaluated according to the four failure criterion discussed in Section 3.2 and is presented in Table 3.2 along with the measured fire resistance from test. According to deflection and the rate of deflection failure criteria, the model predicts a fire resistance value of 125 and 120 minutes respectively, which is lower than that predicted for temperature and strength criteria. The fire resistance predicted by the model using strength criterion is 145 minutes which is lower than that in the test (180 minutes). The difference can be attributed to variation in the high temperature material properties used in the analysis, as discussed above.

3.5.2 T beam B2

The second beam (B2) selected to validate the proposed model is of T cross-section. Since there is no tested beams in literature a representative T beam was designed as per ACI 318 specifications [2008]. Layout of this beam is shown in Figure 3.10 and design details are presented in Appendix C.

The simply supported beam has a span length of 7.62 m (25 feet). The flange is of 1905 mm wide x 152 mm deep while the web is of 317 mm wide x 550 mm deep. The beam is assumed to be made up of siliceous aggregate concrete having a compressive strength of 28 MPa. The beam has 3Ø20 mm bars as tensile reinforcement and 2Ø20 mm bars as

compressive reinforcement. The shear reinforcement consists of #4 (Ø12.7mm) stirrups spaced at 317.5 mm. The yield strength of the reinforcing steel is assumed to be equal to 413 MPa. A concrete cover thickness of 61 mm (clear cover of 38 mm) was provided to the center of tension reinforcement from both sides while that to the center of compression reinforcement was 61 mm from the top of beam. The room temperature capacity of the beam was calculated according to ACI 318 specification [2008] and was found to be 260 kN-m. The beam was analyzed using the current model and SAFIR computer program. The applied load on the beam was 18.1 kN/m, which corresponds to a load ratio of 50%. For the analysis of the beam, the thermal and mechanical properties specified in Eurocode 2 and incorporated into SAFIR were used. The analysis was carried out by exposing the beam from three sides (bottom and two sides) to ASTM E119 standard fire exposure while the top surface was maintained at ambient conditions. Layout of the beam along with the cross-sectional details is shown in Figure 3.10 and the parameters used in the analysis are shown in Table 3.3.

Figure 3.11 and Figure 3.12 shows the variation of temperatures at bottom central rebar and at three different concrete locations respectively as predicted by the current model and SAFIR. The three different concrete locations used to compare the temperatures correspond to quarter depth (175.5 mm), half depth (351 mm) and three quarter depth (526.5 mm) of the beam B2. It can be seen from the figures, that the temperatures predicted by the current model and SAFIR are in good agreement with each other in the entire range of fire exposure time. The temperature at various locations in concrete, as well as the rebar, increases with fire exposure time. Also from Figure 3.12, it can be observed that the temperatures decrease with increasing distance from fire exposed

bottom surface of the beam. This can be attributed to low thermal conductivity and high thermal capacity of concrete that slows down heat transfer to the inner layers of concrete. Variation of mid-span deflection predicted by the current model and SAFIR are plotted in Figure 3.13 as a function of fire exposure time. The predicted fire resistance from the current macroscopic finite element model is slightly higher and also there is large increase in deflection of the beam prior to failure. The higher fire resistance predicted by the proposed model can be attributed to the fact that the current model accounts for softening of the concrete and SAFIR does not take this into consideration [Franssen et al. 2004, Kodur and Dwaikat 2008]. Rapid increase in deflection prior to failure can be attributed to yielding of steel and creep strains which become significant during the later stages of fire exposure. SAFIR does not explicitly account for high temperature creep in concrete and steel.

Results from current model was used to evaluate the fire resistance for beam B2 using the four sets of failure criterion and is compared with fire resistance obtained from SAFIR analysis in Table 3.2. The current model predicts a fire resistance of 205 minutes (based on strength criteria) while SAFIR predicts a value of 187 minutes. The difference can be attributed to the fact that the current model accounts for softening effect in concrete (descending branch of stress-strain curve). However SAFIR does not take this into consideration. Therefore failure in the current model corresponds to concrete attaining ultimate strain while in SAFIR it corresponds to concrete reaching peak strain. A representative stress-strain curve for concrete is shown in Figure 3.14 along with the ultimate strain and the strain corresponding to peak stress.

As can be seen from Table 3.2, the fire resistances predicted by rebar temperature and strength failure criterion is higher than that of deflection and rate of deflection failure criterion. Though actual failure in a beam occurs when the strength limit state is reached, deflection and rate of deflection may be important in various applications in order to maintain the integrity of the structure. Therefore under some fire exposures, deflection and rate of deflection failure criterion might govern the failure of RC beam and hence governs its fire resistance. It should be noted that the current provisions in ASTM E119 does not specify deflection and rate of deflection limit states.

3.5.3 I beam B3

The third beam selected for validation is of I cross-section (B3) and the beam was designed as per ACI 318 specifications [2008]. The room temperature capacity of this I beam, calculated according to ACI 318 specification [2008], is 260 kN-m, which is same as that of a T beam B2. Design details of beam B3 are presented in Appendix C.

Sectional dimensions and other characteristics of the beam are illustrated in Figure 3.15. The beam is assumed to have same material properties as that of Beam B2 and analyzed using the current model and SAFIR. The analysis is carried out with an applied load of 18.1 kN/m by exposing it to ASTM E119 standard fire exposure from three sides. Layout of the beam along with the cross-sectional details is shown in Figure 3.15 and the various parameters used for the analysis are presented in Table 3.4.

Variation of temperatures at bottom central rebar and at three different concrete locations as predicted by the current model and SAFIR are presented in Figures 3.16 and 3.17 respectively. It can be seen from Figs 3.16 and 3.17 that the temperatures predicted by the

70

proposed model and SAFIR are in good agreement with each other in the entire range of fire exposure time. As expected, the predicted temperatures increase with increasing depth from the top surface of the beam due to low thermal conductivity and high thermal capacity of concrete.

Figure 3.18 compares mid-span deflections of beam B3 as predicted by the proposed model and SAFIR. It can be seen in the figure that the mid-span deflection increases continuously throughout the fire exposure time. This can be attributed to the gradual decrease in stiffness of the beam with increasing fire temperature. It can also be seen from the figure that the deflections predicted by the proposed model and SAFIR are in close agreement with each other in the entire duration of fire exposure. The current model predicts a large increase in deflection prior to failure as compared to SAFIR. This is on the expected lines as the current model accounts for high temperature creep and transient strains which play a significant role during the later stages of fire exposure.

Table 3.2 shows the fire resistance values for beam B3 computed using the four sets of failure criterion discussed in Section 3.2 along with the fire resistance obtained from SAFIR analysis. The current model predicts a fire resistance of 270 minutes (based on strength criteria) while SAFIR analysis gives a values of 230 minutes. The difference in the fire resistance values can be attributed to the fact that the current model uses ultimate strain to predict the failure in the beam whereas SAFIR predicts failure of the beam at a strain corresponding to maximum stress, as explained in previous section. It can be seen from Table 3.2 that the fire resistance values predicted by deflection and rate of deflection are lower than those predicted by rebar temperature and strength failure criterion. Thus the deflection or rate of deflection failure criteria might play a crucial role

71

in some applications where the integrity of the structure has to be maintained and hence govern fire resistance of beams.

3.6 Summary

This Chapter presents the development of a macroscopic finite element based numerical model for tracing the fire response of RC beams with rectangular, T, I or inverted T cross-section. The main steps associated with the numerical procedure namely: calculating fire temperature, thermal analysis, and structural analysis of the beam are described in detail. The high temperature material properties of concrete and steel used in the model are also described in this chapter. The validity of the computer model is established by comparing the predictions from the model with that obtained from test data and other numerical models such as SAFIR. Based on the results obtained in the study, it is concluded that the proposed model is capable of predicting the fire response of RC beams under realistic conditions. The numerical model described here will be used to undertake a set of parametric studies for quantifying the influence of various factors on fire resistance of RC beams.

Tables

Table 3.1 - Summary of properties of Beam B1

Summary of various properties used in the analysis of Beam B1		
Strength	Concrete	$f_c' = 58.2$ MPa
	Steel	$f_y = 420$ MPa
Aggregate type	Carbonate	
Thermal properties	Concrete	ASCE manual
	Steel	ASCE manual
Mechanical properties	Concrete	ASCE manual
	Steel	ASCE manual
Number of longitudinal segments	20	
A_s	3Φ19 mm bars	
A_s'	2Φ13 mm bars	

Table 3.2 - Summary of fire resistance values predicted for the analyzed beams using various failure criterion

Beam	Fire resistance(min)				
	Rebar	Strength	Deflection	Rate of deflection	Test/SAFIR
Rectangular beam (B1)	220	145	125	120	180
T beam (B2)	245	205	195	190	187
I beam (B3)	280	270	260	255	230

Table 3.3 - Summary of various properties used in the analysis of Beam B2

Summary of various properties used in the analysis of Beam B2		
Strength	Concrete	$f_c' = 28$ MPa
	Steel	$f_y = 413$ MPa
Aggregate type	Siliceous	
Thermal properties	Concrete	Eurocode
	Steel	Eurocode
Mechanical properties	Concrete	Eurocode
	Steel	Eurocode
Number of longitudinal segments	20	
A_s	3Φ20 mm bars	
A_s'	2Φ20 mm bars	

Table 3.4 - Summary of various properties used in the analysis of Beam B3

Summary of various properties used in the analysis of Beam B3		
Strength	Concrete	$f_c' = 28$ MPa
	Steel	$f_y = 413$ MPa
Aggregate type	Siliceous	
Thermal properties	Concrete	Eurocode
	Steel	Eurocode
Mechanical properties	Concrete	Eurocode
	Steel	Eurocode
Number of longitudinal segments	20	
A_s	3Φ20 mm bars	
A_s'	2Φ20 mm bars	

Figures

(a) Simply supported beam

(b) Cross section

Rectangular   T

(c) Idealized along span

Rectangular   T

(d) Idealized along cross section (segment)

Figure 3.1 - Layout of typical RC beam and its idealization for analysis
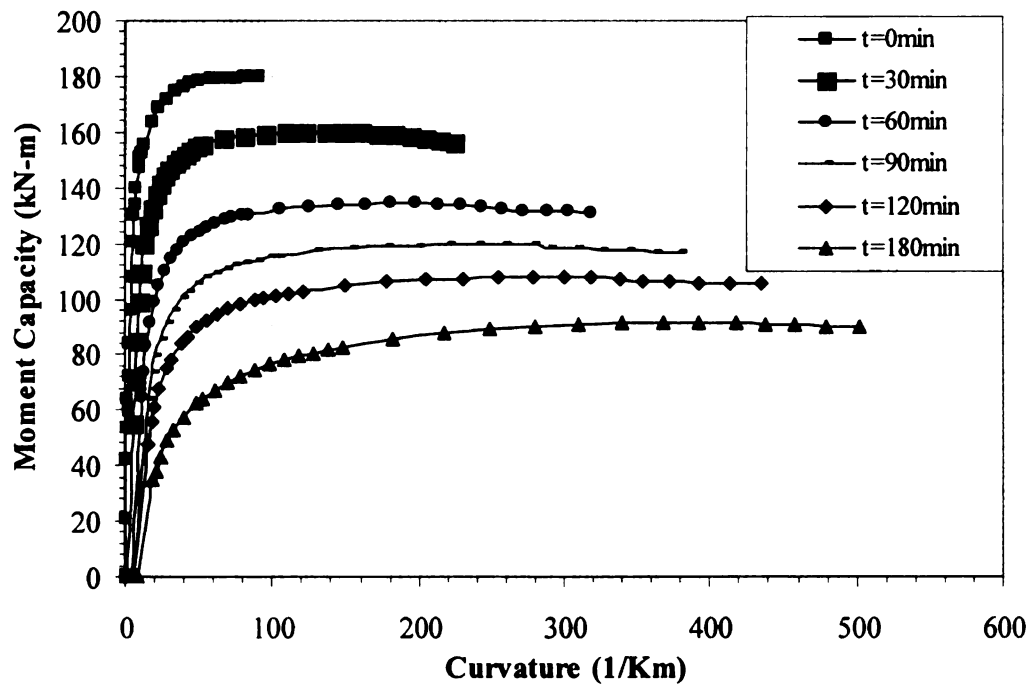
Figure 3.2 – Typical moment-curvature relationships for an RC beam
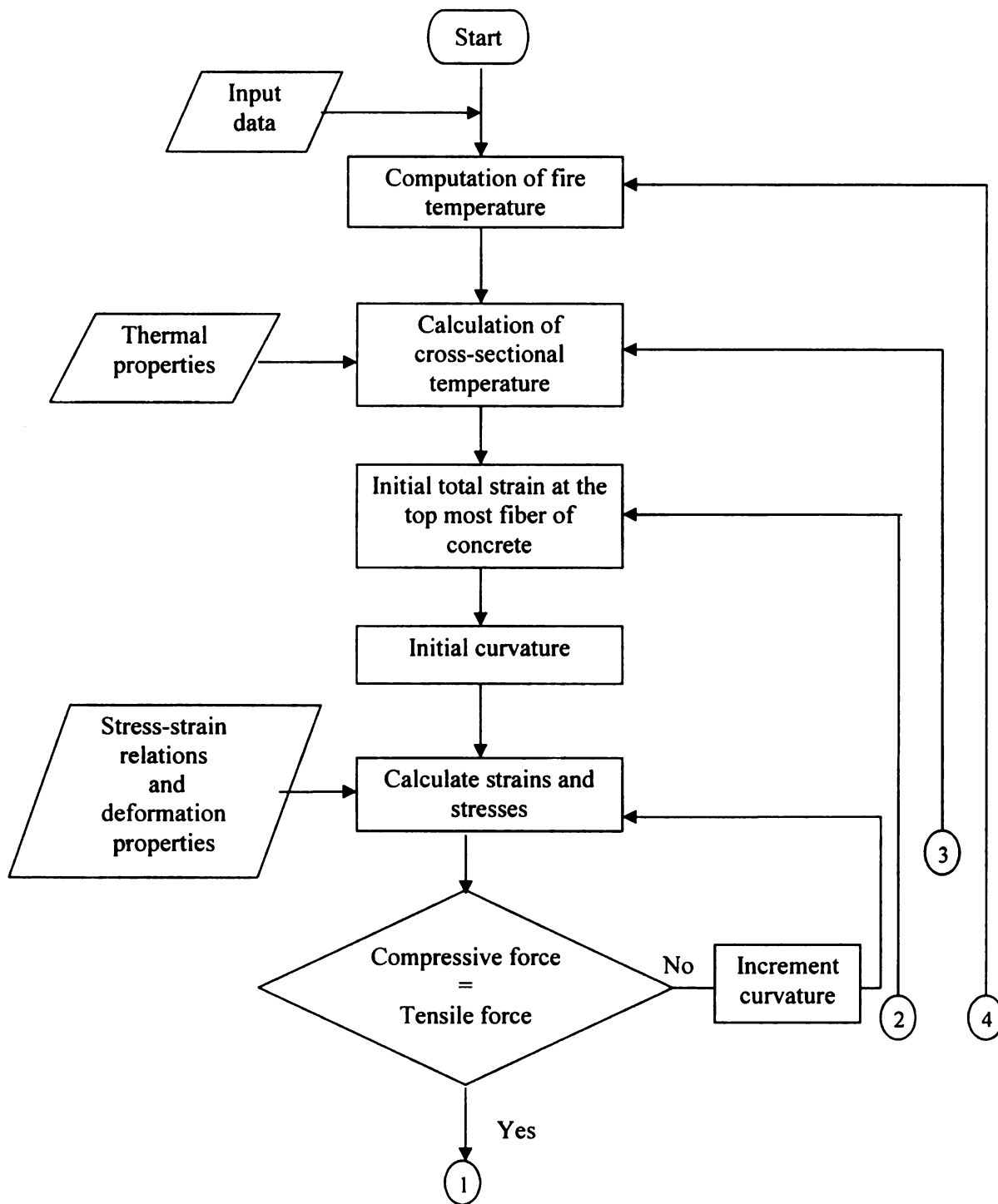
Figure 3.3 – Flow chart showing the numerical procedure associated with analysis of RC beam exposed to fire
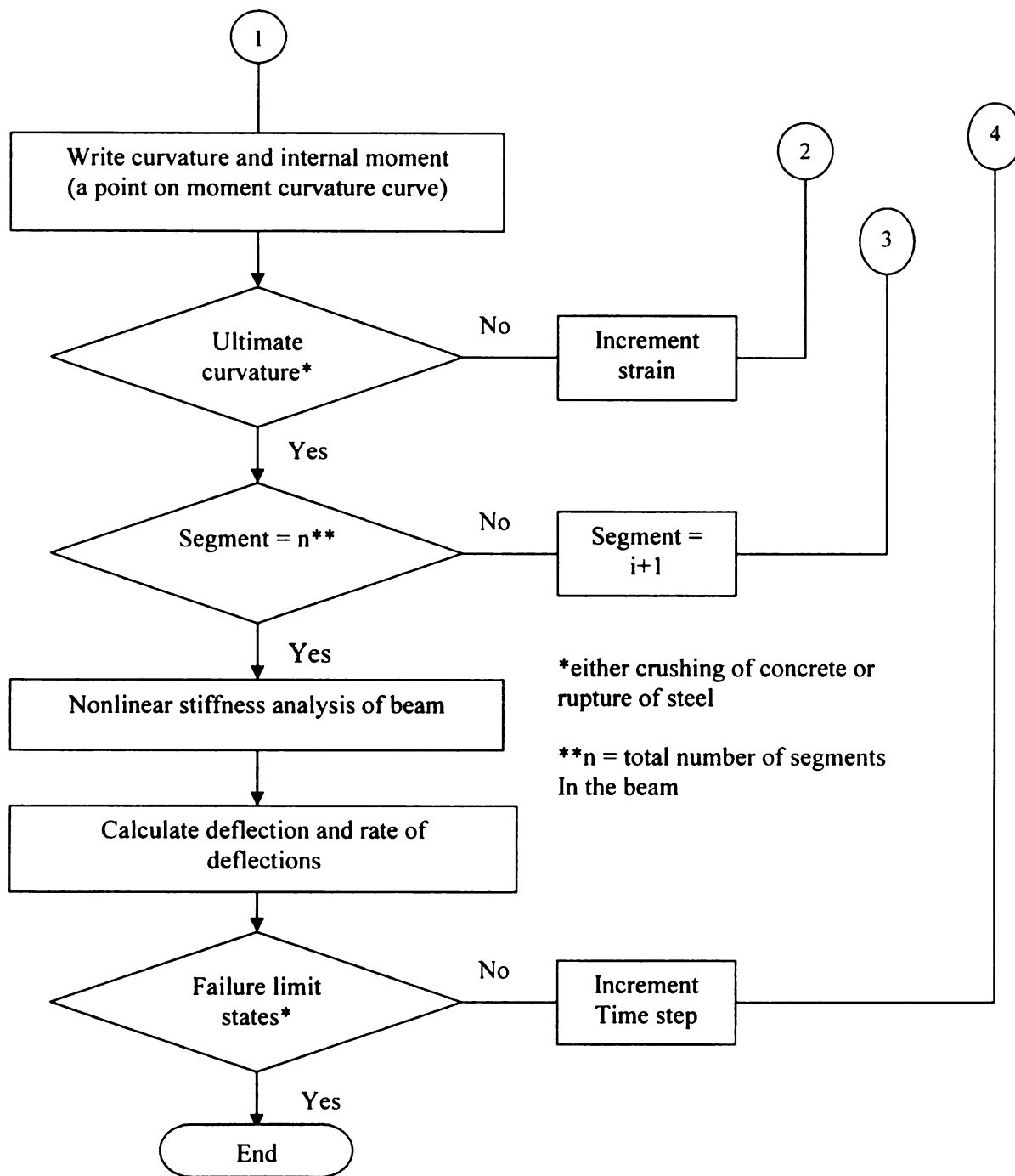
Figure 3.3 (continued) – Flow chart showing the numerical procedure associated with analysis of RC beam exposed to fire

(a) Simply supported T beam

(b) Cross-sectional details   (c) Discretization   (d) Boundary conditions
for
Heat transfer analysis
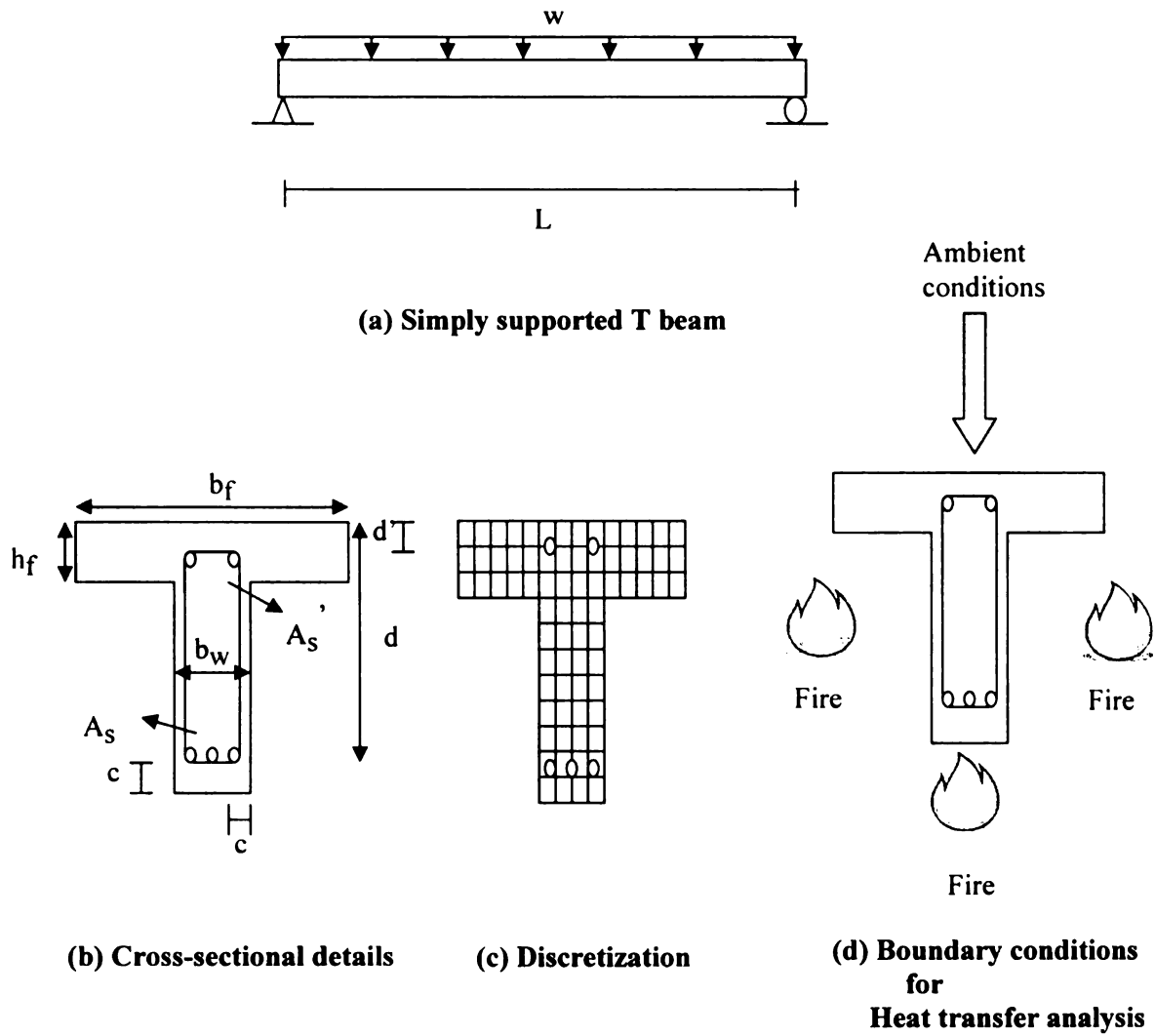
Figure 3.4 – Cross-sectional discretization of T-beam for analysis
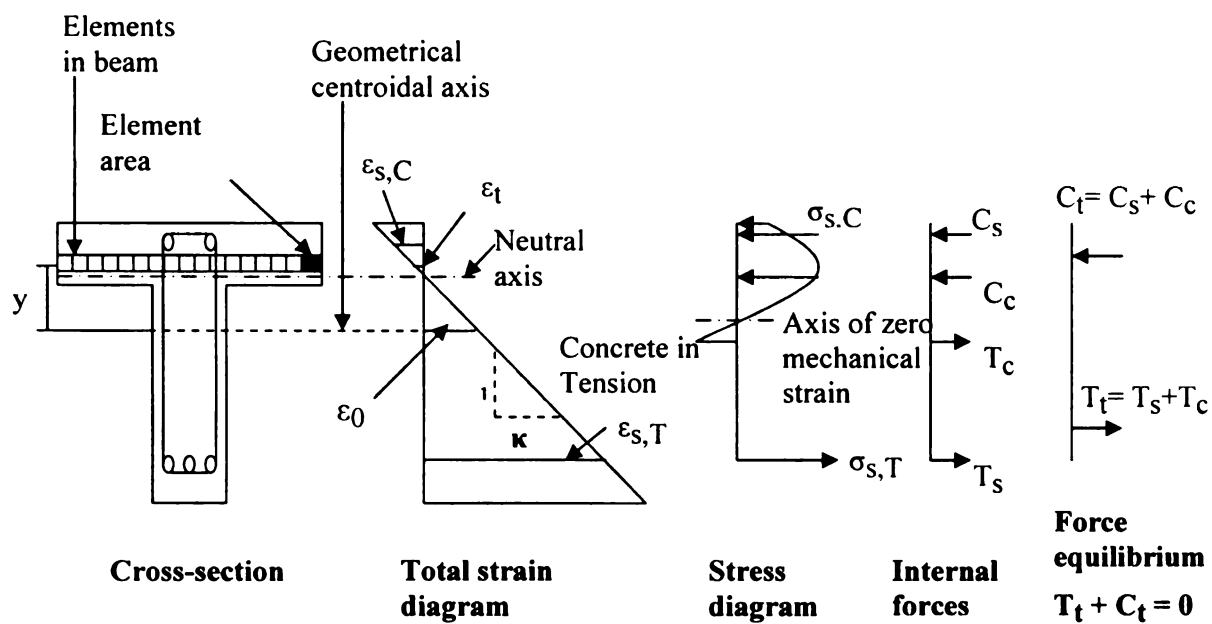
Figure 3.5 – Variation of strain, stress and internal forces in a typical beam cross-section exposed to fire

a) Bending moment diagram

b) Moment-curvature relationship

c) Curvature along the span of the beam

d) Rotation along the span of the beam

e) Deflection along the span of the beam
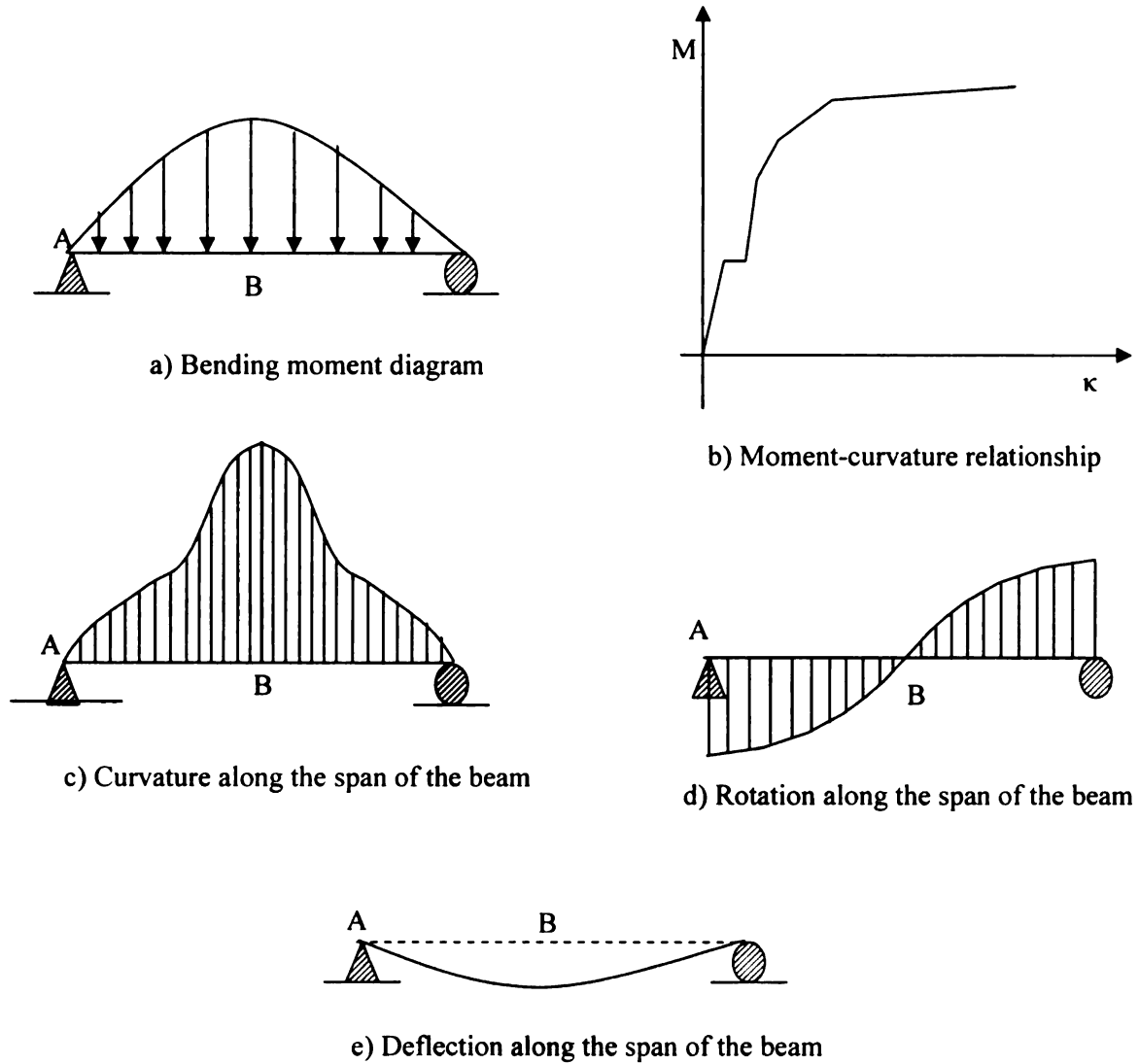
Figure 3.6 – Step-by-step approach for evaluating the mid-span deflection of the beam using M-κ relationship
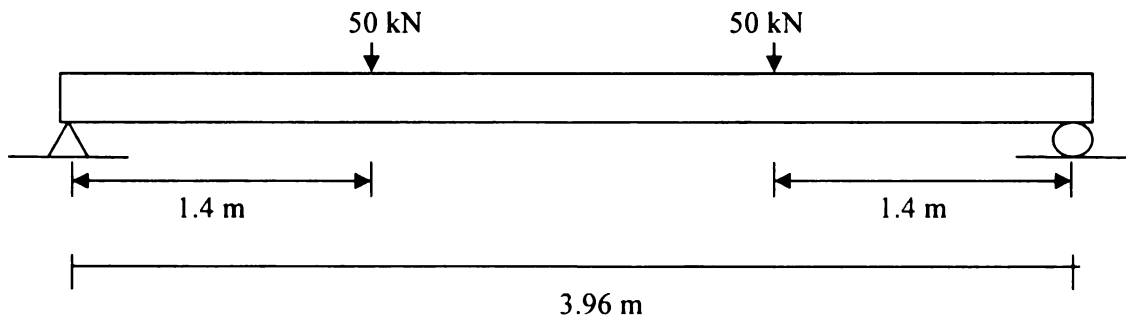
(a) Elevation for Simply Supported Beam
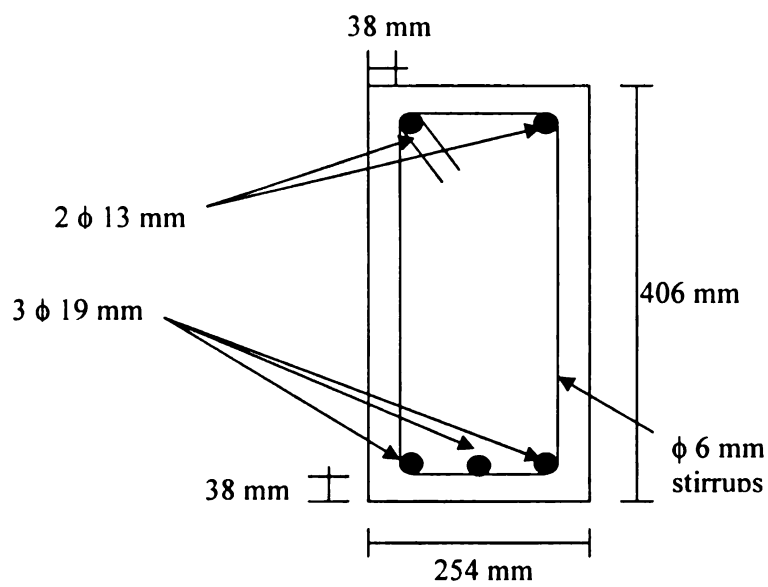
(b) Cross Section

Figure 3.7 – Elevation and cross section of RC beam B1
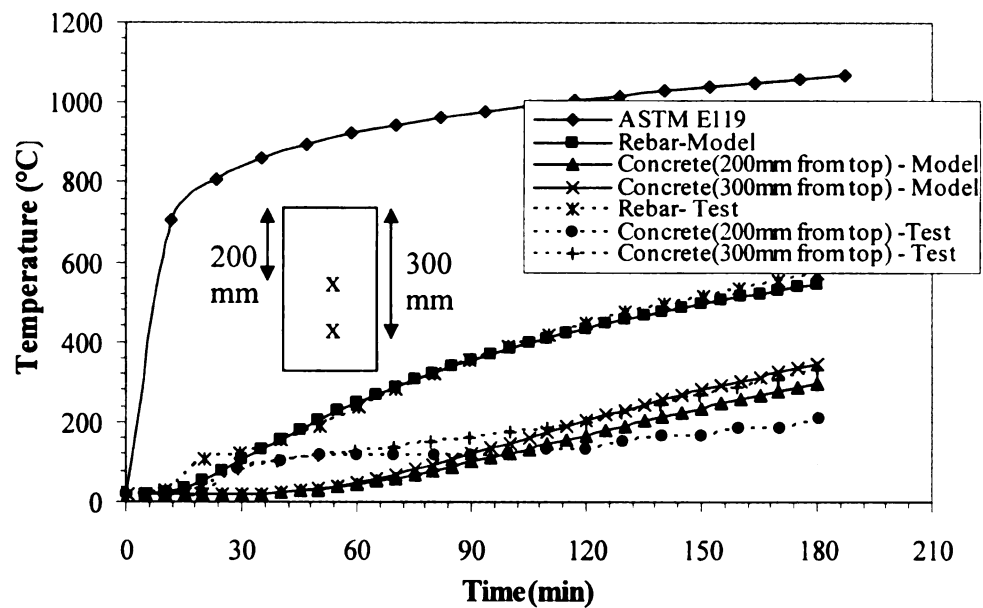
Figure 3.8 – Comparison of measured and predicted average rebar and concrete
temperature as a function of time for beam B1
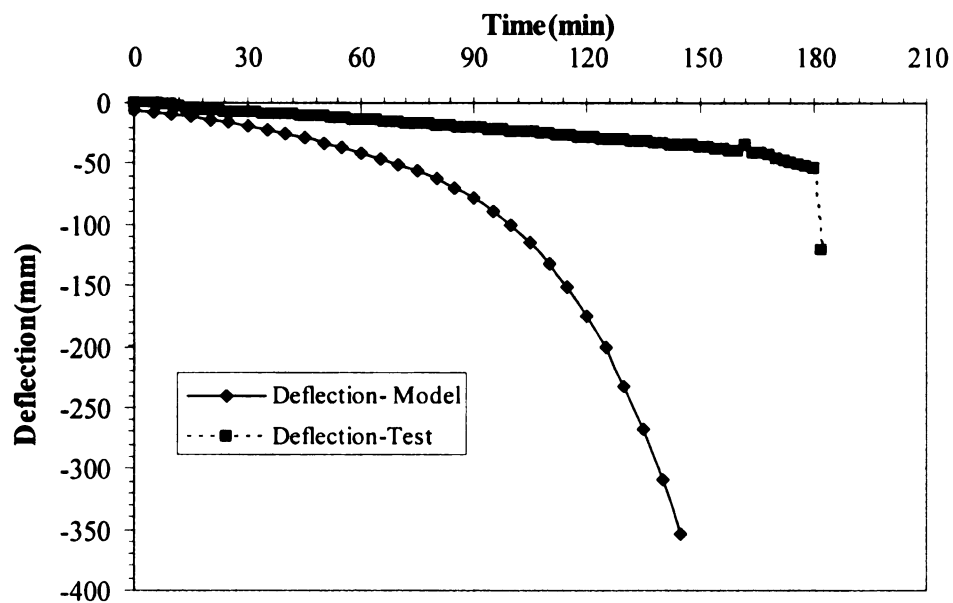
Figure 3.9 – Comparison of measured and predicted mid-span deflection as a function of
time for beam B1

18.1 kN/m

(a) Elevation for Simply Supported T Beam

1905 mm

152 mm

61 mm

2Ø20mm

550 mm

635 mm

3Ø20 mm

61 mm

61 mm

317 mm
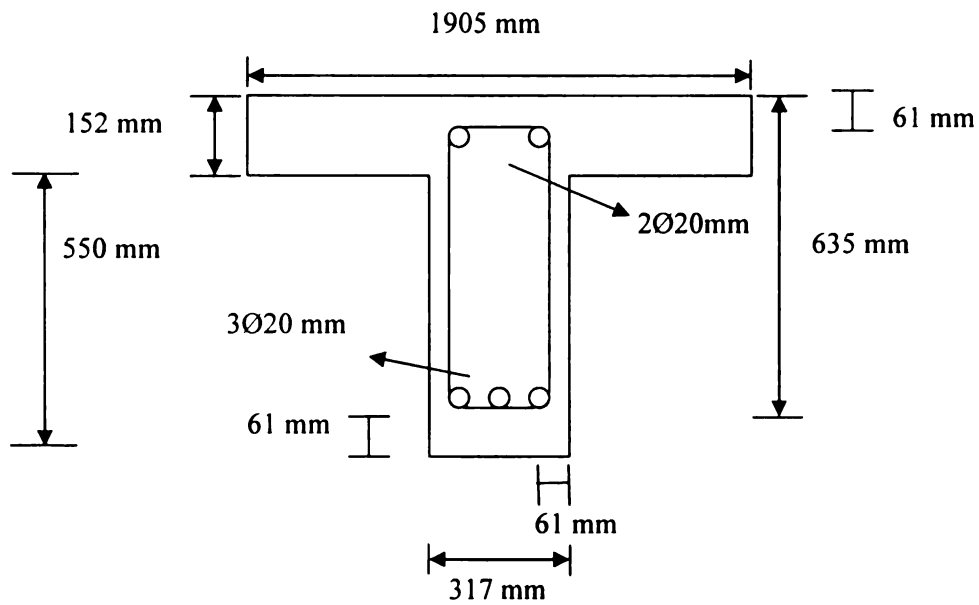
(b) Cross Section

Figure 3.10 – Elevation and cross section of RC Beam B2
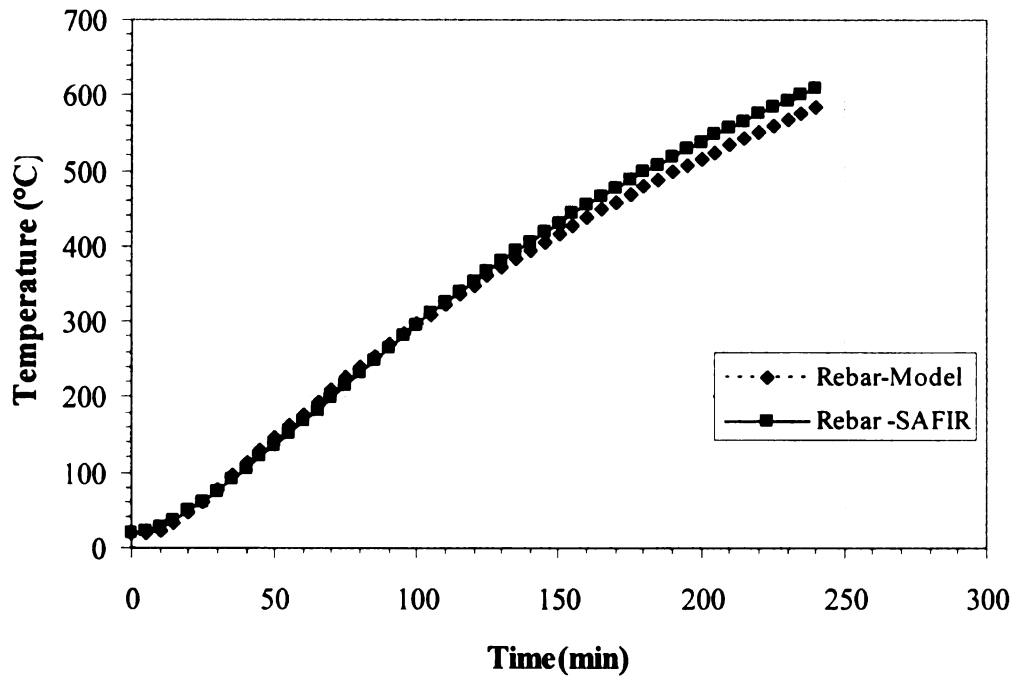
Figure 3.11 – Variation of rebar temperature for Beam B2 as obtained from proposed model and SAFIR
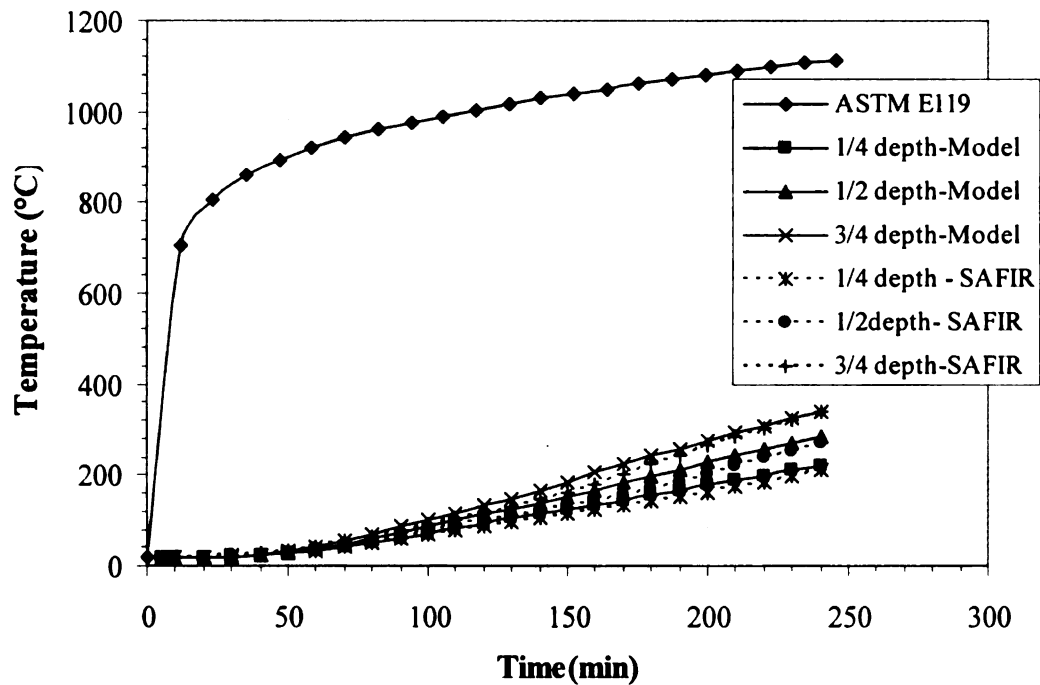
Figure 3.12 – Variation of temperature at three different concrete locations in beam B2 predicted by the proposed model and SAFIR
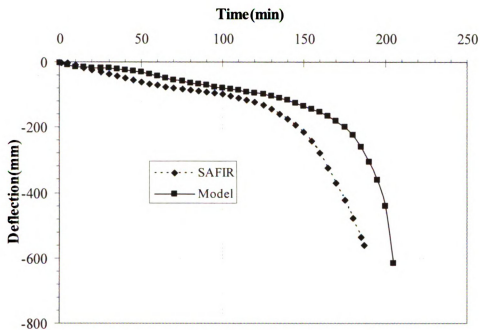
Figure 3.13 – Variation of mid-span deflection for Beam B2 as predicted by the proposed model and SAFIR
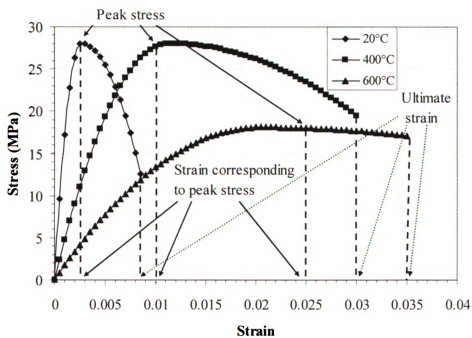
Figure 3.14 – Representative stress-strain curves of concrete with ultimate strain and strain corresponding to peak stress value
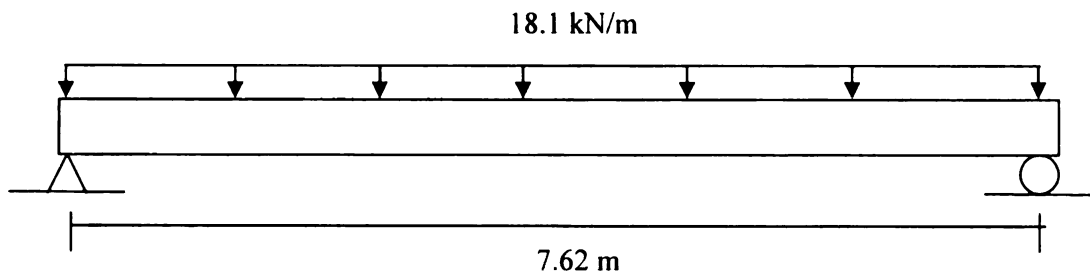
(a) Elevation for Simply Supported Beam
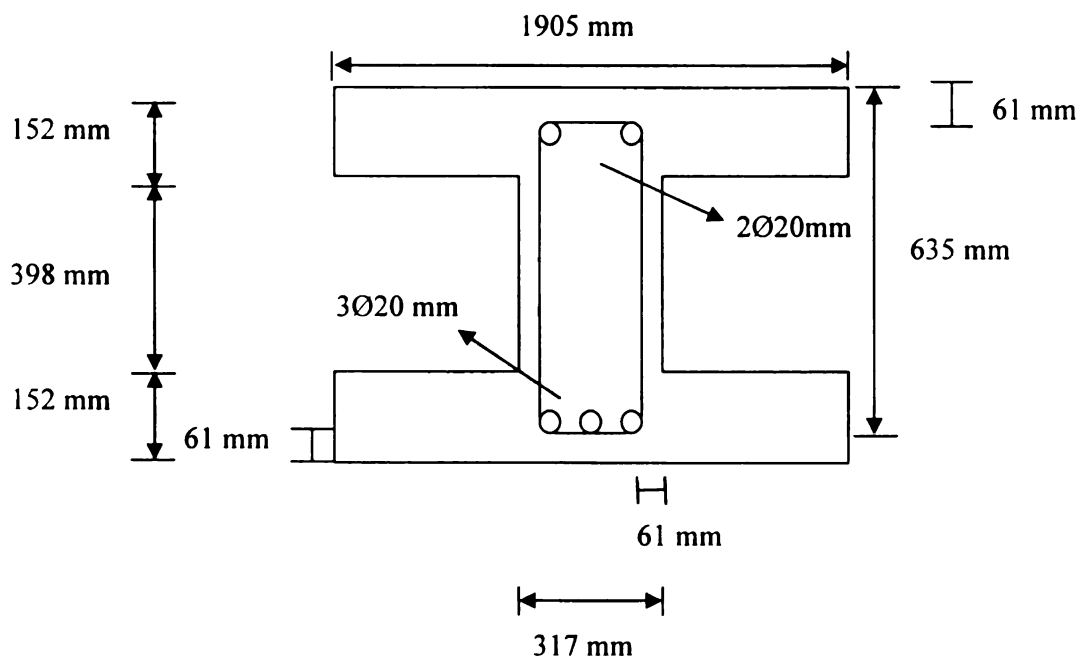
(b) Cross Section

Figure 3.15 – Elevation and cross section of RC I beam B3

87
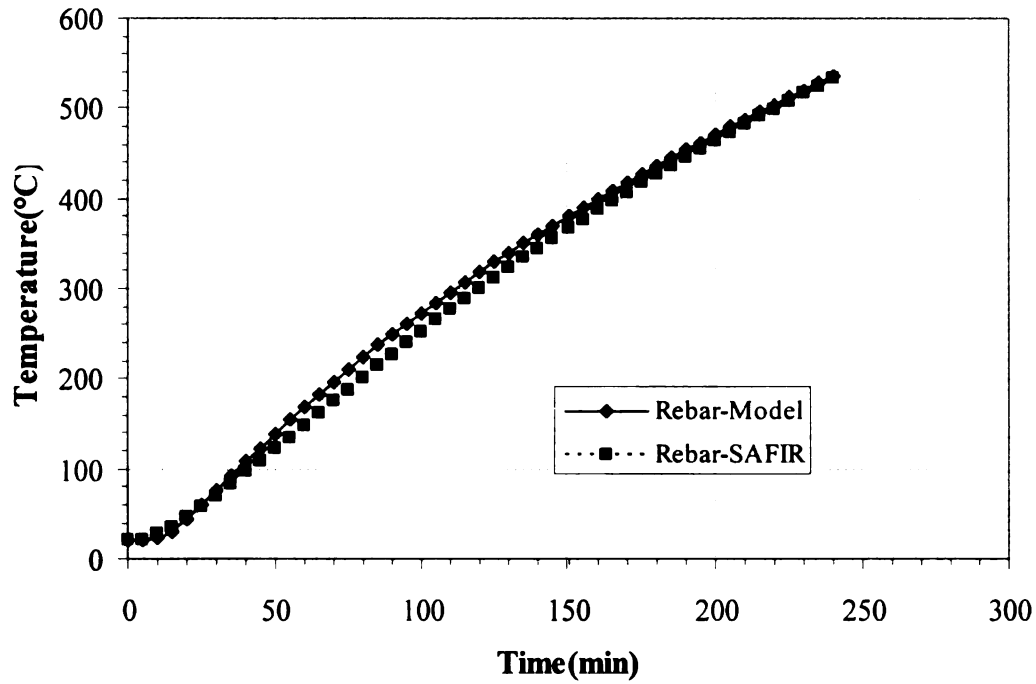
Figure 3.16 – Variation of rebar temperature for Beam B3 as obtained from proposed model and SAFIR
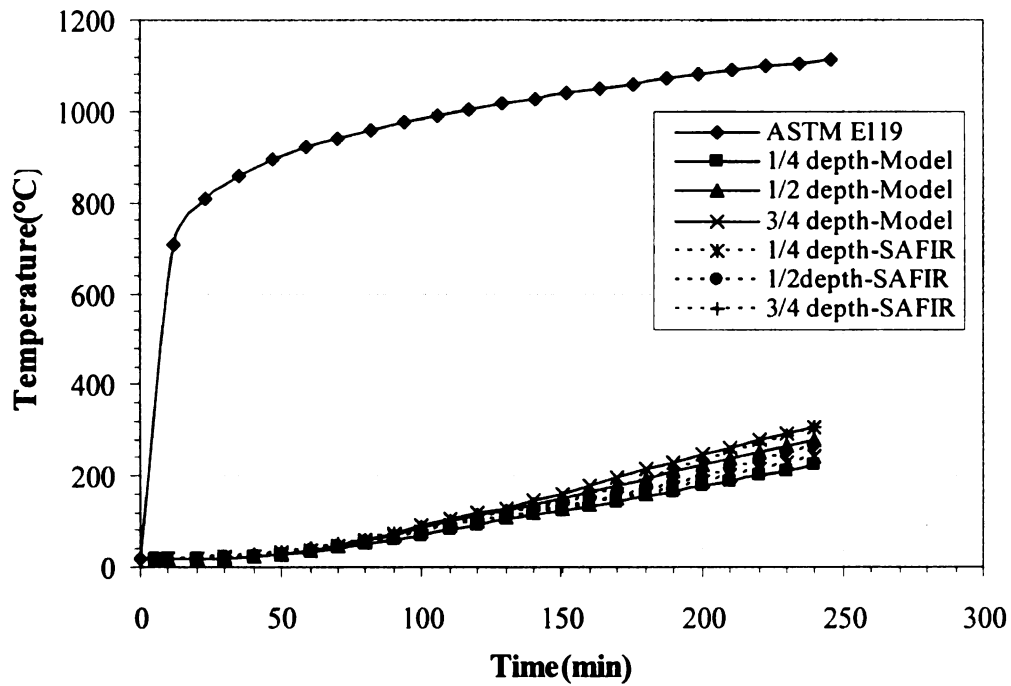
Figure 3.17 – Variation of temperature at three different concrete locations in Beam B3 predicted by the proposed model and SAFIR
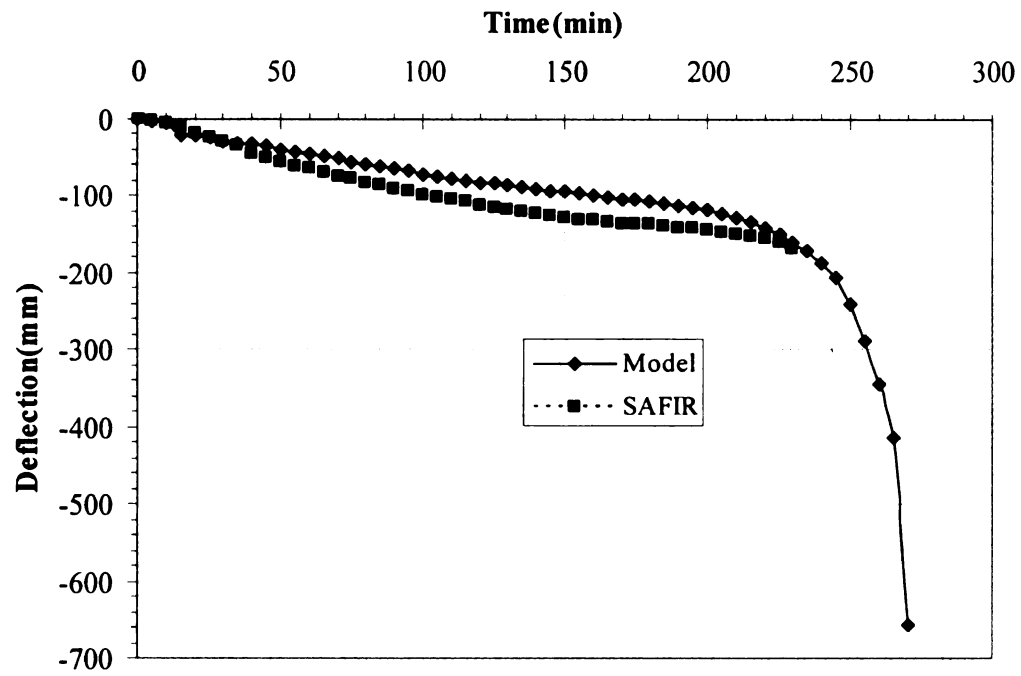
Figure 3.18 – Variation of mid-span deflection for beam B3 (I beam) as predicted by the proposed model and SAFIR

CHAPTER 4

4. PARAMETRIC STUDIES

4.1 General

The review of experimental and analytical studies on RC beams, presented in Chapter 2, indicate that most of the previous studies were carried out under standard conditions and did not take into consideration critical factors such as realistic fire scenario, loading and failure criteria, which influence the fire response of RC beams. Therefor to investigate the effect of various parameters on the fire performance of RC beams, a parametric study was conducted on RC beams using the macroscopic finite element model presented in Chapter 3. The parameters that are studied include load level, aggregate type, fire scenario and concrete strength. Results from the analysis were used to quantify the influence of various parameters on the fire response of RC beams. Details of the parametric study are presented in this chapter.

4.2 Critical factors influencing fire resistance

A review of literature presented in Chapter 2 indicates that fire response of RC beams is influenced by a number of factors. Recent numerical studies (conducted by Kodur and Dwaikat [2008b] and Dwaikat and Kodur [2008a]) on RC beams with rectangular cross-section have shown that the most important factors that influence the fire response of RC beams are:

- Load ratio,

- Aggregate type,

- Fire scenario,

- Concrete strength,

- Failure criteria,

- Concrete cover thickness,

- Location of axial restraint,

- Span-to-depth ratio, and

- Axial and rotational restraint

Dwaikat [2009] conducted a parametric study to investigatie the effect of section characteristics, load ratio (LR) , concrete type, aggregate type, span-to-depth ratio, degree of axial restraint (k_r), location of axial (Y/H) restraint, rotational restraint, fire scenario, concrete strength, spalling and failure criteria on the fire performance of rectangular RC beams. Results of the parametric study obtained for rectangular RC beams are reproduced in Table 4.1. Different cross-sections used for the analysis are presented in Table 4.2. All the analyzed beams were designated by five characters from left to right as follows:

- Concrete type (N for NSC, H for HSC),

- Aggregate type(S for siliceous and C for carbonate aggregate),

- Cross-section number (1,2,3,4 as described in Table 4.2),

- Support conditions (S for simply supported, A for axially restrained, R for rotationally restrained and AR for axially and rotationally restrained beams),

- Span-to-depth ratio (S for small span-to-depth ratio of 8, M for medium span-to-depth ratio of 13 and L for large span-to-depth ratio of 18)

For some beams and additional sixth character (number) is used for designation of different beams whose first five characters are same.

Results from the parametric study indicate that an increase in beam width and concrete cover thickness enhances the fire resistance of the beam by reducing the heat transmission to the cross-section and subsequently to the rebars. Increasing load ratio increases deflection in the beam due to yielding of steel reinforcement and increase in plastic and creep strains. As seen from Table 4.1, beams made with carbonate aggregate have lower deflections than those made with siliceous aggregate due to high thermal capacity and low thermal conductivity of carbonate aggregate. Axial restraint of the beams has significant effect on the fire resistance of the beams and it depends on span-to-depth ratio of the beam. Rotationally restrained beams have higher fire resistance due to the presence of moment redistribution in the beam. Beams subjected to design fire exposure have higher fire resistance than those subjected to standard fire exposure. This can be attributed to the presence of decay phase in design fires during which the beam recovers part of its strength and stiffness.

In summary, the author concluded that fire scenario, load ratio, span-to-depth ratio, location of axial and rotational restraint have significant influence while sectional

dimensions, aggregate, concrete strength, spalling and failure criteria have moderate influence on fire response of rectangular beams.

However the effect of these parameters on RC beams with T and I cross-sections have not been studies. Therefore a set of numerical studies have been conducted to quantify the influence of the above mentioned factors on the fire resistance of T and I cross-section beams.

4.3 Numerical studies on T and I cross-sections

4.3.1 Beam characteristics

Reinforced concrete beams with two different cross-sectional shapes namely T cross-section and I cross-sectional shapes were selected for the analysis. The T beam and I beam used for the parametric studies are the same as those described in Section 3.5.2 and Section 3.5.3 respectively. These beams are designed as under reinforced sections as per the specifications described in ACI 318 [2008]. Both beams are fabricated with concrete having a compressive strength of 28 MPa and the yield strength of steel reinforcement is assumed to be 413 MPa. Cross-sectional dimensions and other characteristics of T and I beams are illustrated in Figures 4.1. For concrete and steel, high temperature property relationships specified in ASCE manual are used as input data for the analysis. All the beams are assumed to be made up of carbonate aggregate as coarse aggregate except those used to study the effect of aggregate type.

4.3.2 Analysis variables

The RC beams were analyzed using three load ratios (30%, 50% and 60%), two aggregate types (siliceous and carbonate aggregate), four values of compressive strength for concrete (30 MPa, 40 MPa, 50 MPa and 60 MPa). The effect of fire scenarios is investigated by subjecting the beams to a standard fire (ASTM E119) exposure and six design fire scenarios namely: FS3, FS6, FS7, FS11, F16 and FS17. Figure 4.2 shows the time-temperature curves for the six design fire scenarios and the ASTM E119a standard fire scenario. It can be seen from Figure 4.2 that the standard fire scenario does not have a decay phase. However, the six design fire scenarios have a well defined decay phase.

The parametric fire time temperature curve [Magnusson SE, Thelandersson S 1970] proposed in Eurocode 1 [1994] and the recent modifications suggested by Feasey and Buchanan [2002] are implemented to arrive at different design fire scenarios. According to Eurocode 1, a design fire consists of a growth phase and a decay phase. Feasey and Buchanan [2002] showed that both the growth and decay phases of the fire are influenced by compartment properties such as the fuel load, ventilation opening and wall linings.

The design fires are selected to cover wide range of compartment characteristics and fuel loads that are encountered in different types of occupancies (buildings). The design fires are assumed to occur in a room of dimension 6 m x 4 m x 3 m. Values of fuel loads ranging from 400 MJ/m^2 to 1200 MJ/m^2 of floor area are used. Opening dimensions are assumed such that the ventilation factor is between 0.02–0.04 $m^{0.5}$. In order to account for the realistic nature of lining material such as gypsum board, concrete and composite construction material, values b (given by Eq. (2.9)) are assumed to vary from 488

94

$Ws^{0.5}/m^2K$ to 1900 $Ws^{0.5}/m^2K$. The different compartment characteristics utilized to establish the design fire scenarios are presented in Table 4.3.

All the beams were analyzed as having simply supported end condition and each beam is discretized into twenty longitudinal segments. The cross-section of each segment was idealized into elements having different sizes in horizontal and vertical directions. Since the dimensions of the flange in T beam and flanges in I beam are relatively larger compared to that of the web and also due to the presence of thermal gradients, the cross-section is idealized into elements having sizes ranging from 2mm to 10mm in the vertical direction and 2.5mm to 25mm in the horizontal direction. Segmental and cross-sectional discretization of the analyzed beams is illustrated in Figure 4.3.The analysis was carried out using the macroscopic finite element model, presented in Chapter 3, in 5 minute time increments for a total duration of four hours or till failure occurred in the beam. Fire resistance of the beams is evaluated based on the thermal, strength, deflection and rate of deflection failure criterion (described in Section 3.2). Results from the parametric studies are used to quantify the influence of various parameters on the overall fire performance of RC beams.

4.4 Results of parametric studies

Results from the parametric studies are presented in Table 4.4 and Figures 4.4 to 4.11. These results are used to discuss the influence of various parameters on the fire response of RC beams.

4.4.1 Effect of load ratio

In order to evaluate the effect of load ratio on the fire response, the beams were analyzed by subjecting them to ASTM E119 standard fire exposure under three load ratios of 30%, 50% and 60%. The load ratio is defined as the ratio of applied load under fire conditions to the capacity of the beam at room temperature.

The influence of load ratio on the fire performance of beams is illustrated in figures 4.4-4.5 and Table 4.4. Figures 4.4 and 4.5 show the variation of mid-span deflection of the beam with fire exposure time and it can be seen that the load ratio has significant influence on the response of the beam. The deflection as well as rate of deflection, of the beam increases with increasing load ratio and this can be attributed to early yielding of the steel reinforcement under higher loads and also increasing high temperature creep effects under large loads. The early yielding leads to decrease in the stiffness of the beam and increases the deflection.

Fire resistance values evaluated based on different failure criterion are presented in Table 4.4. As can be seen from the table an increase in load ratio significantly reduces the fire resistance of RC beams. However, the current prescriptive based approaches evaluate the fire resistance of the beam under an assumed load ratio of 50%. Thus the results from the current approaches may not represent the realistic assessment of RC beams if a different load ratio is used.

4.4.2 Effect of aggregate type

The effect of aggregate type on the fire resistance of RC beams is illustrated in figures 4.6 and 4.7 and Table 4.4. The two figures show the variation of deflection with fire

exposure time for the simply supported T and I beams respectively. It can be seen from both figures that the deflection of the beam with carbonate (calcareous) aggregate type is lower that of the siliceous aggregate RC beam. The difference in deflection can be attributed to the fact that the carbonate aggregate has a high thermal capacity resulting from an endothermic reaction that occurs due to dissociation of dolomite. Also the thermal conductivity of carbonate aggregate concrete is generally lower that that of siliceous aggregate concrete [Dwaikat 2009]. High thermal capacity and low thermal conductivity of carbonate aggregate results in lower temperature increases which in turn produces lower deflection. Hence, the deflection of beam made with carbonate aggregate is lower that that of siliceous aggregate RC beam. A summary of fire resistance values computed based on various failure criteria is presented in Table 4.4.

4.4.3 Effect of fire scenario

The effect of fire scenario on the fire response of RC T and I beams was evaluated by subjecting them to one standard fire scenario namely ASTM E119a [2008], and six design fire scenarios.

The variation of mid-span deflection with fire exposure time for T and I beams are shown in Figures 4.8 - 4.9 respectively. It can be seen from the figures that the deflection and the rate of deflection of the beam exposed to fire increases during the early stages of fire exposure. However, beams exposed to design fires show decrease in deflection towards the later stages of fire exposure. This is due to the presence of decay phase in design fires during which the beam starts cooling and regains part of its strength and stiffness.

Results of fire resistance values computed based on different failure criteria (see Table 4.4) show that the fire exposure has significant influence on the fire resistance of RC beams. It can be seen that the beams exposed to ASTM E119 standard fire exposure attained failure while those subjected to design fire exposure did not fail. Thus the results show that the fire resistance value of beam computed using standard fire exposure will give conservative results if the same beam is exposed to design fire scenario.

4.4.4 Effect of concrete strength

The effect of concrete strength on the fire resistance of T and I beams is investigated by analyzing each of the beams with four different concrete strengths namely: 30, 40, 50 and 60 MPa. Figures 4.10 - 4.11 shows the effect of concrete strength on the mid-span deflection of simply supported T and I beams respectively. It can be seen from both the figures that the concrete strength does not have a significant effect on the fire response of beams. This is due to the fact that the moment capacity of simply supported beams depends mostly on the tension rebar temperature.

From Table 4.4 it can be seen that the fire resistance values computed for different concrete strengths are almost similar implying that the concrete strength has a minor influence on the fire performance of RC beams.

4.4.5 Effect of failure criteria

The fire resistance of T and I beams analyzed in the study was computed according to strength, deflection and rate of deflection failure criterion as shown in Table 4.4. Rebar temperature failure criterion is not considered as it does not represent the actual failure of

the beam [Dwaikat 2009]. It can be seen from Table 4.1 that the deflection and rate of deflection failure criteria predicts lower fire resistance values as compared to strength failure criteria for all the beams. Deflection and rate of deflection failure criterion are important because the integrity of the beam cannot be maintained if it experiences large deflections. The increased deflections lead to cracking in the bottom portion of the beam which exposes the tension rebars to fire. Exposing the tension rebars to fire results in rapid reduction of rebar strength and hence the beam fails early. However, the current provisions in ASTM E119 do not specify deflection or rate of deflection failure criteria.

4.5 Summary

This chapter presents results of parametric studies conducted to quantify the effect of load ratio, aggregate type, fire scenario, concrete strength and failure criterion on the fire response of RC beams. Results from the parametric study show that load ratio, fire scenario and failure limit states have significant influence on the fire resistance of RC beams, while aggregate type and failure criteria have moderate influence. However, the variation in concrete strength has negligible influence on the fire response of RC beams. Further, current codes and standards do not account for critical factors such as realistic fire exposure, deflection and rate of deflection failure criterion, which play an important role in determining the realistic fire resistance of RC beams. Results obtained from the parametric studies are used for developing an energy based time equivalent approach for evaluating fire resistance of RC beams under design fire scenarios.

Tables

Table 4.1 – Summary of fire resistance values for the rectangular beams

Studied parameter	Beam designation	LR (%)	Y/H	k_r (kN/mm)	Fire resistance based on failure criterion (minutes)		
					Strength	Deflection	Rate of Deflection
Section characteristics	NS1SM	50	0.5	0	135	123	115
	NS2SM	50	0.5	0	215	192	189
	NS3SM	50	0.5	0	183	165	166
	NS4SM	50	0.5	0	233	217	218
	NC1AM	50	0.5	50	143	NF	138
	NC2AM	50	0.5	50	228	227	223
	NC3AM	50	0.5	50	195	NF	192
	NC3AM	50	0.5	50	253	NF	249
Load ratio	NS1SS1	30	0.5	0	168	160	143
	NS1SS2	50	0.5	0	135	128	115
	NS1SS3	70	0.5	0	108	105	93
	NC3AM1	30	0.5	50	258	NF	254
	NC3AM	50	0.5	50	195	NF	192
	NC3AM2	70	0.5	50	145	NF	NF
Aggregate type	NS2SM	50	0.5	0	215	192	189
	NC2SM	50	0.5	0	283	245	244
	NS4AM	50	0.5	50	198	NF	194
	NC4AM	50	0.5	50	253	NF	249
Span-to-depth ratio	NS1AS	50	0.5	50	200	NF	194
	NS1AM	50	0.5	50	110	NF	106
	NS1AL	50	0.5	50	75	74	70
Degree of axial restraint	NS1SS2	50	0.5	0	135	128	115
	NS1AS	50	0.5	50	200	NF	194
	NS1AS1	50	0.5	100	210	NF	206
	NS1SL1	50	0.5	0	135	117	115
	NS1AL	50	0.5	50	75	74	70
	NS1AL3	50	0.5	100	63	61	56
Location of axial restraint	NS1AS1	50	0.3	50	123	NF	115
	NS1AS2	50	0.4	50	143	NF	137
	NS1AS	50	0.5	50	200	NF	194
	NS1AS4	50	0.6	50	378	NF	373
	NS1AS5	50	0.7	50	588	NF	582
	NS1AL1	50	0.3	50	98	96	91
	NS1AL2	50	0.4	50	90	88	83
	NS1AL	50	0.5	50	75	74	70
	NS1AL4	50	0.6	50	80	NF	77
	NS1AL5	50	0.7	50	110	NF	106
Rotational restraint	NS2SM	50	0.5	0	215	192	189
	NS2RM	50	0.5	0	363	NF	NF
	NS4AM	50	0.5	50	198	NF	194
	NS4ARM	50	0.5	50	498	NF	NF

100

Table 4.1 (Continued) – Summary of fire resistance values for the rectangular beams

Studied parameter	Beam designation	LR (%)	Y/H	k_r (kN/mm)	Fire resistance based on failure criterion (minutes)		
					Strength	Deflection	Rate of Deflection
Fire scenario	NC1SL1	50	0.5	0	170	146	149
	NC1SL2	50	0.5	0	133	113	113
	NC1SL3	50	0.5	0	NF	105	105
	NC1SL4	50	0.5	0	NF	NF	NF
	NC1SL5	50	0.5	0	NF	NF	NF
	NC1AS1	30	0.5	200	428	NF	425
	NC1AS2	30	0.5	200	425	NF	423
	NC1AS3	30	0.5	200	NF	NF	NF
	NC1AS4	30	0.5	200	NF	NF	NF
	NC1AS5	30	0.5	200	NF	NF	NF
Concrete type and spalling	NS1SM	50	0.5	0	135	123	113
	HS1SM	50	0.5	0	130	118	105
	NS1AM1	50	0.5	200	98	NF	95
	HS1AM	50	0.5	200	80	NF	75
	NS1RM	50	0.5	0	318	307	298
	HS1RM	50	0.5	0	120	NF	NF

N/H – NSC/HSC   S/C – Siliceous/Carbonate aggregate
1/2/3/4 – Cross-sectional size (refer to Table 4.2 for cross-sectional sizes)
S/A/R/AR – simply supported/axially restrained/rotationally restrained/axially and rotationally restrained
S/M/L – small/medium/large span-to-depth ratio
NF – No failure

Table 4.2 – Properties for concrete cross-sections used in the analysis of rectangular beams

Property	Cross-section #			
	1	2	3	4
Cross-section (mm x mm)	300 x 900	400 x 800	700 x 400	600 x 600
Reinforcement for simply supported and axially restrained	2 Φ 14 mm top bars	2 Φ 14 mm top bars	3 Φ 14 mm top bars	3 Φ 14 mm top bars
	5 Φ 20 mm bottom bars	3 Φ 35 mm bottom bars	6 Φ 20 mm bottom bars	8 Φ 20 mm bottom bars
Reinforcement for rotationally restrained beams	5 Φ 20 mm top bars	3 Φ 35 mm top bars	6 Φ 20 mm top bars	8 Φ 20 mm top bars
	4 Φ 20 mm bottom bars	3 Φ 30 mm bottom bars	4 Φ 20 mm bottom bars	5 Φ 20 mm bottom bars
f_c' (Mpa) (for NSC beams)	40	60	30	50
f_c' (Mpa) (for HSC beams)	100	100	100	100
f_y (Mpa)	413	413	413	413
Concrete cover thickness (mm)	40	60	40	50

Table 4.3 – Compartment characteristics used for developing different design fire scenarios

| Fire Scenario	Fuel Load (MJ/m^2 floor area)	Ventilation factor (m$^{0.5}$)	b (Ws$^{0.5}$/m^2°K)
FS 3	1200	0.04	488
FS 6	800	0.04	1900
FS 7	400	0.026	1900
FS 11	1000	0.02	1900
FS 16	1100	0.04	800
FS 17	1000	0.02	1200

Table 4.4 – Summary of fire resistance values for the beams analyzed

Parameter analyzed	Beam type	Aggregate	Concrete strength (MPa)	Fire scenario	Load ratio (%)	Fire resistance (min) Strength	Fire resistance (min) Deflection	Fire resistance (min) Rate of deflection
Load ratio	T	C	28	E119	30	NF	430	NF
	T	C	28	E119	50	300	240	275
	T	C	28	E119	60	190	160	170
	I	C	28	E119	30	NF	430	470
	I	C	28	E119	50	305	245	270
	I	C	28	E119	60	210	185	190
Aggregate type	T	C	28	E119	50	300	230	275
	T	S	28	E119	50	240	195	210
	I	C	28	E119	50	375	290	360
	I	S	28	E119	50	305	245	275
Concrete strength	T	C	30	E119	50	300	230	275
	T	C	40	E119	50	305	235	275
	T	C	50	E119	50	310	240	280
	T	C	60	E119	50	310	240	280
	I	C	30	E119	50	305	245	280
	I	C	40	E119	50	305	250	280
	I	C	50	E119	50	305	250	280
	I	C	60	E119	50	305	250	285
Fire scenario	T	C	28	FS3	50	NF	NF	NF
	T	C	28	FS6	50	NF	NF	NF
	T	C	28	FS7	50	NF	NF	NF
	T	C	28	FS11	50	NF	NF	NF
	T	C	28	FS16	50	NF	NF	NF
	T	C	28	FS17	50	NF	NF	NF
	T	C	28	E119	50	300	240	275
	I	C	28	FS3	50	NF	NF	NF
	I	C	28	FS6	50	NF	NF	NF
	I	C	28	FS7	50	NF	NF	NF
	I	C	28	FS11	50	NF	NF	NF
	I	C	28	FS16	50	NF	NF	NF
	I	C	28	FS17	50	NF	NF	NF
	I	C	28	E119	50	305	245	270

*NF – No failure; C/S – Carbonate/Siliceous aggregate;

Figures
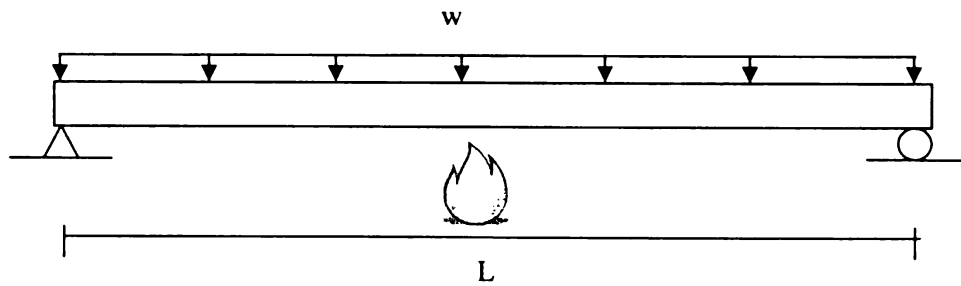
(a) Elevation of simply supported beam
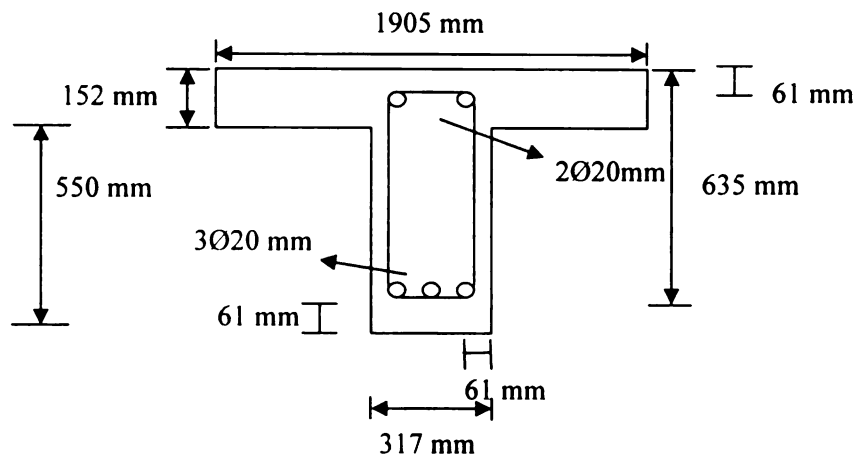
(b) Beam with T cross-section
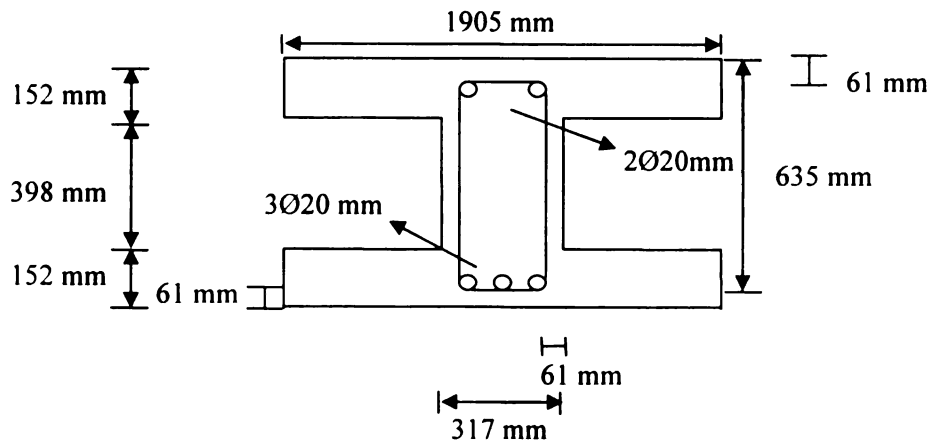
(c) Beam with I cross-section

Figure 4.1 – Elevation and cross-sectional details of RC beams used in parametric studies

104
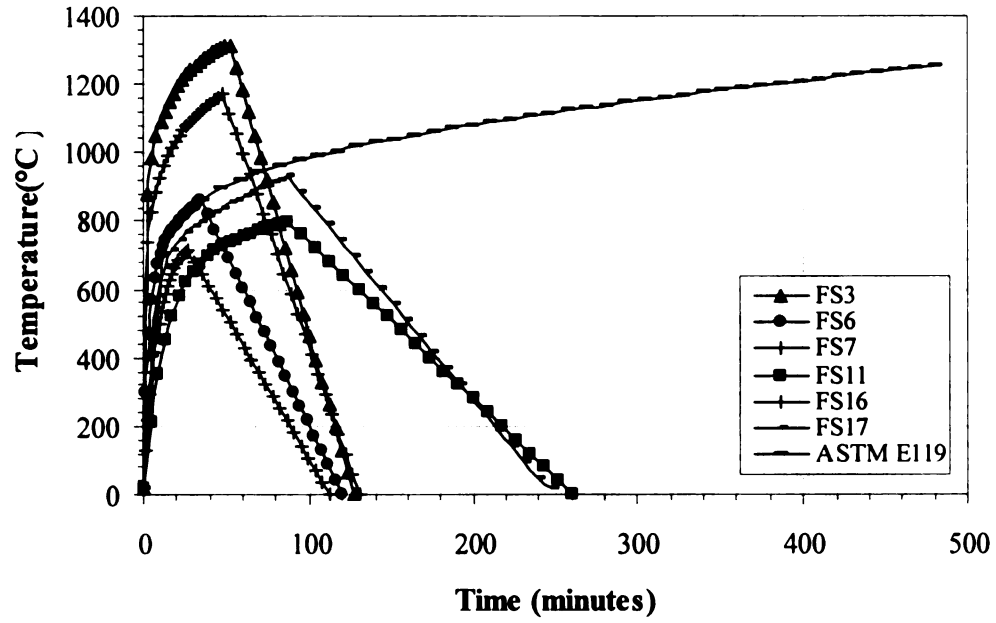
Figure 4.2 - Time-temperature curves for design and standard fire exposures used in the analysis
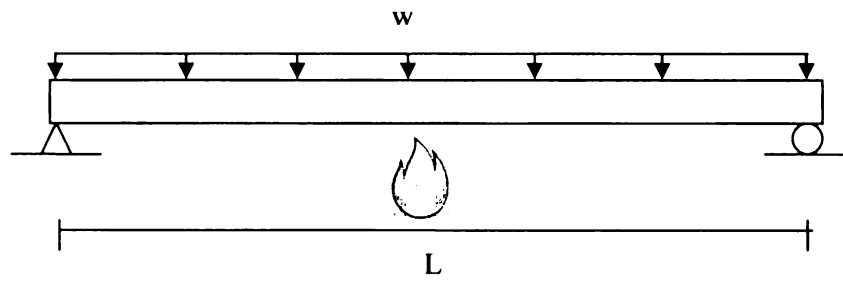
(a) Elevation of simply supported beam
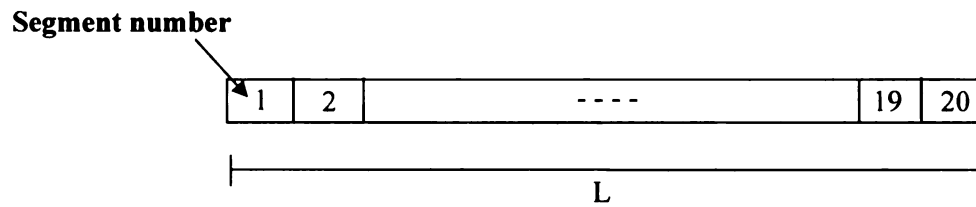
(b) Segmental discretization of the beam
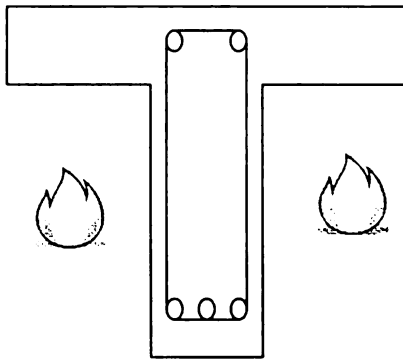
(c) Cross-section details
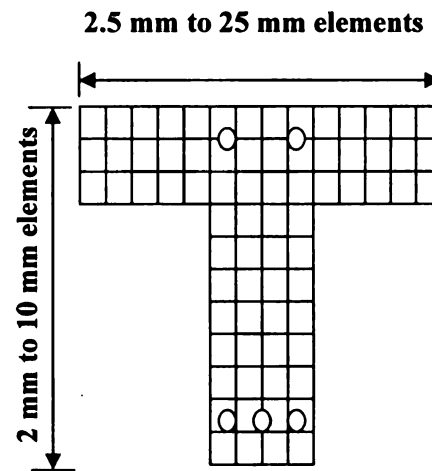
(d) Cross-sectional discretization

Figure 4.3 – Cross-section and segmental discretization of the analyzed beams
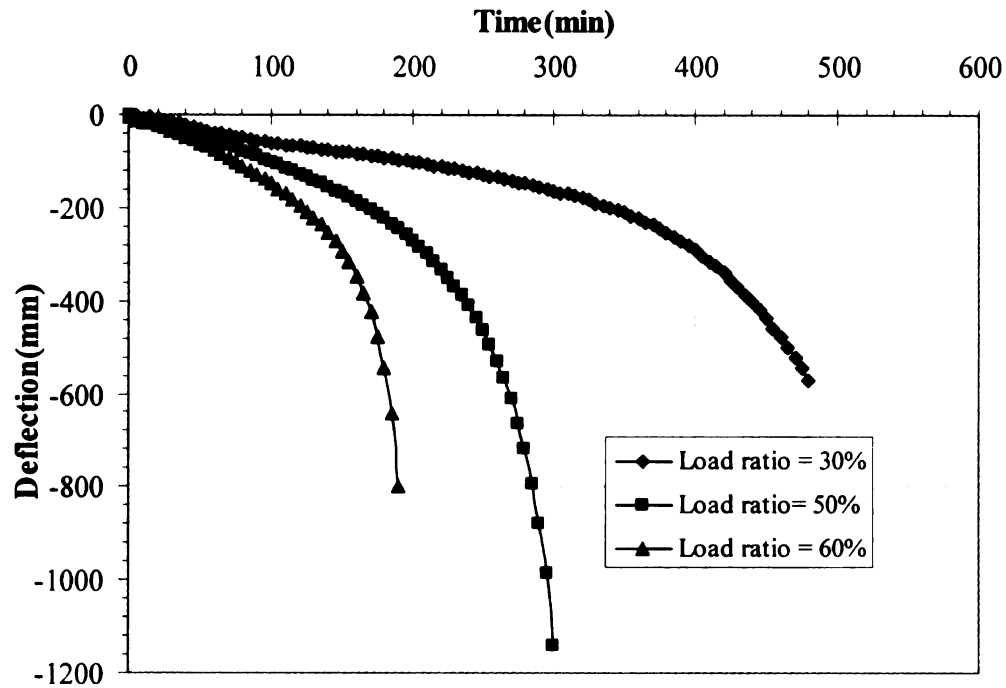
Figure 4.4 – Influence of load ratio on the mid-span deflection of simply supported T-beam exposed to fire
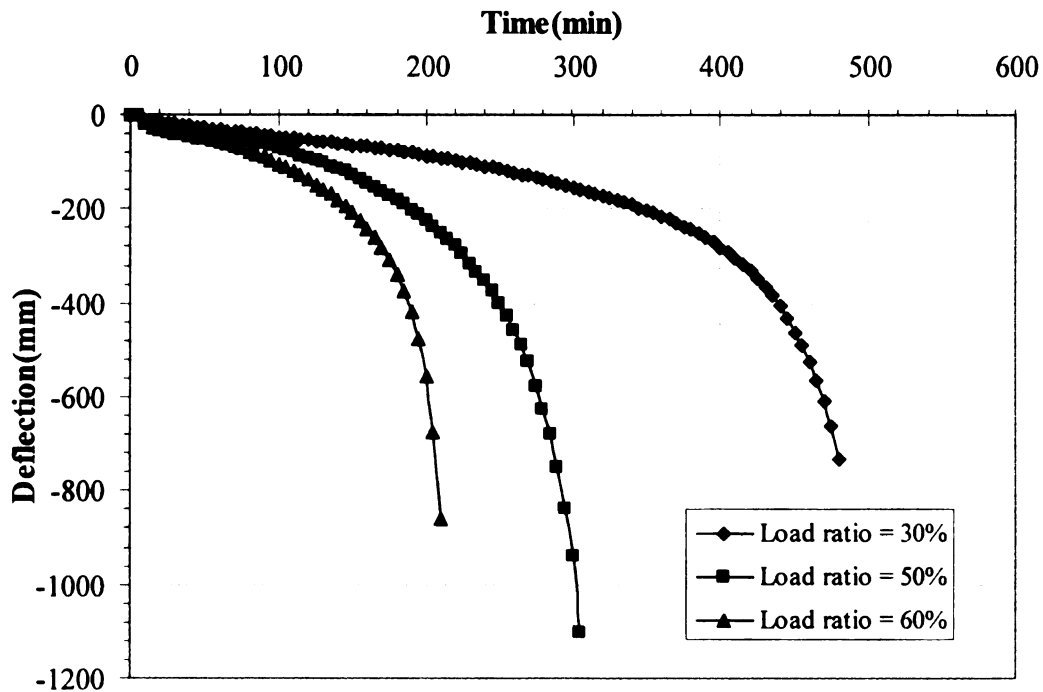
Figure 4.5 – Influence of load ratio on the mid-span deflection of simply supported I-beam exposed to fire
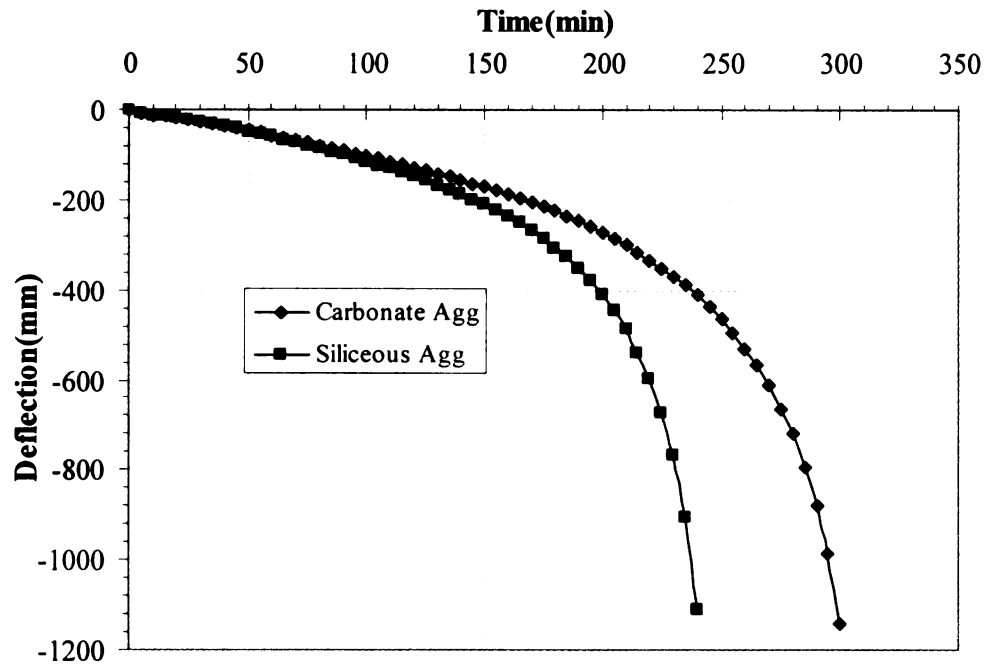
Figure 4.6 – Effect of aggregate type on the mid-span deflection of simply supported T-beam exposed to fire
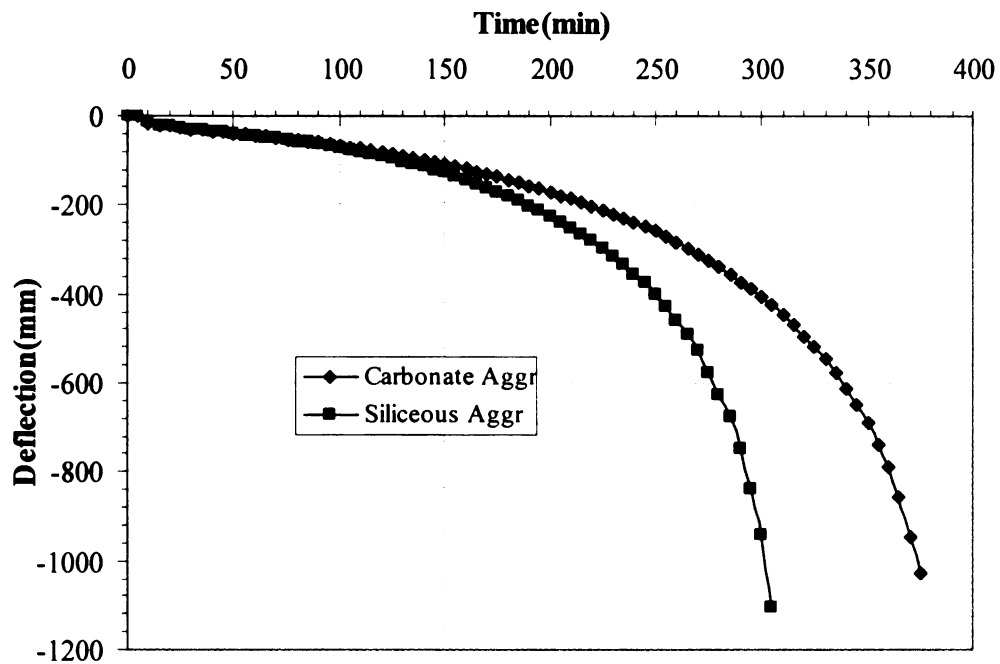
Figure 4.7 – Effect of aggregate type on the mid-span deflection of simply supported I-beam exposed to fire
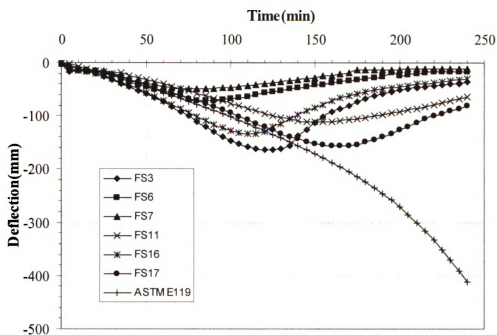
Figure 4.8 – Effect of fire scenario on the deflection of a simply supported T beam
exposed to six design fires and a standard fire
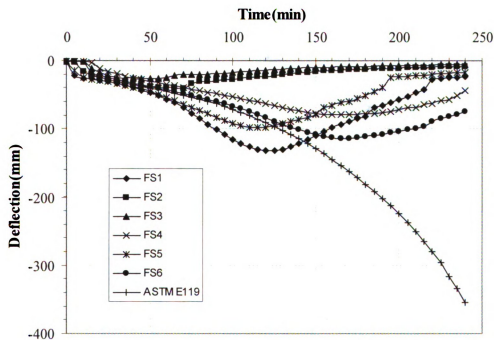
Figure 4.9 – Effect of fire scenario on the deflection of simply supported I beam exposed
to six design fires and a standard fire
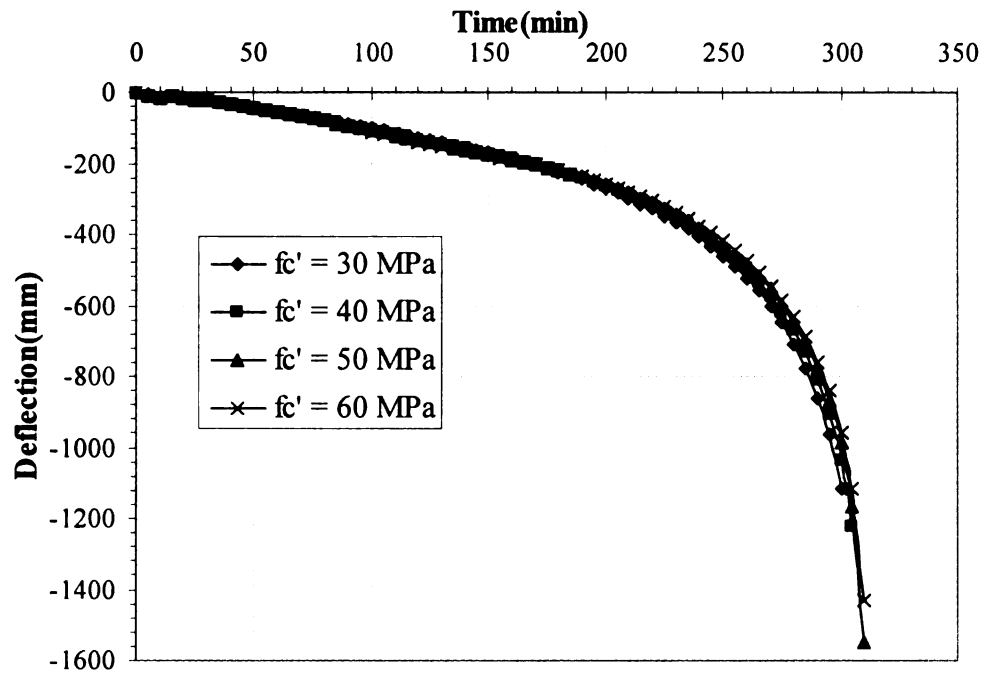
Figure 4.10 – Effect of concrete strength on the deflection of simply supported T beam exposed to fire
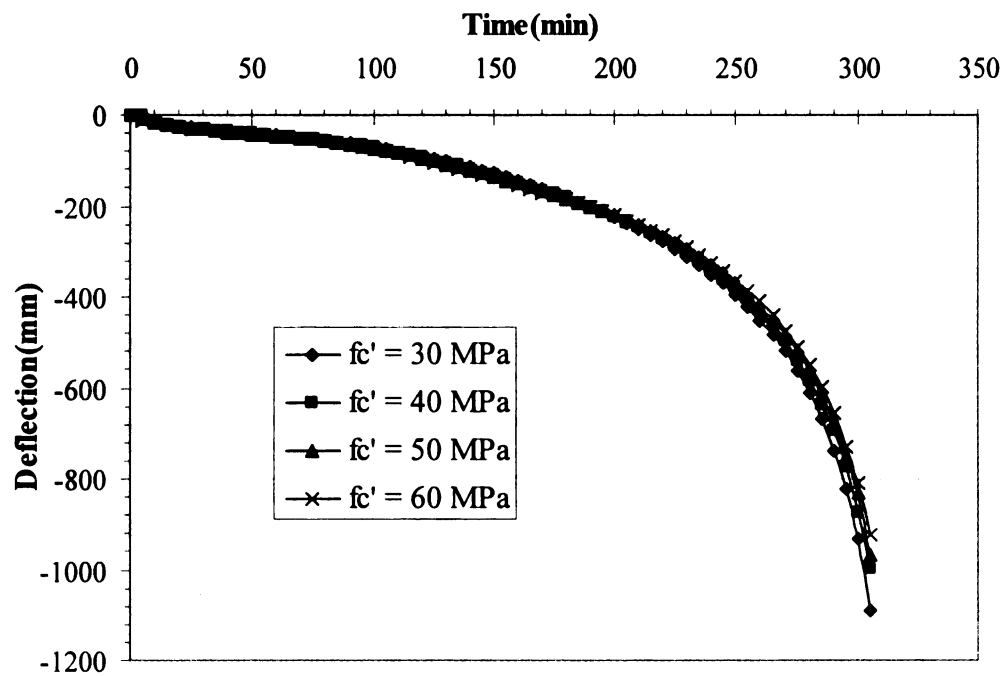
Figure 4.11 – Effect of concrete strength on the deflection of simply supported I beam exposed to fire

CHAPTER 5

5. ENERGY BASED EQUIVALENT APPROACH

5.1 General

The current approach of evaluating fire resistance of RC beams is based on prescriptive

based approaches which are derived from standard fire tests. In these standard fire tests,

the fire resistance of RC beams is evaluated under a standard fire exposure which follows

a predefined time-temperature relationship. This time-temperature relationship does not

provide a realistic representation of typical compartmentation fire conditions since it does

not consider the actual fuel and ventilation conditions present in buildings. Hence the

standard fire tests do not provide a rational and realistic fire resistance assessment of RC

beams. Thus the current prescriptive based methods may not be fully applicable for

undertaking performance based fire design of structural members. For realistic

assessment of fire resistance of the beam, performance of the beam should be evaluated

under realistic fire exposure, loading and failure criteria. However, conducting full scale

fire tests under realistic fire exposure may not be practical or economical since numerous types of fire exposure conditions have to be considered. Alternatively "time equivalency" concept which relates the severity of a design fire to that of a standard fire exposure can be applied to evaluate fire resistance under design fire. However, there is lack of reliable time equivalency methods for evaluating fire resistance of RC members. In this chapter, an energy based time equivalent approach is developed for evaluating the fire resistance of RC beams under any given design fire scenarios.

5.2 Energy based time equivalent approach

5.2.1 General approach

A review of literature presented in Chapter 2 indicates that the current methods for evaluating time equivalent of structural members are not consistent. The time equivalent (fire resistance) predicted by various methods shows a significant variation even for the same fire exposure. In addition, most of the empirical formulae are derived for protected steel members and hence they may not be applicable for RC members. To overcome some of the drawbacks, an energy based time equivalent approach has been developed for establishing equivalency between design and standard fire exposure.

The proposed approach utilizes energy equivalence to compute the time equivalent of design fires with respect to standard fire exposure. According to this method, time equivalent can be computed through the following steps:

- Evaluate fire temperatures (both for design fire and standard fire exposures) in the entire duration of fire exposure time,

112

- Using the above calculated fire temperatures, compute the total amount of energy transferred to RC beam from design fire exposure,

- Similarly using the standard fire temperatures, the amount of energy transferred to RC beam from standard fire exposure is calculated at various time steps,

- Identify a time on the standard fire energy curve where the total amount of energy transferred by design fire exposure is equal to the cumulative energy transferred by standard fire exposure up to that time. The time point at which the energies are equal is defined as the time equivalent.

The fire temperatures for the design fire are computed, as a function of time, based on the compartment characteristics such as dimensions of the compartment, size of the openings and the amount of combustible fuel load present. These fire temperatures are evaluated using the parametric fire time-temperature relationships provided in Eurocode 1 [1994]. For the standard fire exposure, the temperatures are computed using the predefined time-temperature relationships specified in codes. Following this energy transferred to the RC beam under standard and design fire exposures is computed. By equating two energies under standard and real fire exposure, time equivalency is established for an RC beam.

5.2.2 Evaluating fire energy transferred to beam

The proposed approach computes time equivalent based on amount of energy transferred to the beam (energy equivalence) from two fires under comparison. The approach is based on the principle that a structural member is said to experience same level of fire severity if same amount of energy is transferred to the member from two different fire scenarios. The amount of energy transferred is mainly by the heat flux transferred from

113

the fire exposed surfaces to the beam through convection and radiation heat transfer mechanisms. The convection and radiation heat flux on the boundary of an RC beam exposed to fire can be expressed by the following two formulae respectively [Buchanan 2002]

$$q_c = h_c(T_f - T_c)$$ (5.1)

$$q_r = \sigma\varepsilon(T_f^4 - T_c^4)$$ (5.2)

where

q_c = convective heat flux (W/m^2),

q_r = radiative heat flux (W/m^2),

h_c = convective heat transfer coefficient (W/m^2°K),

T_f = temperature of fire (°C or °K),

T_c = temperature on the surface of boundary (°C or °K),

σ = Stefan-Boltzmann constant (5.67x10^{-8} W/m^2°K^4) and

ε = emissivity.

Generally the temperature on the surface of boundary (T_c) is close the temperature of fire (T_f) itself. Thus, the radiative heat flux can be approximated as follows:

$$q_r = \sigma\varepsilon(T_f{}^4 - T_c{}^4)$$

$$= \sigma\varepsilon(T_f^2 + T_c^2)(T_f^2 - T_c^2)$$

$$= \sigma\varepsilon(T_f^2 + T_c^2)(T_f + T_c)(T_f - T_c) \tag{5.3}$$

$$\approx \sigma\varepsilon(T_f^2 + T_f^2)(T_f + T_f)(T_f - T_c)$$

$$\approx 4\sigma\varepsilon T_f{}^3(T_f - T_c)$$

Hence, the total heat flux transferred to an RC beam can be written as:

$$q = q_c + q_r \approx h_c(T_f - T_c) + 4\sigma\varepsilon T_f{}^3(T_f - T_c) \tag{5.4}$$

Further if we assume $T_f - T_c = \alpha T_f$, (where α is a constant), Eq.(5.4) can be rewritten as:

$$q \approx \alpha(4\sigma\varepsilon T_f{}^4 + h_c T_f) \tag{5.5}$$

Then the total amount of energy transferred to an RC beam for a particular fire exposure (design or standard) can be approximated by the following formula:

$$E = \int qA\,dt \approx \int A\alpha(4\sigma\varepsilon T_f^4 + h_c T_f)\,dt \tag{5.6}$$

where

      A = area of boundary exposed to fire and

      E = total energy.

As both A and α are constants, Eq (5.6) can be rearranged as follows

$$E = \alpha A \int (4\sigma\varepsilon T_f{}^4 + h_c T_f)\,dt \tag{5.7}$$

or

$$E = \alpha A \times \left(\text{Area under heat flux curve } \left(\frac{q}{\alpha}\right) \right) \tag{5.8}$$

This 'E' is the total energy bound by the time-temperature curve for a given fire exposure.

5.2.3 Computation of time equivalent

The third step in the energy based approach involves the computation of time equivalent. The amount of energy transferred to RC beam from the design fire exposure (E_d) is computed as described in the previous section. Similarly the amount of energy transferred to RC beam from standard fire exposure (E_s) is also computed. Thus using this approach, a design fire will have the same severity as that of the standard fire if

$$E_s = E_d \tag{5.9}$$

where

E_s = total energy under the heat flux ($\frac{q}{\alpha}$) curve of the standard fire, and

E_d = total energy under the heat flux ($\frac{q}{\alpha}$) curve of the design fire

Consequently, the equivalent time can be computed by equating the total area under the heat flux ($\frac{q}{\alpha}$) curve for the design fire with the area under the heat flux ($\frac{q}{\alpha}$) curve for the standard fire as shown in Figure 5.1 (for the standard and design fires). To arrive at equivalency, first the total area under the heat flux curve for the design fire (area B in Figure 5.1) is computed. The area under the heat flux of a standard fire (area A in Figure 5.1) is computed at various time steps. The time at which area A (which varies as a function of time) equals area B is defined as the time equivalent of the design fire.

5.3 Numerical studies

The development of above discussed energy based time equivalent approach requires large set of fire resistance data on RC beams under standard and design fire exposures. Such data can be generated through numerical simulations on RC beams under various fire scenarios. For the analysis, the macroscopic finite element (FE) based computer program developed in Chapter 3 was selected. The advantage of utilizing the FE program is that various fire, and support conditions can be accounted for in evaluating the fire response of RC beams.

Rectangular RC beams were analyzed under 18 fire scenarios and four different support conditions resulting in 72 beam-fire combinations. Results from FE analysis was used to establish fire resistance time equivalent of each beam under a given design fire exposure. This predicted time equivalent is considered to be reliable since finite element analysis accounts for various factors such as support conditions, high temperature material properties and fire scenario that influence fire resistance of RC beams. Fire resistance data generated through these numerical simulations is used to verify the energy based approach under different scenarios. Details on the computer program, the analysis and the analyzed beams are discussed in the following section.

5.3.1 Design parameters

For generating time equivalent data, four rectangular RC beams (each with different support conditions) were analyzed. The four beams had a simply supported, axially restrained, rotationally restrained and both axially and rotationally restrained end conditions. Details of the beam and boundary conditions are illustrated in Figure 5.2. The

boundaries restraining the beam are idealized as a spring of stiffness (k) as shown in Figure 5.2. Two values of axial restraint stiffness, namely 0 and 20 kN/mm, are selected for the analyzed beams. An axial restraint stiffness value of zero represents a simply supported condition and stiffness of 20 kN/mm represents a restrained condition.

All the beams are of rectangular cross section (300 mm × 500 mm) having a span of 6 m as shown in Figure 5.2. The beams are assumed to be made of concrete with a compressive strength of 30 MPa and reinforced with steel rebars having yield strength of 400 MPa. The applied load on simply supported and axially restrained beams was 14 kN/m (equivalent to a load ratio of 40%), while the corresponding applied load on rotationally restrained, rotational and axially restrained beams was 30 kN/m (equivalent to a load ratio of 40%). Load ratio is defined as the ratio of expected loads on the beam during a fire to the loads that would cause collapse of beam at room temperatures. The fire resistance analysis was carried out in 2.5 minute time increments for a maximum fire exposure time of 8 hours. Data from fire resistance analysis was used to derive time equivalent for the seventeen design fires with respect to that of standard fire exposure.

5.3.2 Fire exposure scenarios

In order to generate data for applying equivalent fire severity concept, the beams were analyzed under one standard fire [ASTM E119a, 2008] and seventeen design fire scenarios namely FS1 through FS17. ASTM E119 fire represents the fire scenario used in standard fire resistance tests and is similar to other standard fire scenarios specified in standards such as ISO 834 [1974]. Figure 5.3 shows the time-temperature curves for the standard and various design fires (FS1 through FS17) used in the analysis. The design

fires are selected to cover wide range of compartment characteristics and fuel loads that are encountered in different types of occupancies (buildings). The parametric fire time temperature curve [Magnusson SE, Thelandersson S 1970] proposed in Eurocode 1 [1994] and the recent modifications suggested by Feasey and Buchanan [2002] are implemented to arrive at different design fire scenarios. According to Eurocode 1, a design fire consists of a growth phase and a decay phase. Feasey and Buchanan [2002] showed that both the growth and decay phases of the fire are influenced by compartment properties such as the fuel load, ventilation opening and wall linings. These design fires are assumed to occur in a room of dimension 6 m x 4 m x 3 m. Values of fuel loads ranging from 400 MJ/m^2 to 1600 MJ/m^2 of floor area are used. Opening dimensions are assumed such that the ventilation factor is between 0.02–0.04 m$^{0.5}$. In order to account for the realistic nature of lining material such as gypsum board, concrete and composite construction material, values of b (given by Eq. (2.9)) are assumed to vary from 488 $Ws^{0.5}/m^2K$ to 1900 $Ws^{0.5}/m^2K$. The different compartment characteristics utilized to establish the design fire scenarios are presented in Table 5.1.

5.3.3 Determining time equivalent

The time equivalent for the analyzed beams was evaluated by the maximum deflection method using the results obtained from FE analysis described in previous chapters. The maximum deflection method is selected (over minimum load capacity method) since the failure of an RC beam under fire exposure is generally governed by deflection failure criteria. This was the case for most of the beam analyzed in Chapters 3 and 4. It should be

noted that the fire resistance based on deflection criteria is very close to that obtained from strength criterion.

5.3.4 Evaluating time equivalent from current methods

The analysis of four types of rectangular RC beams under one standard fire and seventeen design fires produced seventy two time-deflection curves. The time-deflection curve of a beam under design fire is compared with standard fire exposure to establish the time equivalent for each beam-fire combination using the maximum deflection method. The time equivalent for each combination is also evaluated using the currently available empirical formulae and the equal area method. The comparative study did not include the minimum load capacity and the maximum temperature methods since these methods may not provide realistic fire resistance values and also because these methods require detailed finite element analysis which limits their use for design purposes, as discussed in Section 2.4.4. The time equivalency predicted by maximum deflection method is considered to be the most reliable value for time equivalency. Maximum deflection method is considered to be reliable because the integrity of the beam cannot be maintained under large deflections. Further increasing deflection results in cracking of the beam, which exposed the rebars directly to the fire, causing premature failure of the beam. A comparison of estimated time equivalent values based on equal area method and empirical formulae (CIB, Law and Eurocode) with that predicted by the maximum deflection method for the 72 beam-fire combinations are shown in Figure 5.4. The conservative and unconservative regions for the data points are also shown in Figure 5.4.

120

An observation of time equivalent values presented in Figure 5.4 show that Law formula predicts lower fire resistance for all the fire scenarios.

It can be seen from Figure 5.4, that there is significant variation in the time equivalent (t_e) values predicted by empirical formulae and equal area method. Almost all the time equivalent values predicted by CIB formula are unconservative and the variation in the predicted t_e values increases as the severity of the design fire increases (as the time equivalent value increase). Similar to the CIB formula, the time equivalent values predicted by the Law formula and Eurocode formula are also on the unconservative side and are highly scattered for increasing values of time equivalent (i.e., for severe design fire exposures). In general, the time equivalent values predicted by empirical formulae are unconservative and the accuracy of prediction decreases as the fire severity increases. The unconservative nature of time equivalent values predicted by empirical formulae can be attributed to the fact that these formulae were derived using the maximum temperature concept for protected steel members under design fire scenarios. Thus they may not be fully applicable for predicting the time equivalent of RC members.

As can be seen in Figure 5.4, the time equivalent values predicted by the equal area method have less variation than those predicted by the empirical formulae. However, similar to different empirical formulae, the variation in the time equivalent values predicted by equal area method becomes significant for severe design fire scenarios. Also, equal area method gives unconservative predictions for almost half of the time equivalent values computed in this study. This can be related to the fact that the equal area method predicts the same time equivalent value for different shaped time-temperature curves provided that they have equal areas under time-temperature curves.

This clearly indicates that the time equivalent computed based on the equal area method may not be conservative under many fire scenarios.

In summary, the time equivalent values predicted by equal area method and empirical formulae are generally unconservative and have significant variation. Thus, the current time equivalent methods do not yield reliable fire resistance predictions for RC beams. To overcome these drawbacks, a semi-empirical energy based approach for establishing time equivalency of RC beams is proposed.

5.4 Calibration

To improve the accuracy of predictions from the proposed method, estimated time equivalency values from energy based approach have been calibrated against time equivalent values obtained from finite element analysis. An analysis of results indicate that there exists a correlation between the ratio $(t_{e(FE)}/\ t_{e(energy)})$ of the two time equivalent values (predicted by the FE method and the equal energy method) and the maximum temperature of design fire as shown in Figure 5.5. It can be seen from Figure 5.5 that the ratio of time equivalent predicted by the FE method to that predicted by equal energy method decreases with increase in the maximum temperature of design fire. This can be attributed to the fact that the extent of fire damage in the beam depends not only on energy transferred from fire but also on other factors such as temperature distribution and resulting thermal gradients across the beam. These thermal gradients are large in case of fires with high maximum temperatures.

Data generated from FE analysis was randomly divided into two sets. The first set was used for the calibration of the method and the second set was used to validate the method.

Almost half of the beam-fire combinations have been selected at random and the ratio of time equivalents obtained by FE and energy method are plotted against the maximum temperature reached in respective fire scenarios as can be seen from Figure 5.5. Least sum of square of error analysis is carried out to obtain a best fit and a conservative line for that correlation and is shown in Figure 5.5. Accordingly, the equation of conservative line for predicting the ratio between the two time equivalents $(t_{e(FE)}/ t_{e(energy)})$ is given as

$$\frac{t_{e(FE)}}{t_{e(energy)}} = 1.6 - 0.00042 * T_{max} \tag{5.10}$$

where

$t_{e(FE)}$ = time equivalent computed from maximum deflection method (or FE analysis),

$t_{e(energy)}$ = time equivalent computed from equivalent energy method and

T_{max} = maximum temperature of design fire

Thus, the actual time equivalent of a design fire can be estimated by the following equation

$$t_{e(FE)} = (1.6 - 0.00042 * T_{max}) * t_{e(energy)} \tag{5.11}$$

A 95% confidence interval for the variation of temperature was determined for the above data set used for calibration. Accordingly, the lower and upper confidence interval limits are found to be equal to 1008°C and 1168°C.

5.5 Validation

To illustrate the validity of the proposed method, time-equivalent values computed based on the energy method are compared with those obtained from FE analysis and equal area method. Three cross-sectional types of RC beams namely rectangular, T and I beams are used for validation. The rectangular beams are same as that described in Section 5.3.1 and shown in Figure 5.2, while T and I beams are those described in Section 3.7.2 and Section 3.7.3 respectively. As mentioned earlier (Section 5.4) data generated from FE analysis for rectangular beams was divided into two sets. First set of data was used for calibration of the proposed method while the second set of data was used for validation. In order to generate data for T and I beams, both beams are subjected to six randomly selected design fire scenarios (namely FS3, FS6, FS7, FS11, FS16 and FS17) and time equivalent values are computed through finite element analysis using the macroscopic finite element model. A summary of computed t_e values for rectangular RC beams is presented in Table 5.2.

Figures 5.6 -5.8 shows variation of time equivalent values predicted by equal area method, empirical formulae, FE analysis and proposed equal energy method along with conservative and unconservative regions for rectangular, T and I beams respectively. It can be seen from the figures that almost all the time equivalent values predicted by the equal energy method are on the conservative side throughout the range of fire scenarios considered. Time equivalents predicted by equal area method shows less scatter as compared to empirical formulae. The figures also show that the time equivalent computed based on equal energy method has less variation as compared to other methods.

Thus, equal energy method can be considered as a reliable method for estimating time equivalent of design fires.

In order to illustrate the applicability of the proposed method (Eq. 5.11) to an independent set of data, four RC beams were analyzed under six design fire scenarios. Cross-sectional details and properties of the beams used for this analysis are presented in Table 5.3 and selected fire scenarios are shown in Figure 5.9. A comparison of time equivalent obtained from the proposed method with those obtained from macroscopic finite element model (described in Chapter 3) is shown in Figure 5.10. It can be seen from Figure 5.10 that the predictions from the proposed method are in good agreement with finite element results, and are conservative for most of the beams. The coefficient of determination was found to be equal to 0.94 indicating that the proposed equation is sufficiently accurate in estimating time equivalent in comparison with detailed finite element analysis. A comparison of figures 5.6 and 5.10 show that time equivalent computed from the proposed method has less variation than other methods. Thus the proposed method can be used in predicting conservative and relatively better estimate of time equivalent under design fires.

5.6 Numerical example

In order to illustrate the applicability of the proposed energy based time equivalent method to practical design situations, fire resistance of an RC beam is evaluated by applying the proposed energy based approach. A simply supported rectangular beam of 6 m span length and made of concrete with a compressive strength of 30 MPa and reinforced with steel rebars having yield strength of 400 MPa is selected. The beam is

assumed to be exposed to design fire FS5 (as shown in Figure 5.3) and the time equivalent is evaluated. Detail step-by-step procedure involved in computing the time equivalent is presented in Appendix D.

The total amount of energy transferred to RC beam from FS5 is calculated to be equal to 39814995 Joules. Next, the amount of energy transferred to RC beam from ASTM E119 standard fire is evaluated at various time intervals. Subsequently the difference in total energy of design fire and cumulative energy of standard fire is computed at each time step to find a minimum value. The minimum difference in energy occurs at 150 minutes. Hence according to the equal energy method, design fire FS5 has a time equivalency of 150 minutes. The same beam is analyzed (using the numerical model described in Chapter 3) under ASTM E119 standard fire exposure and fire resistance of the beam is found to be equal to 272 minutes. Since the computed time equivalent is less than the fire resistance (failure time) of the beam, the beam can survive complete burnout under design fire FS5 (without failure). In summary, failure occurs in the beam if time equivalent is greater than the fire resistance of the beam.

5.7 Summary

Currently available empirical formulae for computing the time equivalent are mainly derived for protected steel members and may not be fully applicable for RC members. Further, the time equivalent values predicted by current methods and empirical formulae show significant variation and the accuracy of prediction decreases with increasing fire severity. To overcome these drawbacks, a reliable semi-empirical energy based approach for evaluating the time equivalent of RC beams is presented in this chapter. The proposed

approach is validated by comparing the predicted time equivalent values form the approach with those obtained from existing time equivalent methods and detailed finite element analysis. Based on the results obtained in this study, it is concluded that the proposed approach gives a reliable estimate of time equivalent for RC beams compared to existing methods. In order to facilitate the use of the proposed approach in practical design situations, a simple linear design equation has been developed and validated. Using this equation, time equivalent of RC beams for any design fire exposure with respect to standard fire exposure can be estimated with sufficient accuracy without the need for expensive full-scale fire resistance tests.

Tables

Table 5.1 – Compartment characteristics used for arriving at different design fire scenarios

Fire Scenario	Fuel Load (MJ/m² floor area)	Ventilation Factor (m^0.5)	b (Ws^0.5/m²°K)
FS1	1600	0.02	488
FS 2	1200	0.02	488
FS 3	1200	0.04	488
FS 4	800	0.04	488
FS 5	1600	0.02	1900
FS 6	800	0.04	1900
FS 7	400	0.026	1900
FS 8	1100	0.04	488
FS 9	1300	0.03	1900
FS 10	900	0.04	488
FS 11	1000	0.02	1900
FS 12	700	0.035	1900
FS 13	1100	0.02	488
FS 14	800	0.04	1200
FS 15	800	0.04	1000
FS 16	1100	0.04	800
FS 17	1000	0.02	1200

Table 5.2 – Summary of computed time equivalent values from various methods

Design Fire	Duration of burning period (minutes)	Maximum temperature (°C)	Equal Energy method	Equal area method	Time equivalent (minutes) Finite element analysis			
					Simply supported	Axially restrained	Rotationally restrained	Axially and rotationally restrained
FS1	139	1270	304	294	*	290	292	282
FS2	104	1230	231	223	250	237	227	215
FS3	52	1314	162	125	150	155	145	140
FS4	35	1270	118	93	118	117	115	112
FS5	139	861	150	232	185	150	162	137
FS6	35	861	59	75	73	70	70	65
FS7	27	717	39	57	47	42	40	40
FS8	48	1306	151	117	142	145	137	135
FS9	75	890	99	132	117	115	115	102
FS10	39	1285	129	101	125	127	122	122
FS11	87	798	91	139	105	102	105	92
FS12	35	824	55	72	67	65	65	60
FS13	104	1229	210	223	250	237	227	215
FS14	35	1000	76	82	87	82	85	80
FS15	35	1054	83	85	95	90	90	87
FS16	48	1170	121	111	130	130	127	122
FS17	87	928	118	156	140	135	135	120

* Not applicable as failure occurred before beam reached maximum deflection

129

Table 5.3 – Cross-sectional details and properties of beams used in the analysis

Property	Beam I	Beam II	Beam III	Beam IV
	Simulated by Kodur and Dwaikat [2007]	Tested by Lin et at [1981]	Tested by Dotreppe and Franssen [1985]	Tested by Dwaikat [2009]
Width (mm)	300	305	200	255
Depth (mm)	500	355	600	405
Length (m)	6	6.1	6.5	3.96
Tension reinforcement	3 Φ20 mm	4 Φ19 mm	3 Φ22 mm	3 Φ19 mm
Compression reinforcement	2 Φ14 mm	2 Φ19 mm	2 Φ12 mm	2 Φ13 mm
f_c' (Mpa)	30	30	15	58.2
f_y (Mpa)	400	435.8	300	420
Load ratio	0.5	0.42	0.263	0.576
Applied load (kN)	120	80	65	141.5
Concrete cover (mm)	40	25 (bottom) 38(side)	40	38
Aggregate type	Carbonate	Carbonate	Siliceous	Carbonate
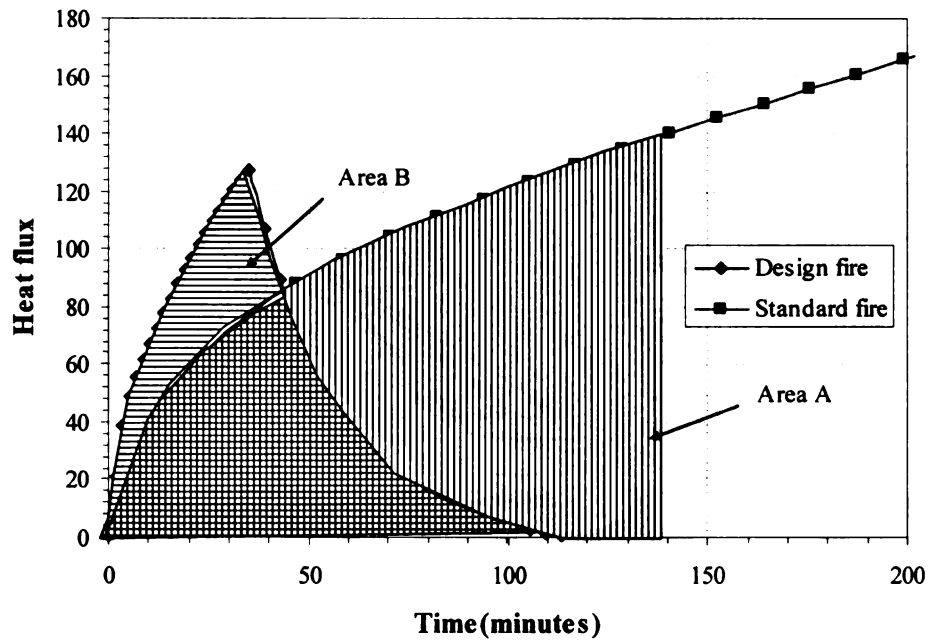
Figure 5.1 – Equivalent energy concept for standard and design fire

(a) Cross section

$f_c' = 30 \text{ MPa}$

$f_y = 400 \text{ MPa}$

40 mm 150 mm

500 mm

6 φ 20 mm

40 mm

φ 10 mm stirrups

300 mm

14 kN/m

k

6 m

(b) Elevation for simply supported restrained beam

30 kN/m

k

6 m

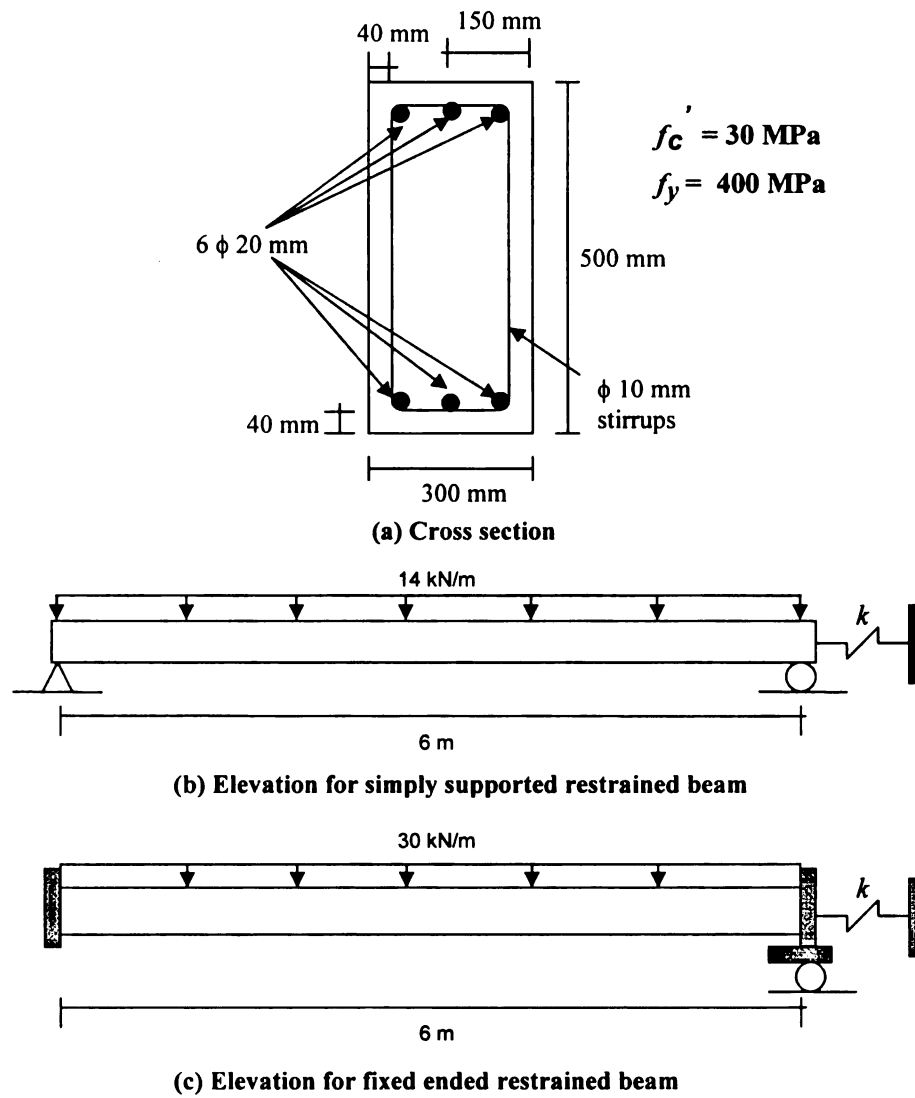**(c) Elevation for fixed ended restrained beam**

Figure 5.2 – Cross section and elevation of RC beam used in the analysis

132

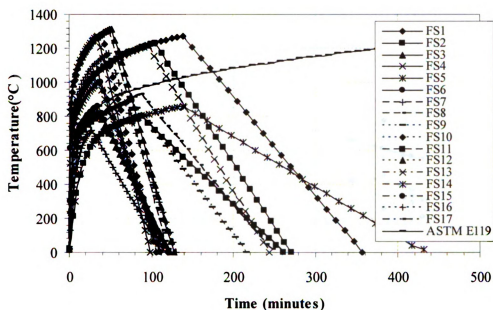Figure 5.3 – Time temperature curves for design and ASTM E119 standard fire exposure
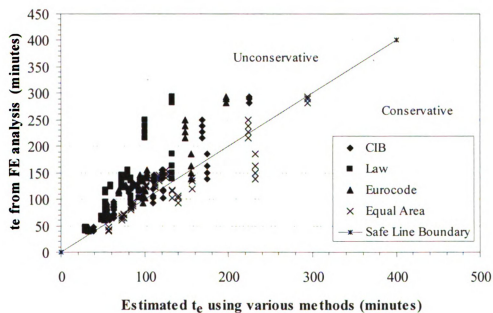
Figure 5.4 – Comparison of time equivalent computed based on FE analysis with that of other methods
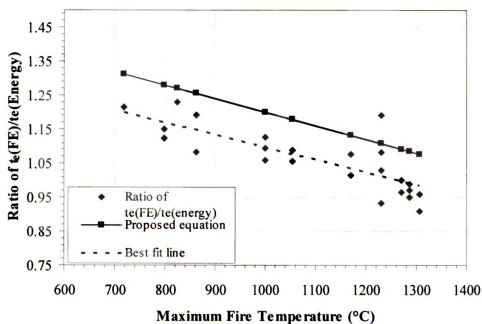
Figure 5.5 – Variation of $\dfrac{t_{e(FE)}}{t_{e(Energy)}}$ with maximum fire temperature
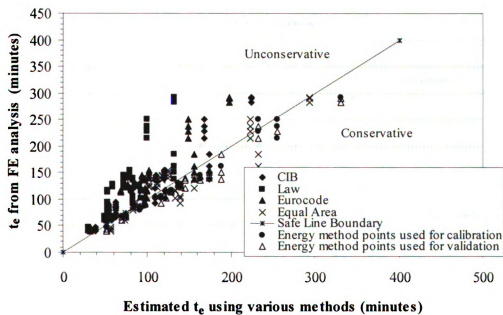
Figure 5.6 – Comparison of time equivalent from equal energy method with predictions from other methods for a rectangular beam
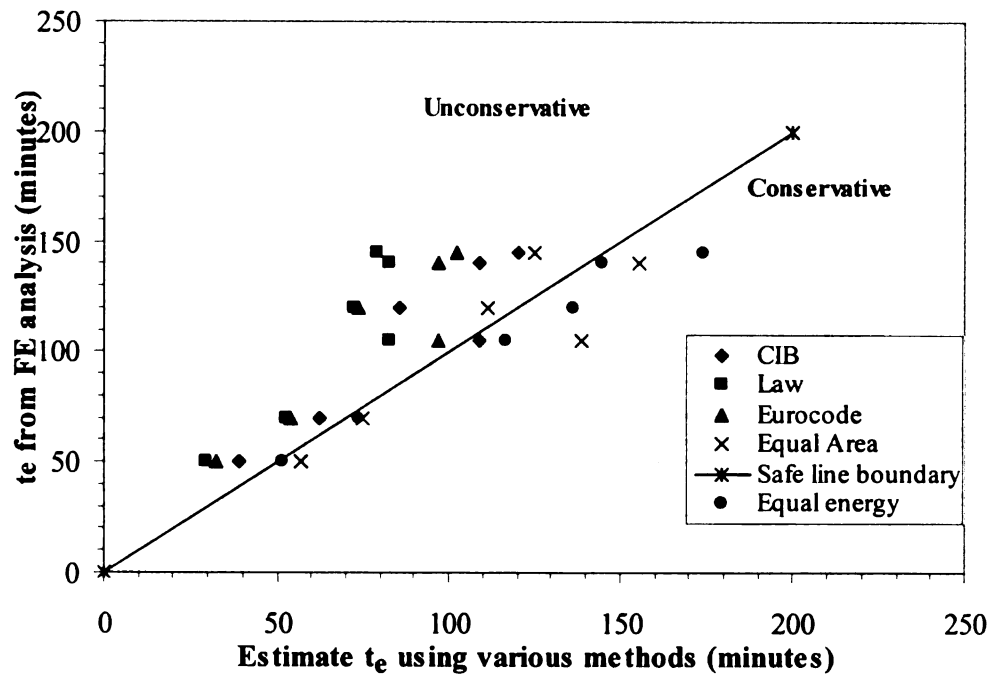
Figure 5.7 – Comparison of time equivalent from equal energy method with predictions from other methods for a T beam

Figure 5.8 – Comparison of time equivalent from equal energy method with predictions from other methods for an I beam

135
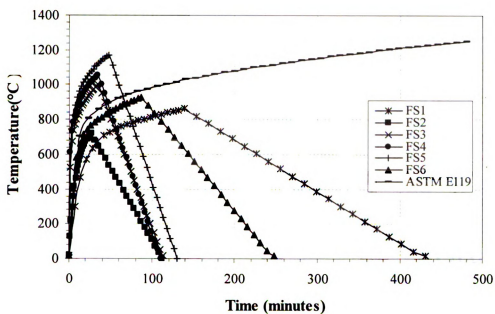
Figure 5.9 – Fire scenarios used in the analysis of RC beams
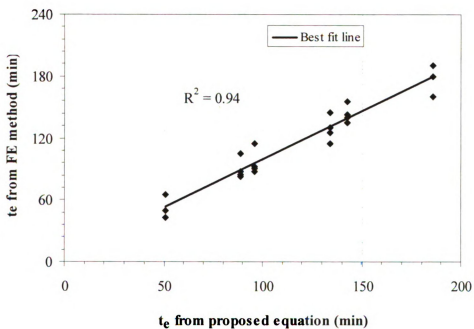
Figure 5.10 – Comparison of time equivalents from the proposed equation and the finite element analysis

<div align="right">**CHAPTER 6**</div>

6. CONCLUSIONS AND RECOMMENDATIONS

6.1 General

The fire response of RC beams exposed to fire is presented in this thesis. A numerical model was developed for tracing the fire response of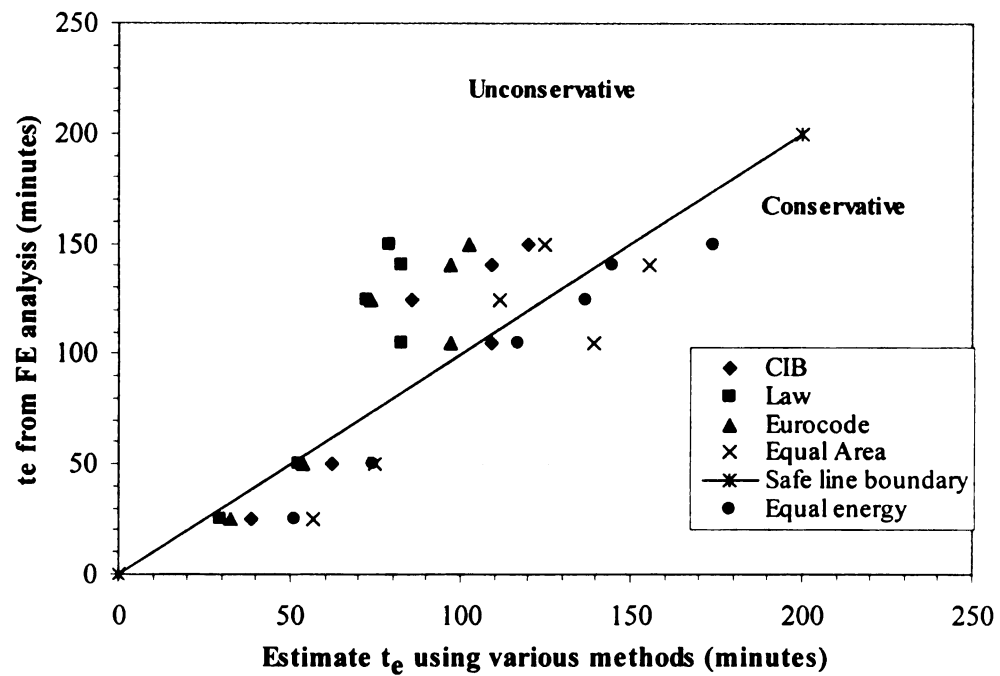 RC beams under realistic fire and loading conditions. The model is based on macroscopic finite element approach and uses moment-curvature relationships to predict the response of rectangular, T and I cross-section RC beams. The model accounts for high temperature constitutive material properties, various strain components and different fire exposure conditions. The validity of the model is established by comparing the predictions from the model with those obtained from tests and other numerical programs such as SAFIR. The proposed numerical model was used to undertake a set of parametric studies to quantify the influence of various parameters on the fire response of RC beams. Data generated from the parametric studies was used to develop a semi-empirical energy based approach for evaluating time equivalent of RC beams under design fire scenario. The proposed

approach, which equates energy between a standard and a design fire exposure, can be applied to evaluate fire resistance of RC beams under design fires thus facilitating performance based design.

6.2 Conclusions

Based on the information presented in the thesis, the following conclusions are made:

- There is limited information on response of RC beams under realistic fire and loading conditions, specifically for beams with T and I cross-sections. The current fire resistance provisions in codes and standards are based on prescriptive approaches and may not be applicable for performance based fire design.

- The macroscopic finite element based numerical model developed in this thesis is capable of tracing the fire response of RC beams, with rectangular, T and I corss-sections, under realistic loading and fire scenarios. The model account for critical factors, such as high temperature material properties and various strain components that govern the fire response of RC beams.

- Results from the parametric study show that load ratio and fire scenario have significant influence on the fire resistance of RC beams while aggregate type and failure criteria have moderate influence.

- The proposed energy based approach accounts for critical compartmentation factors such as fuel load and ventilation parameters in establishing time equivalency for design fire exposures. Thus it is capable of providing a realistic assessment of fire resistance of RC beams.

- The energy based approach provides better estimate of time equivalent (fire resistance) of RC beams than current approaches.

6.3 Recommendations

Though the data presented in this study provides valuable information in understanding the response of RC beams under realistic fire conditions, further studies are needed to provide a comprehensive understanding of the fire behavior of RC beams. The following are some of the topics that need to be explored for developing such a comprehensive understanding:

- The macroscopic finite element model proposed here is applicable for reinforced concrete beams only. The model can be extended to cover other cases such as prestressed and FRP strengthened concrete beams. This can be done by modifying the thermal and structural models to account for temperature dependent material properties for FRP, insulation and prestressing steel.

- The numerical model can be further enhanced to model the effects of spalling in concrete. Previous studies have indicated that explosive spalling, which generally occurs in new concrete types such as high strength concrete, has a significant influence on the fire response of concrete structural systems.

- The macroscopic finite element model, presented in this thesis, can model the behavior of simply supported RC beams (for T, I beams) only. The model can be extended for RC beams with different support conditions such as axial restraint, rotational restraint, axial and rotational restraint by incorporating stiffness based formulation to the structural analysis (following the generation of M-κ relationships).

To illustrate the applicability of time equivalence formula for an RC beam per existing methods and empirical formulae, equivalent time subjected to a design fire is computed. The characteristics of design fire are shown in Figure 2.5 and presented in Table 5.1. The RC beam is simply supported and the properties of this beam are explained in section 2.5. Time equivalency computation from different methods is presented below.

<u>CIB formula</u>

$$t_e = k_c w e_f$$

$$w = \frac{A_f}{\sqrt{A_v A_t \sqrt{H_v}}}$$

$b = 1900 \ \text{Ws}^{0.5}/\text{m}^2\text{K}, \quad F_v = 0.02 \ \text{m}^{0.5}, \quad e_f = 1600 \ \text{MJ/m}^2$ (From Table 5.1)

$k_c = 0.07$ (From Table 2.1)

$$A_t = 2*(6*4+6*3+3*4) = 108m^2 \ , \ A_f = 6*4 = 24m^2 \ , \ A_v = 2.2*1 = 2.2m^2$$

$$A_v\sqrt{H_v} = (2.2*1)*\sqrt{1} = 2.2m^{2.5}$$

$$w = \frac{24}{\sqrt{108*2.2}} = 1.56$$

$$t_e = 0.07*1.56*1600 = 174 \text{ minutes}$$

<u>Law formula</u>

$$t_e = \frac{A_f e_f}{\Delta H_c \sqrt{A_v(A_t - A_v)}}$$

$e_f = 1600 \ \text{MJ/m}^2$ (From Table 5.1)

$\Delta H_c = 19$ MJ/kg

$$A_t = 2*(6*4+6*3+3*4) = 108m^2, \quad A_f = 6*4 = 24m^2, \quad A_v = 2.2*1 = 2.2m^2$$

$$t_e = \frac{24*1600}{19\sqrt{2.2*(108-2.2)}} = 132 \text{ minutes}$$

Eurocode formula

$$t_e = k_b w e_f$$

$k_b = 0.055$ (from Table 2.1)

$e_f = 1600$ MJ/m^2 (From Table 5.1)

$$w = \left(\frac{6.0}{H_r}\right)^{0.3}\left[0.62 + \frac{90(0.4-\alpha_v)^4}{1+b_v\alpha_h}\right] > 0.5$$

$$\alpha_v = \frac{A_v}{A_f} = \frac{2.2}{24} = 0.0917 \qquad 0.025 \leq \alpha_v \leq 0.25$$

$$\alpha_h = \frac{A_h}{A_f} = \frac{0}{24} = 0 \qquad \alpha_v \leq 0.2$$

$$b_v = 12.5(1+10\alpha_v - \alpha_v^2) = 12.5*(1+10*0.0917 - 0.0917^2) = 23.86$$

$$w = \left(\frac{6.0}{H_r}\right)^{0.3}\left[0.62 + \frac{90(0.4-\alpha_v)^4}{1+b_v\alpha_h}\right] = \left(\frac{6.0}{3.0}\right)^{0.3}\left[0.62 + \frac{90(0.4-0.0917)^4}{1+23.86*0}\right] = 1.76 > 0.5$$

$$t_e = k_b w e_f = 0.055*1.76*1600 = 155 \text{ minutes.}$$

Equal area method

Cumulative area under time-temperature curve for FS5 = 3740.3 minutes centigrade.

Time at which area under ASTM E119 time-temperature curve is 3740.3 minutes

centigrade is equal to 232 minutes (Refer to Figure.2.1). These areas are computed using

the procedure discussed in Chapter 2.

Therefore, t_e = 232 minutes.

B.1 Material Properties

Table B.1 – Constitutive relationships for high temperature properties of concrete

ASCE Manual 1992 (NSC)	
Stress-strain relationships	$$\sigma_c = \begin{cases} f'_{c,T}\left[1-\left(\dfrac{\varepsilon - \varepsilon_{max,\,T}}{\varepsilon_{max,\,T}}\right)^2\right], & \varepsilon \le \varepsilon_{max,\,T} \\[4mm] f'_{c,T}\left[1-\left(\dfrac{\varepsilon_{max,\,T} - \varepsilon}{3\varepsilon_{max,\,T}}\right)^2\right], & \varepsilon > \varepsilon_{max,\,T} \end{cases}$$ $$f'_{c,T} = \begin{cases} f'_c & ,20\,°C \le T \le 450\,°C \\[2mm] f'_c\left[2.011-2.353\left(\dfrac{T-20}{1000}\right)\right] & ,450\,°C < T \le 874\,°C \\[2mm] 0 & ,874\,°C < T \end{cases}$$ $$\varepsilon_{max,T} = 0.0025 + \left(6.0T + 0.04T^2\right)\times 10^{-6}$$
Thermal capacity	Siliceous Aggregate Concrete $$\rho c = \begin{cases} 0.005T +1.7 & 20\,°C \le T \le 200\,°C \\ 2.7 & 200\,°C < T \le 400\,°C \\ 0.013T - 2.5 & 400\,°C < T \le 500\,°C \\ 10.5 - 0.013T & 500\,°C < T \le 600\,°C \\ 2.7 & 600\,°C < T \end{cases}$$ Carbonate Aggregate Concrete. $$\rho c = \begin{cases} 2.566 & 20\,°C \le T \le 400\,°C \\ 0.1765T - 68.034 & 400\,°C < T \le 410\,°C \\ 25.00671 - 0.05043T & 410\,°C < T \le 445\,°C \\ 2.566 & 445\,°C < T \le 500\,°C \\ 0.01603T - 5.44881 & 500\,°C < T \le 635\,°C \\ 0.16635T - 100.90225 & 635\,°C < T \le 715\,°C \\ 176.07343 - 0.22103T & 715\,°C < T \le 785\,°C \\ 2.566 & 785\,°C < T \end{cases}$$

Table B.1 (Continued) – Constitutive relationships for high temperature properties of concrete

	ASCE Manual 1992 (NSC)
Thermal conductivity	Siliceous Aggregate Concrete. $$k_c = \begin{cases} -0.000625T + 1.5 & 20\,°C \leq T \leq 800\,°C \\ 1.0 & 800°C < T \end{cases}$$ Carbonate Aggregate Concrete. $$k_c = \begin{cases} 1.355 & 20\,°C \leq T \leq 293\,°C \\ -0.001241T + 1.7162 & 293\,°C < T \end{cases}$$
Thermal strain	All types : $$\varepsilon_{th} = \left[0.004\left(T^2 - 400\right) + 6(T - 20)\right] \times 10^{-6}$$

144

Table B.1 (Continued) – Constitutive relationships for high temperature properties of concrete

	Normal strength and high strength concrete – Eurocode 2[2004]
Stress-strain relationships	$$\sigma_c = \dfrac{3\varepsilon\, f'_{c,T}}{\varepsilon_{c1,T}\left(2 + \left(\dfrac{\varepsilon}{\varepsilon_{c1,T}}\right)^3\right)}\ ,\varepsilon \leq \varepsilon_{cu1,T}$$ For $\varepsilon_{c1(T)} < \varepsilon \leq \varepsilon_{cu1(T)}$, the Eurocode permits the use of linear as well as nonlinear descending branch in the numerical analysis. For the parameters in this equation refer to Table A.2

Thermal capacity	*Specific heat (J/kg C)*
	 $c = 900,$ *for* $20°C \leq T \leq 100°C$
	 $c = 900 + (T - 100),$ *for* $100°C < T \leq 200°C$
	 $c = 1000 + (T - 200)/2,$ *for* $200°C < T \leq 400°C$
	 $c = 1100,$ *for* $400°C < T \leq 1200°C$
	
	 Density change (kg/m^3)
	 $\rho = \rho(20°C) = Reference\ density$
	      for $20°C \leq T \leq 115°C$
	 $\rho = \rho(20°C)\ (1 - 0.02(T - 115)/85)$
	      for $115°C < T \leq 200°C$
	 $\rho = \rho(20°C)\ (0.98 - 0.03(T - 200)/200)$
	      for $200°C < T \leq 400°C$
	 $\rho = \rho(20°C)\ (0.95 - 0.07(T - 400)/800)$
	      for $400°C < T \leq 1200°C$
	
	 Thermal Capacity $= \rho \times c$

Table B.1 (Continued) – Constitutive relationships for high temperature properties of concrete

	Normal strength and high strength concrete – Eurocode 2[2004]
Thermal conductivity	All types : Upper limit: $k_c = 2 - 0.2451 \ (T/100) + 0.0107 \ (T/100)^2$ for $20°C \leq T \leq 1200°C$ Lower limit: $k_c = 1.36 - 0.136 \ (T/100) + 0.0057 \ (T/100)^2$ for $20°C \leq T \leq 1200°C$
Thermal strain	*Siliceous aggregates:* $\varepsilon_{th} = -1.8 \times 10^{-4} + 9 \times 10^{-6} T + 2.3 \times 10^{-11} T^3$ for $20°C \leq T \leq 700°C$ $\varepsilon_{th} = 14 \times 10^{-3}$ for $700°C < T \leq 1200°C$ *Calcareous aggregates:* $\varepsilon_{th} = -1.2 \times 10^{-4} + 6 \times 10^{-6} T + 1.4 \times 10^{-11} T^3$ for $20°C \leq T \leq 805°C$ $\varepsilon_{th} = 12 \times 10^{-3}$ for $805°C < T \leq 1200°C$

Table B.2 – Values for the main parameters of the stress-strain relationships of normal strength concrete at elevated temperatures [Eurocode 2]

Temp. °C	Normal Strength Concrete					
	Siliceous Aggregate			Calcareous Aggregate		
	$\dfrac{f'_{c,T}}{f'_c(20°C)}$	$\varepsilon_{c1,T}$	$\varepsilon_{cu1,T}$	$\dfrac{f'_{c,T}}{f'_c(20°C)}$	$\varepsilon_{c1,T}$	$\varepsilon_{cu1,T}$
20	1	0.0025	0.02	1	0.0025	0.02
100	1	0.004	0.0225	1	0.004	0.023
200	0.95	0.0055	0.025	0.97	0.0055	0.025
300	0.85	0.007	0.0275	0.91	0.007	0.028
400	0.75	0.01	0.03	0.85	0.01	0.03
500	0.6	0.015	0.0325	0.74	0.015	0.033
600	0.45	0.025	0.035	0.6	0.025	0.035
700	0.3	0.025	0.0375	0.43	0.025	0.038
800	0.15	0.025	0.04	0.27	0.025	0.04
900	0.08	0.025	0.0425	0.15	0.025	0.043
1000	0.04	0.025	0.045	0.06	0.025	0.045
1100	0.01	0.025	0.0475	0.02	0.025	0.048
1200	0	-	-	0	-	-

147

Table B.3 – Constitutive relationships for high temperature properties of reinforcing steel

	ASCE Manual [1992]
Stress-strain relationships	$\sigma_s = \begin{cases} \dfrac{f(T,0.001)}{0.001}\varepsilon_s & \varepsilon_s \le \varepsilon_p \\ \dfrac{f(T,0.001)}{0.001}\varepsilon_p + f(T,\varepsilon_s - \varepsilon_p + 0.001) - f(T,0.001) & \varepsilon_s > \varepsilon_p \end{cases}$ $f(T,x) = 6.9(50 - 0.04T)\left[1 - \exp((-30 + 0.03T)\sqrt{x}\,\right]$ $\varepsilon_p = 4 \times 10^{-6} f_{y,20}$ where: σ_s and ε_s = stress(MPa) and strain in steel reinforcement, respectively, and $f_{y,20}$ is the yield strength of reinforcing steel(MPa) at room temperature.
Thermal strain	$\varepsilon_{ths} = [0.004(T^2 - 400) + 6(T - 20)] \times 10^{-6} \quad T < 1000^o C$

Table B.3 (Continued) – Constitutive relationships for high temperature properties of reinforcing steel

	Eurocode 2[2004]
Stress-strain relationships	$$\sigma_s = \begin{cases} \varepsilon_s E_{s,T} & \varepsilon_s \le \varepsilon_{sp,T} \\ f_{sp,T} - c + (b/a)\left(a^2 - (\varepsilon_{sy,T} - \varepsilon_s)^2\right)^{0.5} & \varepsilon_{sp,T} < \varepsilon_s \le \varepsilon_{sy,T} \\ f_{sy,T} & \varepsilon_{sy,T} < \varepsilon_s \le \varepsilon_{st,T} \\ f_{sy,T}\left(1 - \dfrac{\varepsilon_s - \varepsilon_{st,T}}{\varepsilon_{su,T} - \varepsilon_{st,T}}\right) & \varepsilon_{st,T} < \varepsilon_s \le \varepsilon_{su,T} \\ 0 & \varepsilon_s > \varepsilon_{su,T} \end{cases}$$ Parameters $$\varepsilon_{sp,T} = \dfrac{f_{sp,T}}{E_{s,T}} \qquad \varepsilon_{sy,T} = 0.02 \qquad \varepsilon_{st,T} = 0.15 \qquad \varepsilon_{su,T} = 0.2$$ Functions $$a^2 = (\varepsilon_{sy,T} - \varepsilon_{sp,T})\left(\varepsilon_{sy,T} - \varepsilon_{sp,T} + \dfrac{c}{E_{s,T}}\right)$$ $$b^2 = c(\varepsilon_{sy,T} - \varepsilon_{sp,T})E_{s,T} + c^2$$ $$c = \dfrac{(f_{sy,T} - f_{sp,T})^2}{(\varepsilon_{sy,T} - \varepsilon_{sp,T})E_{s,T} - (f_{sy,T} - f_{sp,T})}$$ Values of $f_{sp,T}$, $f_{sy,T}$ and $E_{s,T}$ can be obtained from Table B.4
Thermal strain	$$\varepsilon_{ths} = \begin{cases} 1.2 \times 10^{-5}T + 0.4 \times 10^{-8}T^2 - 2.416 \times 10^{-4} & 20^{\circ}C \le T \le 750^{\circ}C \\ 1.1 \times 10^{-2} & 750^{\circ}C < T \le 860^{\circ}C \\ 2 \times 10^{-5}T - 6.2 \times 10^{-3} & 860^{\circ}C < T \le 1200^{\circ}C \end{cases}$$

Table B.4 – Values for the main parameters of the stress-strain relationships of reinforcing steel at elevated temperatures [Eurocode 2]

Steel temperature T(°C)	$\dfrac{f_{yT}}{f_y}$	$\dfrac{f_{sp}}{f_y}$ *	$\dfrac{E_{sT}}{E_s}$ *
20	1	1	1
100	1	1	1
200	1	0.807	0.9
300	1	0.613	0.8
400	1	0.42	0.7
500	0.78	0.36	0.6
600	0.47	0.18	0.31
700	0.23	0.075	0.13
800	0.11	0.05	0.09
900	0.06	0.0375	0.0675
1000	0.04	0.025	0.045
1100	0.02	0.0125	0.0225
1200	0	0	0

* f_y and E_s are yield strength and modulus of elasticity at room temperature

This appendix presents a detailed step-by-step calculations involved in the design of T and I beams. Both the beams are designed as under reinforced section using ACI 318 [2008] provisions. Theoretically design of I beams is exactly similar to that of T beams. Hence the detailed design procedure for T beams is presented here and it is also used for the design of I beams. Both the beams are assumed to be located in a building having a span of 7.62m (25 feet). The effective depth of the section is assumed to be equal to one-twelfth of the span length. The width of the top flange for T beam and top and bottom flanges for I beam is assumed to be equal to one-fourth of the span length while the width of the web is equal to one-half of the depth of the section. The height of the top flange for T beam and top, bottom flanges for I beam is assumed to be equal to 152mm (6 inches). Each beam is assumed to be made of siliceous aggregate concrete having a compressive strength of 28 MPa. The beams were provided with 3Ø20 mm bars as tensile reinforcement and 2Ø20 mm bars as compressive reinforcement. The yield strength of the reinforcing steel is 413 MPa. A clear concrete cover thickness of 51mm was provided to the center of tension reinforcement from both sides while that to the top of compression reinforcement was 51mm from the top of beam. The cross-sectional details along with bending moment diagram and shear force diagram are shown in Figure C.1 while the design calculations are as follows:

$f_c^1 = 28$ MPa (4 ksi) $f_y = 413$ MPa (60 ksi)

Modulus of elasticity of steel $E_s = 206842.8$ MPa (30000 ksi)

Yield strain of steel $\varepsilon_y = \dfrac{f_y}{E_s} = \dfrac{413}{206842.8} \approx 2*10^{-3}$

Length of the beam (L) = 7.62 m = 7620 mm

Effective depth of the section (d) = $\dfrac{Length}{12} = \dfrac{7620}{12} = 635$ mm

Width of the flange (b$_f$) = $\dfrac{Length}{4} = \dfrac{7620}{4} = 1905$ mm

Width of the web (b$_w$) = $\dfrac{Effective\ depth}{2} = \dfrac{635}{2} = 317$ mm

Thickness of the flanges = 152 mm

Clear concrete cover to top and bottom reinforcement = 51 mm

Diameter of tension reinforcement = 20 mm

Diameter of compressive reinforcement = 20 mm

Area of tension reinforcement $A_s = 3 * \dfrac{\pi}{4} * 20^2 = 942.5\ mm^2$

Area of compressive reinforcement $A'_s = 2 * \dfrac{\pi}{4} * 20^2 = 628.3\ mm^2$

Tensile force in bottom steel T = $A_s * f_y = 942.5 * 413 = 389252.5\ N$

Assume that the neutral axis is within the top flange and the top steel reinforcement has also yielded. Let the depth of neutral axis be c from the surface of top flange.

Compressive force in concrete

$C_c = 0.85 * f'_c * b_f * (\beta_1 c) = 0.85 * 28 * 1905 * 0.85 * c$
$\quad = 38538.15c$

Force in top steel $C'_s = A'_s * f_y = 628.3 * 413 = 259487.9\ N$

For equilibrium

$T + C'_s = C_c$

152

$$389252.5 + 259487.9 = 38538.15c$$

$$c = 16.83 \, mm$$

$$\therefore a = \beta_1 c = 0.85 * 16.83 = 14.3 \, mm$$

The strains in the tensile and compressive steel satisfy the assumptions made:

$$\frac{\varepsilon_s}{d-c} = \frac{\varepsilon_c}{c}$$

$$\frac{\varepsilon_s}{635 - 16.83} = \frac{0.003}{16.83}$$

$$\varepsilon_s = 0.11 > \varepsilon_y \quad \therefore Ok$$

$$\frac{\varepsilon_s'}{d' - c} = \frac{\varepsilon_c}{c}$$

$$\frac{\varepsilon_s'}{61 - 16.83} = \frac{0.003}{16.83}$$

$$\varepsilon_s' = 7.87 * 10^{-3} > \varepsilon_y \quad \therefore Ok$$

Thus, the factored moment resistance of the section is:

$$M_n = T.(d - \frac{a}{2}) + C_s'.(d' - \frac{a}{2})$$

$$M_n = 389252.5.(635 - \frac{14.3}{2}) + 259487.9.(61 - \frac{14.3}{2})$$

$$= 258.4 \, kN - m$$

$$\therefore M_n = 258.4 \, kN - m$$

Figures
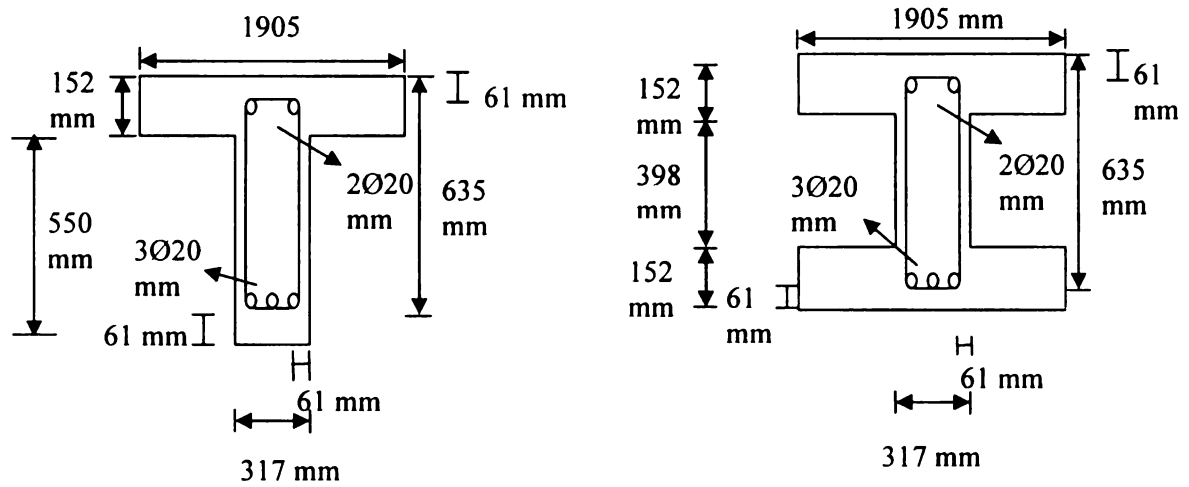
(a) Cross-sectional details of T and I beam

(b) Elevation of the beam

(c) Bending moment diagram

(d) Shear force diagram

Figure C.1 – Cross-section, Elevation, Bending moment diagram and Shear force diagram from T and I beams

Step-by-step procedure

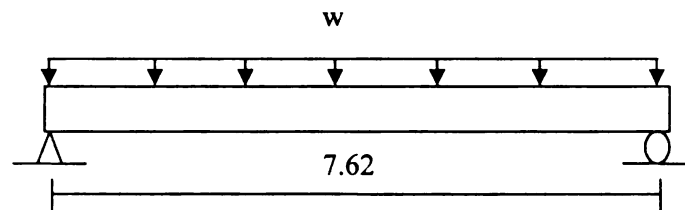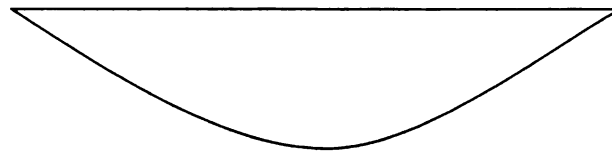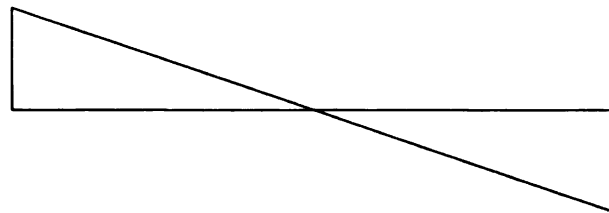Time equivalent of an RC beam exposed to design fire can be evaluated by applying the proposed energy based approach. Various calculations involved in computing the time equivalent can be performed using a spreadsheet program. The three main steps associated with the approach are:

- Computing the total energy of design fire.

- Computing cumulative energy of standard fire and.

- Finding the time equivalent.

The properties of RC beam are as discussed in Section 5.6. The beam is assumed to be exposed to design fire FS5 with a total duration of 425 minutes, as shown in Figure D.1, and the time equivalent is evaluated as follows. Detailed calculations for computing the time equivalent are illustrated in Table D.1.

Computing the total energy of design fire can be divided into the following sub-steps:

- o Dividing the total duration of fire (425 minutes), computed according to Eurocode equations, into half minute ($8.333 * 10^{-3}$ hour) time increments (Δt).

- o Calculation of fire temperatures at each time increment using the time-temperature relationships specified in standards (Eq. 3.2).

- o The fire temperature computed above is used to compute the heal flux (q/α) using Eq.(5.5).

- o At each time step, area under the heat flux curve (energy) is calculated by integrating the area using Trapezoidal rule as shown in Figure D.1. For example,

at any time step, the area is computed as a product of the time increment (Δt) and average value of heat flux during the same time increment.

o The computed values of energy at each time step are summed up to give the total energy of design fire. Thus a total energy transferred to the beam under design fire exposure is of 39814995 Joules.

Computing the cumulative energy of standard fire can be done through the following sub-steps:

o The standard fire used in this case study is ASTME119 with a maximum duration of six hours (480 minutes).

o The total duration of 480 minutes is divided into half minute ($8.333 * 10^{-3}$ hour) time increments.

o At each time step, the temperature of standard fire is computed using the approximate time-temperature relationship provided by Lie[1995] which is expressed below:

$$T = 750(1 - \exp(-3.79553\sqrt{t_h})) + 170.41\sqrt{t_h} + T_o \qquad (D.1)$$

where

t_h = time (hours),

T_o = initial temperature (°C) and

T = fire temperature (°C)

o Using this value of fire temperature, heat flux at each time step is computed using Eq.(5.5) followed by the computation of area under heat flux curve (energy), using Trapezoidal rule. (similar procedure as that for design fire)

o   At each time step the cumulative area under heat flux curve (energy) of the standard fire exposure, which is equal to the energy at the current time step plus the sum of energies till the previous time step is computed.

o   At each time step, the difference between the total energy of design fire and cumulative energy of standard fire is computed.

The difference between two energy values is minimum (approximately zero) at a time of 150 minutes. Hence this time value is defined as the time equivalent by the current method.

In summary, the proposed method predicts a time equivalent value of 150 minutes with respect to ASTM E119 standard fire exposure for the RC beam described in the case study subjected to design fire scenario FS5.

Tables

Table D.1 – Step-by-step calculations for evaluating time equivalent of fire scenario5 (FS5) by equal energy method

Time step	Time (min)	Design fire Temperature (°C)	Heat flux ($q(\alpha)$) (W/m²)		Energy (Joules) = Cumulative area under heat flux curve		Difference in total energy of design fire and cumulative energy of standard fire
			Design fire	Standard fire	Design fire	Standard fire	
1	$t_1 = 0$	$T_{f1} = 20$	Heat flux at time step t_1 (HFt1_DF) calculated using Eq.(5.5) = 8161	Heat flux at time step t_1 (HFt1_SF) calculated using Eq(5.5) = 8161	$ED_1 = 0$	$ES_1 = 0$	$ES_1 - ED_n = (39814995 - 0) = 39814995$
2	$t_2 = t_1 + \Delta t = 0.5$	$T_{f2} = 45$	Heat flux at time step t_2 (HFt2_DF) calculated using Eq.(5.5) = 9124	Heat flux at time step t_2 (HFt2_SF) calculated using Eq.(5.5) = 22102	$ED_2 = 0.5 \times (t2 - t1) \times (HFt1\_DF + HFt2\_DF) + ED_1 = 4321$	$ES_2 = 0.5 \times (t2 - t1) \times (HFt1\_SF + HFt2\_SF) + ES_1 = 8431$	$ES_2 - ED_n = (39814995 - 8431) = 39806564$
⋮							
i	$t_i = 150$	$T_{fi} = 828$	Heat flux at time step t_i (HFti_DF) calculated using Eq.(5.5) = 194094	Heat flux at time step t_i (HFti_SF) calculated using Eq.(5.5) = 367333	$ED_i = 0.5 \times (t_i - t_{i-1}) \times (HFt_{i\_DF} + HFt_{i-1\_DF}) + ED_{i-1} = 22599270$	$ES_i = 0.5 \times (t_i - t_{i-1}) \times (HFt_{i\_SF} + HFt_{i-1\_SF}) + ES_{i-1} = 39785460$	$ES_i - ED_n = (39785460 - 39785460) \approx 0$
⋮							

Table D.1 (Continued) – Step-by-step calculations for evaluating time equivalent of fire scenario5 (FS5) by equal energy method

| Time step	Time (min)	Design fire Temperature (°C)	Heat flux (q/α) (W/m²)		Energy (Joules) = Cumulative area under heat flux curve		Difference in total energy of design fire and cumulative energy of standard fire
			Design fire	Standard fire	Design fire	Standard fire	
n-1	$t_{n-1}=$ 420	$T_{fn-1}=33$	Heat flux at time step t_{n-1} (HF_{n-1_DF}) calculated using Eq.(5.5) = 8622	Heat flux at time step t_{n-1} (HF_{n-1_SF}) calculated using Eq.(5.5) = 602047	$ED_{n-1}=0.5\times(t_{n-1}-t_{n-2})\times(HF_{n-2\_DF}+HF_{n-1\_DF})+ED_{n-2}=$ 39773147	$ES_{n-1}=0.5\times(t_{n-1}-t_{n-2})\times(HF_{n-2\_SF}+HF_{n-1\_SF})+ES_{n-2}=1.71*10^8$	$ES_{n-1}-ED_n=$ (39814995- $1.7*10^8$) = -131185005
n	$t_n=$ 425	$T_{fn}=20$	Heat flux at time step t_n (HF_{n_DF}) calculated using Eq.(5.5) = 8075	Heat flux at time step t_n (HF_{n_SF}) calculated using Eq.(5.5) = 606177	$ED_n=0.5\times(t_n-t_{n-1})\times(HF_{n\_DF}+HFt_{n-1\_DF})+ED_{n-1}=$ 39814995	$ES_n=0.5\times(t_n-t_{n-1})\times(HF_{n\_SF}+HF_{n-1\_SF})+ES_{n-1}=1.74*10^8$	$ES_n-ED_n=$ (39814995- $1.74*10^8$) = -134185005
					Total Energy of design fire	$ED_n=$39814995	

159
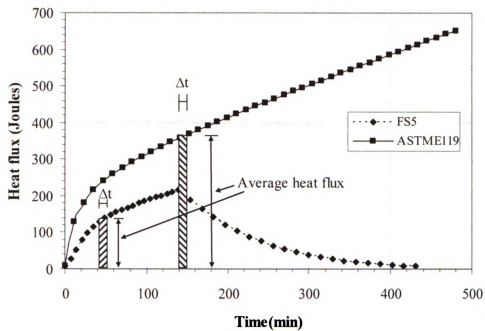
Figures

Figure D.1 – Illustration of computation of area under heat flux curves using Trapezoidal rule

REFERENCES

1. ACI Committee 216.1-07 (2007), "Standard Method for Determining Fire Resistance of Concrete and Masonry Construction Assemblies", American Concrete Institute, Detroit.

2. ACI 318 -2008 (2008), "Building Code Requirements for Reinforced Concrete", ACI 318-08 and Commentary, American Concrete Institute, Detroit, MI.

3. Anderberg Y., and Thelandersson S. (1976), "Stress and Deformation Characteristics of Concrete at High Temperatures, 2. Experimental Investigation and Material Behaviour Model", Lund Institute of Technology, Sweden.

4. ASCE manual No.78 (1992), "Structural Fire Protection", ASCE committee on fire protection, structural division, American Society of Civil Engineers, New York.

5. ASTM (2008), "Standard Methods of Fire Test of Building Construction and Materials", Test Method E119a-08, American Society for Testing and Materials, West Conshohocken, PA.

6. ASTM (1993), "Standard Test Methods for Determining Effects of Large Hydrocarbon Pool Fires on Structural Members and Assemblies", Test Method E1529, American Society for Testing and materials, West Conshohocken, PA.

7. Buchanan, A.H.(2002), "Structural Design for Fire Safety", John Wiley & Sons Ltd., Chichester, England.

8. CIB (1986), Design guide- structural fire safety, CIB-W14. Fire Safety Journal, 10, 2, pp.75-138.

9. Dotreppe J.C., and Franssen J.M.(1985), "The Use of Numerical Models for the Fire Analysis of Reinforced Concrete and Composite Structures", Engineering Analysis, CML Publications, 2(2), pp.67-74.

10. Dwaikat M.B., and Kodur V.R. (2008a), "A Numerical Approach for Modeling the Fire Induced Restraint Effects in Reinforced Concrete Beams", Fire Safety Journal, 43(4), pp.291-307.

11. Dwaikat M.B. (2009), "Flexural response of reinforced concrete beams exposed to fire", PhD Dissertation, Michigan State University, East Lansing, Michigan, USA.

12. Ellingwood B., and Lin T.D. (1991), "Flexure and Shear Behavior of Concrete Beams During Fire", Journal of Structural Engineering, ASCE, 117(2) , pp. 440-458.

13. Eurocode 1 (2002), "EN1991-1-2. Actions on structures. Part 1-2: General Actions-Actions on Structures Exposed to Fire", European Committee for Standardization, Brussels, Belgium.

14. Eurocode 2 (2004), "EN 1991-1-2: Design of Concrete Structures. Part 1-2: General Rules- Structural Fire Design", European Committee for Standardization, Brussels, Belgium.

15. Eurocode 3 (1995), "Eurocode 3: Design of Steel Structures. ENV 1993-1-2: General Rules- Structural Fire Design", European Committee for Standardization, Brussels, Belgium.

16. Feasey,R., and Buchanan, A.H. (2002), "Post-flashover Fires for Structural Design", Fire Safety Journal, 37(1), pp. 83-105.

17. Franssen J.M., Kodur V.K.R., and Mason J.(2004), User Manual for SAFIR, University of Liège, Belgium.

18. Harmathy T.Z.(1967), " A comprehensive Creep Model", Journal of Basic Engineering, 89(2), pp. 496-502.

19. Ingberg, S.H. (1928), Tests of the severity of building fires. National Fire Protection Quarterly,22,1,pp.43-61.

20. ISO 834-1975 (1975), Fire resistance tests – elements of building construction. International Organization for Standardization.

21. Kang S.W., and Hong S.G. (2004), "Analytical Method for the Behavior of a Reinforced Concrete Flexural member at Elevated Temperatures", Fire and materials, 28, pp. 227-235.

22. Kodur V.K.R., Dwaikat M.B. (2008), "A numerical model for predicting the fire resistance of reinforced concrete beams", Journal of Cement & Concrete Composites, 30, pp. 431-443.

23. Kodur V.R., and Dwaikat M.B. (2008b), "Flexural Response of Reinforced Concrete Beams Exposed to Fire", Structural Concrete, 9(1), pp.45-54.

24. Kodur V.R., Dwaikat M.M.S., and Dwaikat M.B. (2008), "High Temperature Properties of Concrete for Fire Resistance Modeling of Structures", ACI Material Journal, 105(5), pp.517-527

25. Law, M. (1971), "A relationship between fire grading and building design and contents", *Fire Research Note No. 877*. Fire Research Station, UK.

26. Lie T.T., and Irwin R.J. (1993), "Method to Calculate the Fire Resistance of Reinforced Concrete Columns with Rectangular Cross-section:. ACI Structural Journal, American Concrete institute, 90(1), pp. 52-60.

27. Lie TT (1995). Fire temperature-time relations. Chapter 4-8, SFPE Handbook of fire protection engineering, second edition, Society of fire protection engineers, USA.

28. Lin T.D., Gustaferro A.H., and Abrams M.S. (1981), "Fire Endurance of Continuous Reinforced Concrete Beams", R&D Bulletin RD072.01B, Portland Cement Association, IL, USA.

29. Lin T.D., and Ellingwood B. (1987), "Flexural and Shear Behavior of Reinforced Concrete Beams during Fire Tests", NBS-GCR-87-536, Portland Cement Association, IL, USA.

30. Magnusson SE, Thelandersson S (1970), "Temperature-time curves of complete process of fire development; Theoretical study of wood fuel fires in enclosed spaces", Civil engineering and building series 65, Acta, Polytechnica, Scandinavia.

31. NBCC (2005), "Fire and Structural Protection of Building", National Building Code of Canada, National Research Council, Canada.

32. Nyman, J.F.(2002), Equivalent Fire Resistance Ratings of Construction Elements Exposed to Realistic Fires, University of Canterbury, May 2002.

33. Pettersson,O. (1973), The connection between a real fire exposure and the heating conditions according to standard fire-resistance tests-with special application to steel structures. Document CECM 3-73/73. European Commission for Constructional Steelwork.

34. Pettersson, O., Magnusson, S.E., and Thor, J.(1976), Fire Engineering design of steel structures. Publication No. 50, Swedish Institute of Steel Construction.

35. Poh K.W., and Bennetts I.D. (1995), "Analysis of Structural members Under Elevated Temperature Conditions", Journal of Structural Engineering, ASCE, 121(4), pp.664-675.

36. Poh, K.W.,and Bennets I.D., (1995), "Behavior of steel columns at elevated temperatures", Journal of Structural Engineering, ASCE, 121(4), pp.676-684.

37. SFPE (2004), "Fire Exposure to Structural Elements – Engineering Guide", Society of Fire Protection Engineers, Bethesda, MD, pp.150.

38. Shi X., Tan T., Tan K., and Guo Z. (2004), "Influence of Concrete Cover on Fire Resistance of Reinforced Concrete Flexural Members", Journal of Structural Engineering, ASCE, 130(8) , pp. 1225-1232.

39. William, B.B. (1990), "A first course in the Finite Element Method", Richard D. Irwin, Inc., US.